NBSIR 82-2465 (A)

Investigation of the Kansas City Hyatt Regency Walkways Collapse

U.S. DEPARTMENT OF COMMERCE
National Bureau of Standards
Washington, DC 20234

Feburary 1982

DEPARTMENT OF COMMERCE
NAL BUREAU OF STANDARDS

NBSIR 82-2465 (A)

INVESTIGATION OF THE KANSAS CITY HYATT REGENCY WALKWAYS COLLAPSE

R. D. Marshall
E. O. Pfrang
E. V. Leyendecker
K. A. Woodward

Center for Building Technology
National Engineering Laboratory

R. P. Reed
M. B. Kasen
T. R. Shives

Center for Materials Science
National Measurement Laboratory

U.S. DEPARTMENT OF COMMERCE
National Bureau of Standards
Washington, DC 20234

February 1982

U.S. DEPARTMENT OF COMMERCE, Malcolm Baldrige, *Secretary*
NATIONAL BUREAU OF STANDARDS, Ernest Ambler, *Director*

ABSTRACT

An investigation into the collapse of two suspended walkways within the atrium area of the Hyatt Regency Hotel in Kansas City, Mo., is presented in this report. The investigation included on-site inspections, laboratory tests and analytical studies.

Three suspended walkways spanned the atrium at the second, third, and fourth floor levels. The second floor walkway was suspended from the fourth floor walkway which was directly above it. In turn, this fourth floor walkway was suspended from the atrium roof framing by a set of six hanger rods. The third floor walkway was offset from the other two and was independently suspended from the roof framing by another set of hanger rods. In the collapse, the second and fourth floor walkways fell to the atrium floor with the fourth floor walkway coming to rest on top of the lower walkway.

Based on the results of this investigation, it is concluded that the most probable cause of failure was insufficient load capacity of the box beam-hanger rod connections. Observed distortions of structural components strongly suggest that the failure of the walkway system initiated in the box beam-hanger rod connection on the east end of the fourth floor walkway's middle box beam.

Two factors contributed to the collapse: inadequacy of the original design for the box beam-hanger rod connection which was identical for all three walkways, and a change in hanger rod arrangement during construction that essentially doubled the load on the box beam-hanger rod connections at the fourth floor walkway. As originally approved for construction, the contract drawings called for a set of continuous hanger rods which would attach to the roof framing and pass through the fourth floor box beams and on through the second floor box beams. As actually constructed, two sets of hanger rods were used, one set extending from the fourth floor box beams to the roof framing and another set from the second floor box beams to the fourth floor box beams.

Based on measured weights of damaged walkway spans and on a videotape showing occupancy of the second floor walkway just before the collapse, it is concluded that the maximum load on a fourth floor box beam-hanger rod connection at the time of collapse was only 31 percent of the ultimate capacity expected of a connection designed under the Kansas City Building Code. It is also concluded that had the original hanger rod arrangement not been changed, the ultimate capacity would have been approximately 60 percent of that expected under the Kansas City Building Code. With this change in hanger rod arrangement, the ultimate capacity of the walkways was so significantly reduced that, from the day of construction, they had only minimal capacity to resist their own weight and had virtually no capacity to resist additional loads imposed by people.

Supplementary material is contained in an appendix to this report and published as NBSIR 82-2465A.

Key Words: building; collapse; connection; construction; failure; steel; walkway.

APPENDIX

Sections A6.10 - A6.11

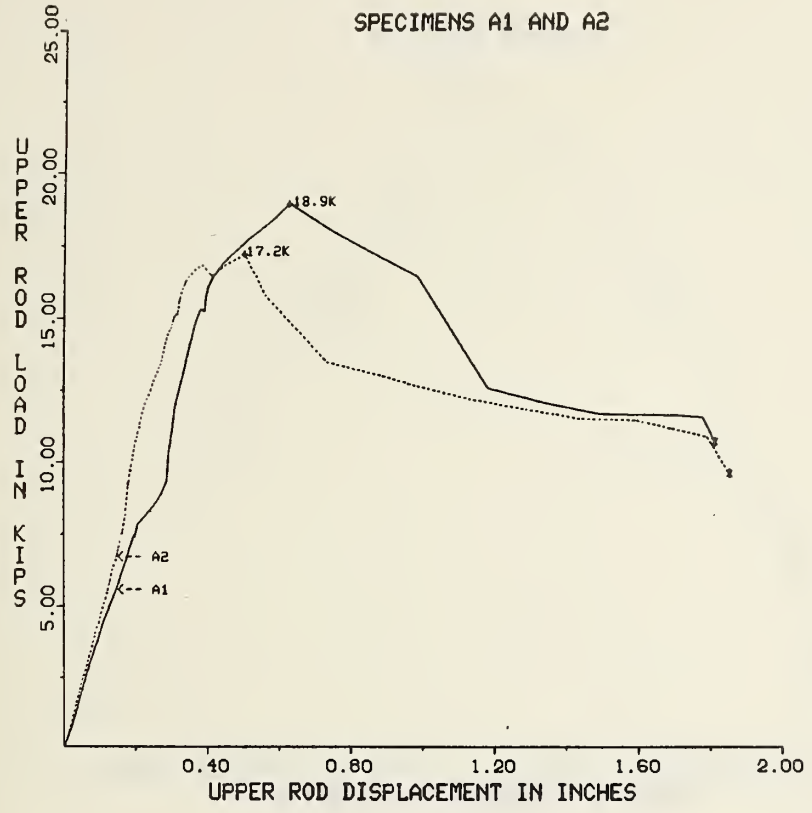

Figure A6.10-1 In-plane load vs displacement curves for specimens A1 and A2.

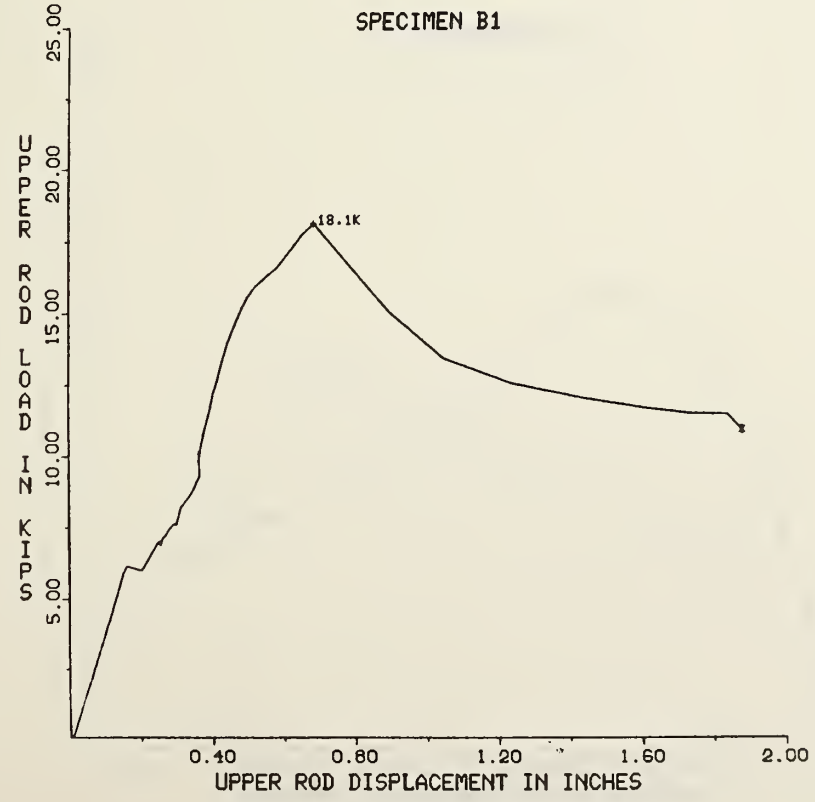

Figure A6.10-2 In-plane load vs displacement curve for specimens B1.

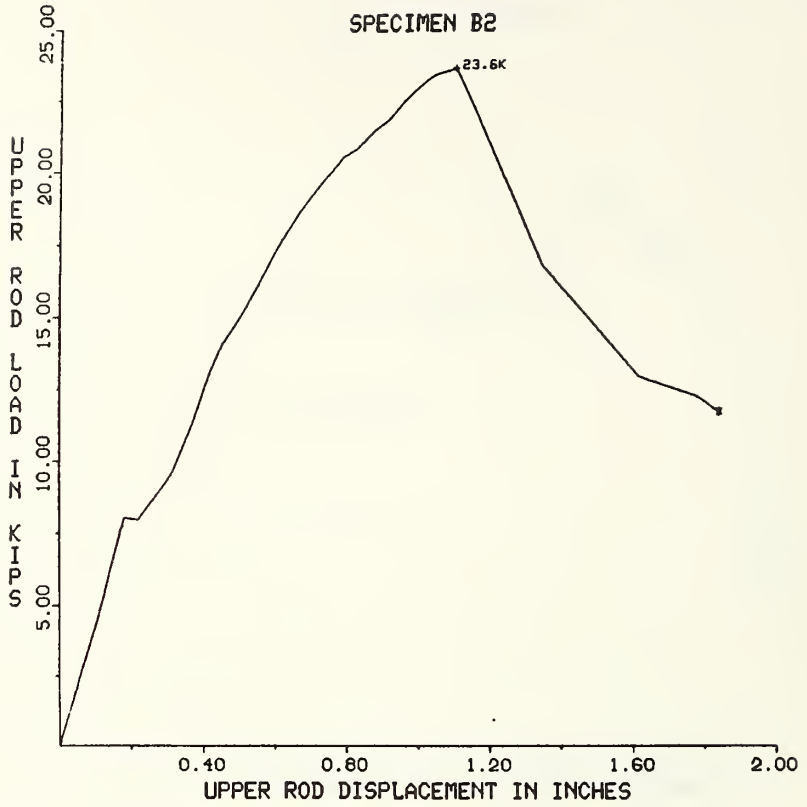

Figure A6.10-3 In-plane load vs displacement curve for specimens B2.

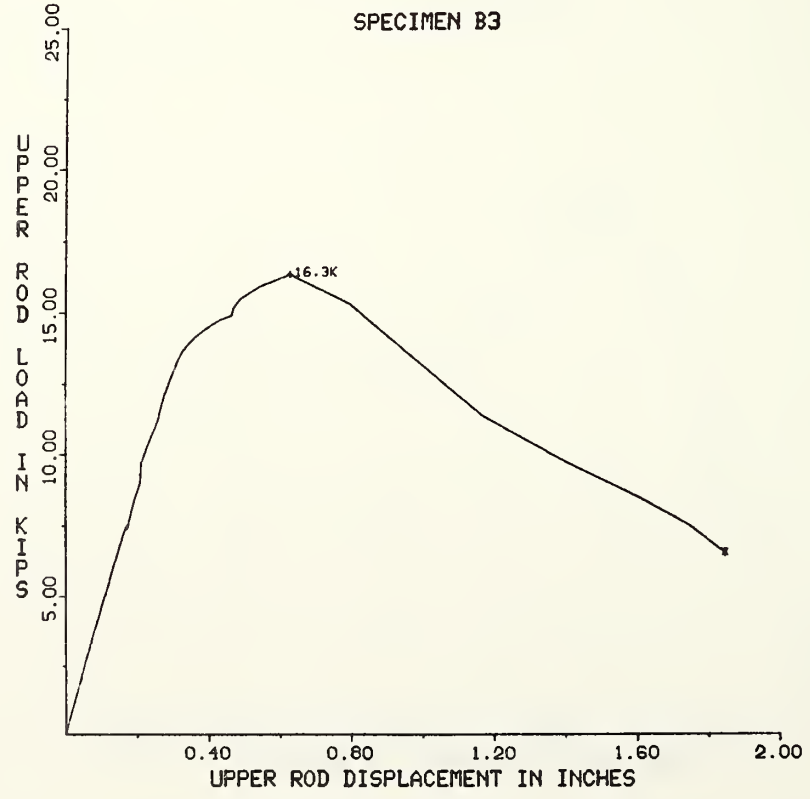

Figure A6.10-4 In-plane load vs displacement curve for specimens B3.

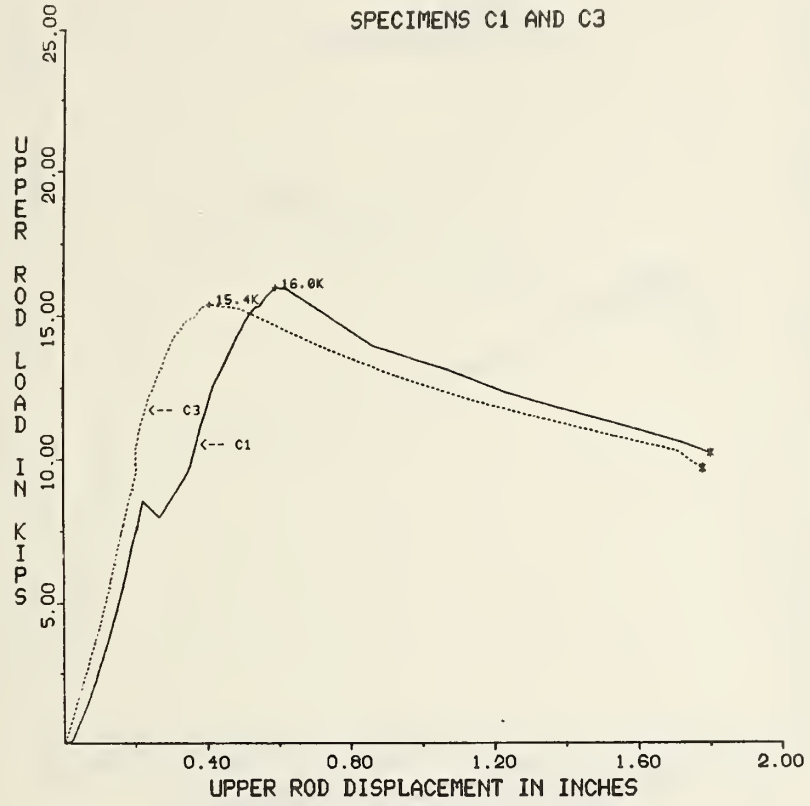

Figure A6.10-5 In-plane load vs displacement curves for specimens C1 and C3.

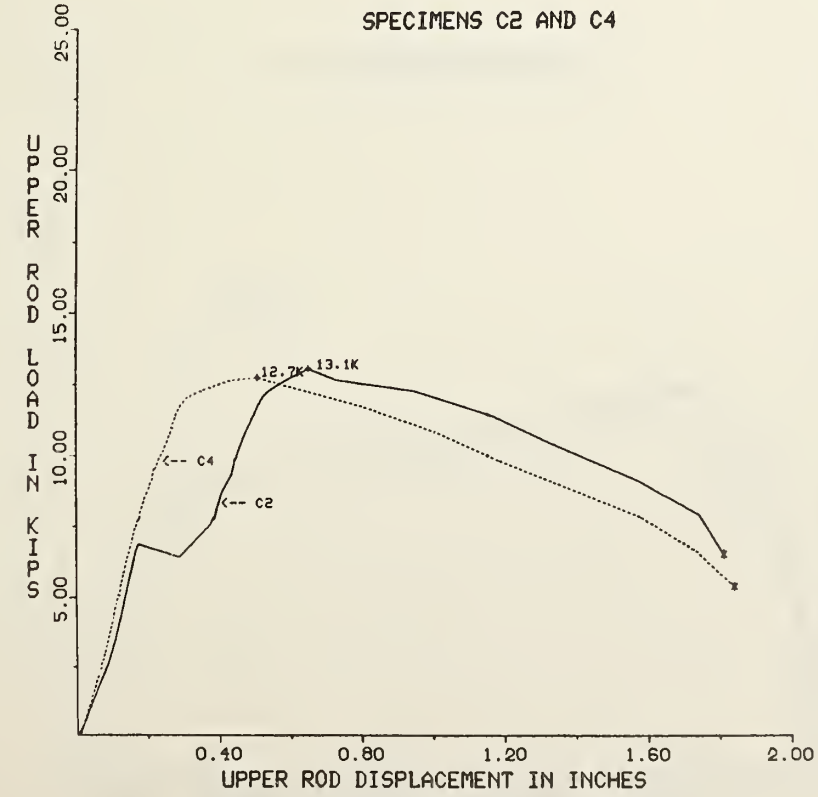

Figure A6.10-6 In-plane load vs displacement curves for specimens C2 and C4.

Figure A6.10-7 In-plane load vs displacement curve for specimens D1.

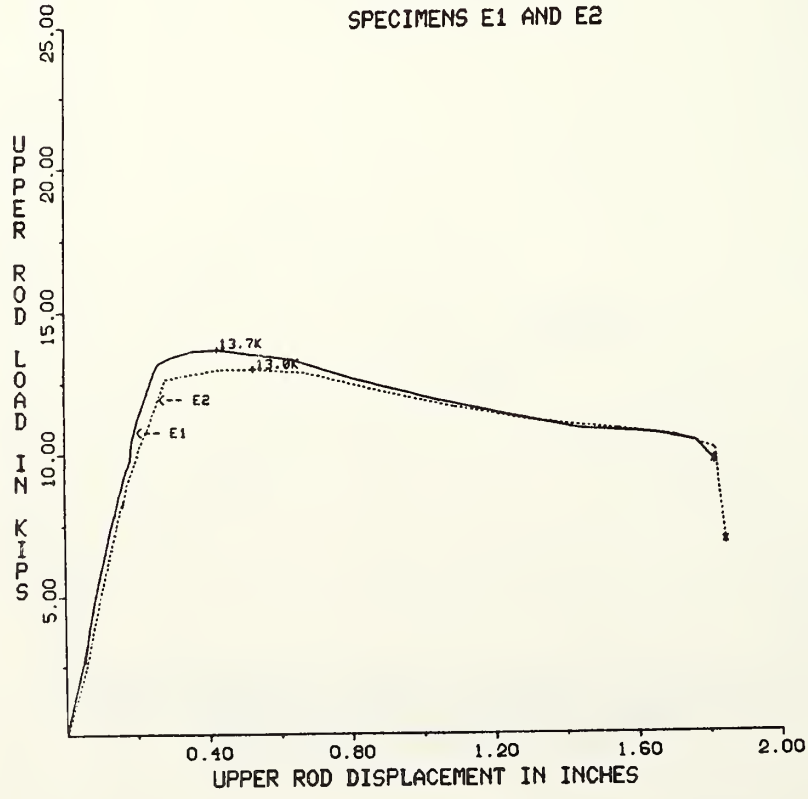

Figure A6.10-8 In-plane load vs displacement curves for specimens E1 and E2.

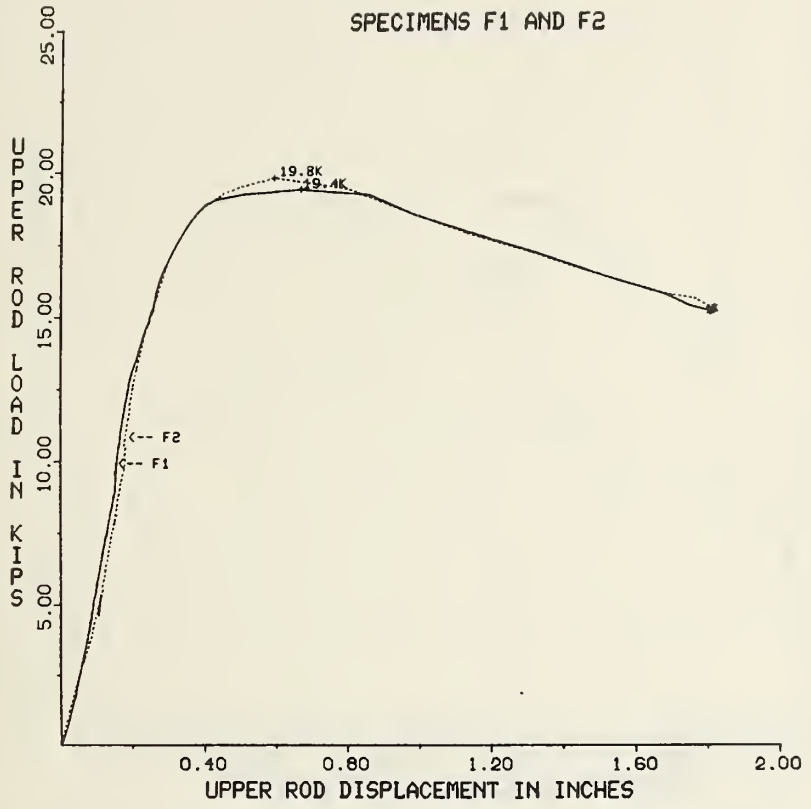

Figure A6.10-9 In-plane load vs displacement curves for specimens F1 and F2.

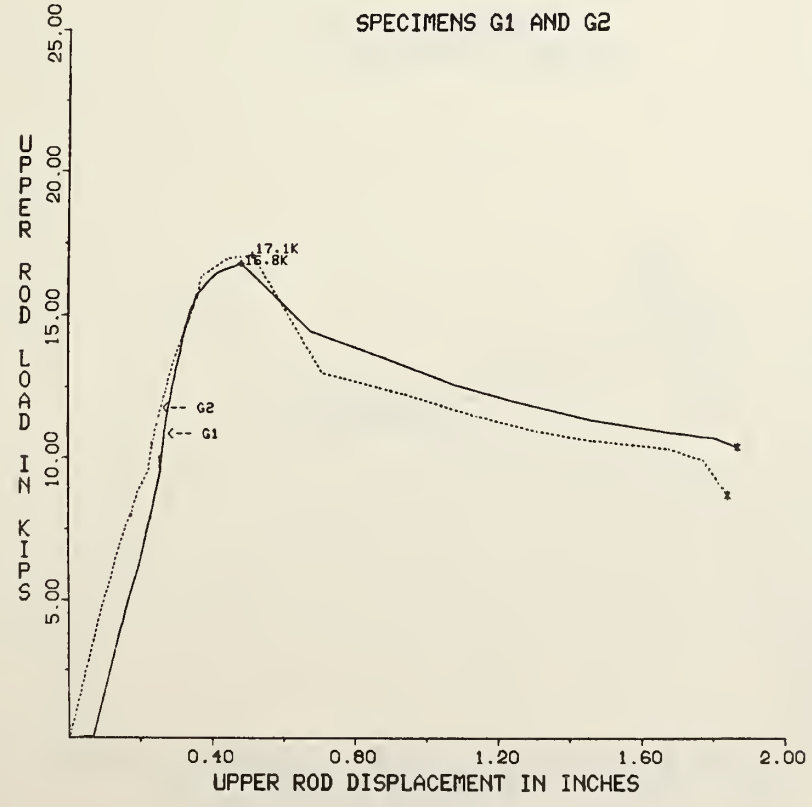

Figure A6.10-10 In-plane load vs displacement curves for specimens G1 and G2.

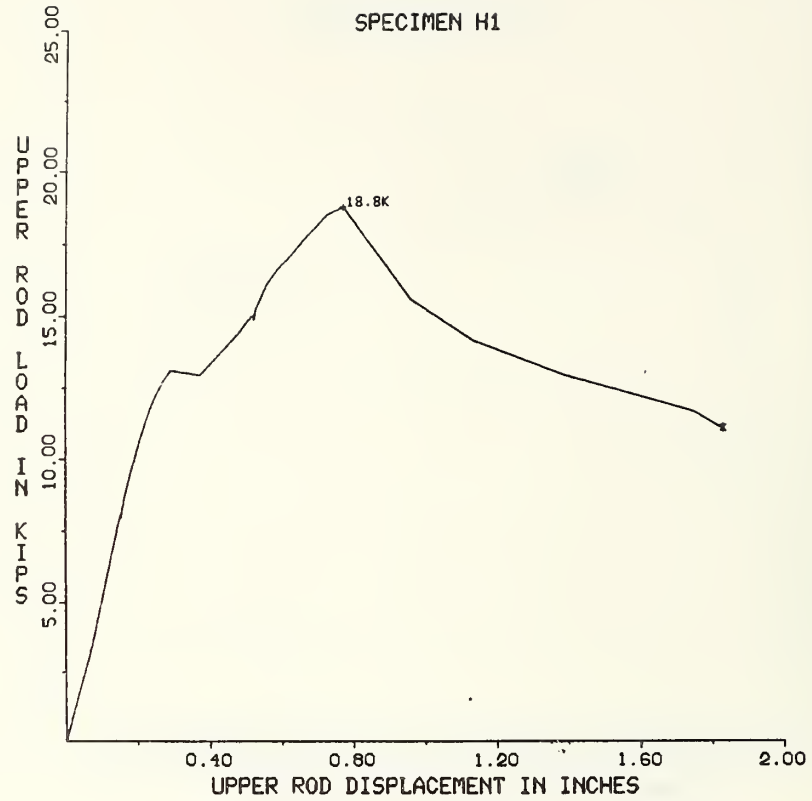

Figure A6.10-11 In-plane load vs displacement curve for specimens H1.

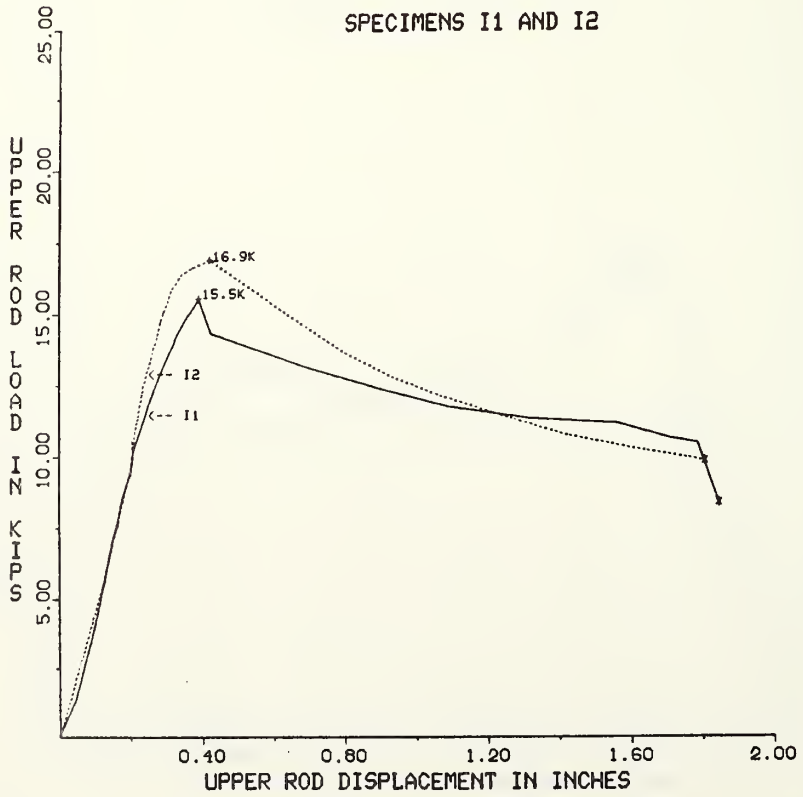

Figure A6.10-12 In-plane load vs displacement curves for specimens I1 and I2.

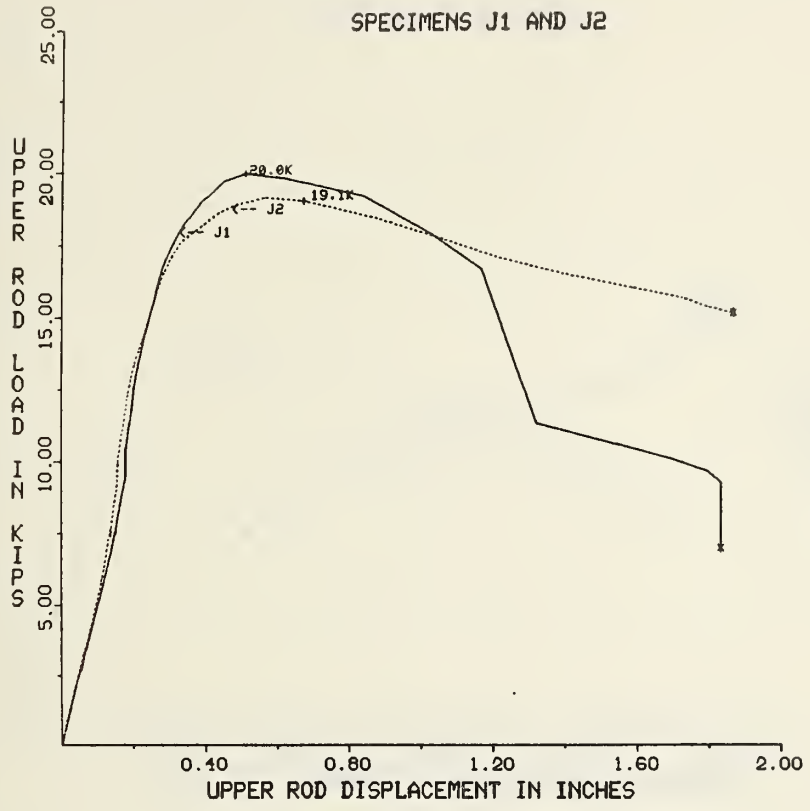

Figure A6.10-13 In-plane load vs displacement curves for specimens J1 and J2.

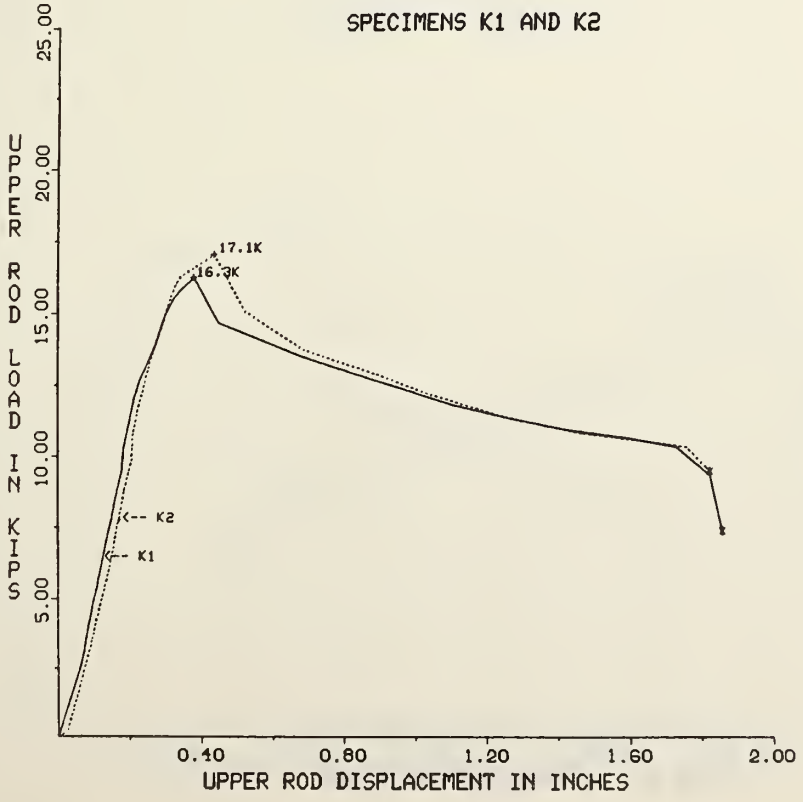

Figure A6.10-14 In-plane load vs displacement curves for specimens K1 and K2.

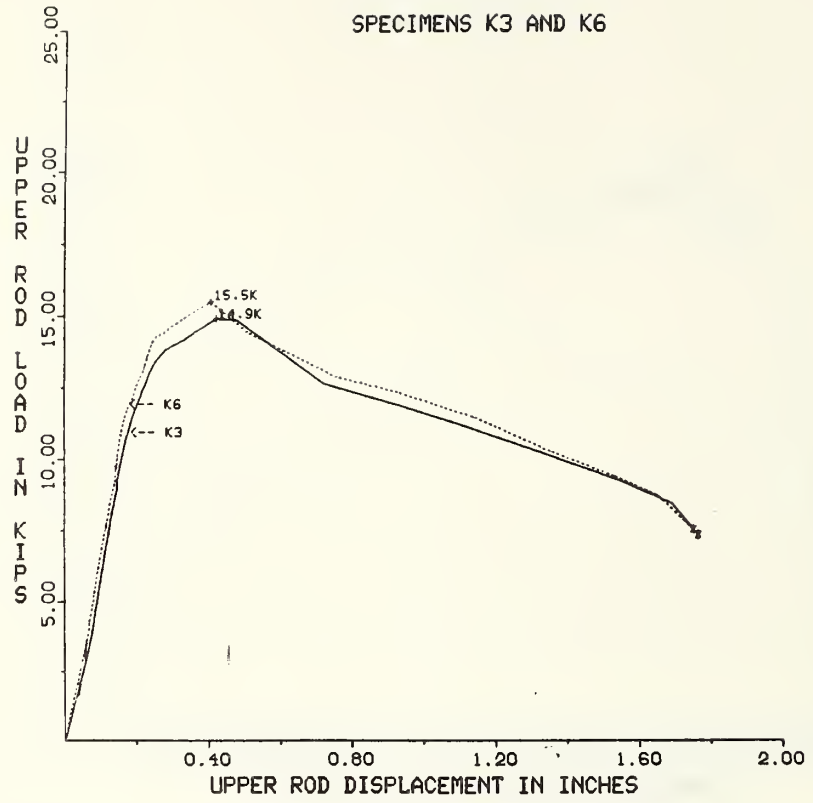

Figure A6.10-15 In-plane load vs displacement curves for specimens K3 and K6.

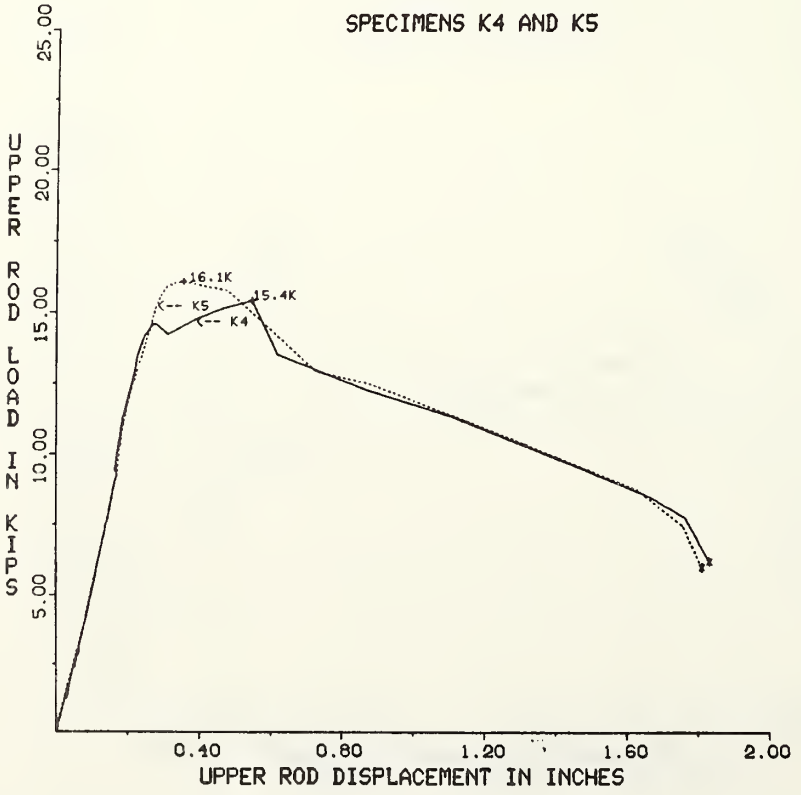

Figure A6.10-16 In-plane load vs displacement curves for specimens K4 and K5.

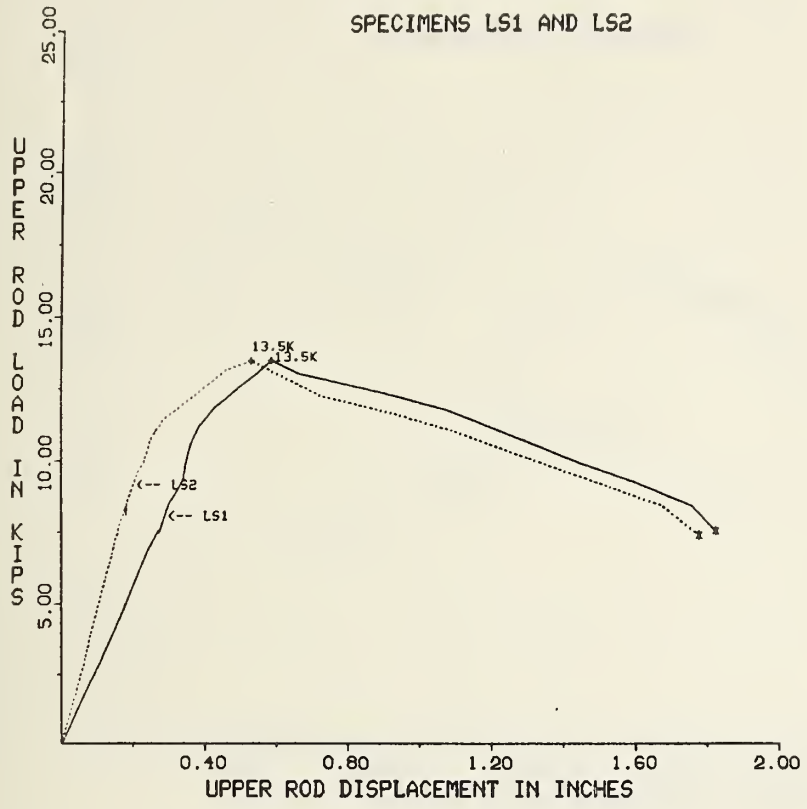

Figure A6.10-17 In-plane load vs displacement curves for specimens LS1 and LS2.

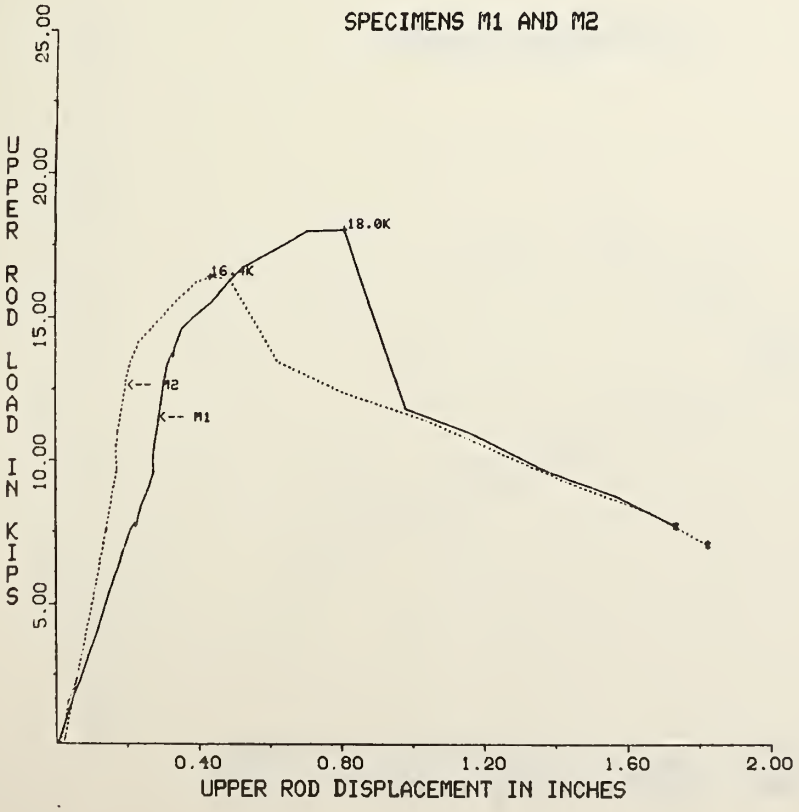

Figure A6.10-18 In-plane load vs displacement curves for specimens M1 and M2.

Figure A6.10-19 In-plane load vs displacement curves for specimens N1 and N2.

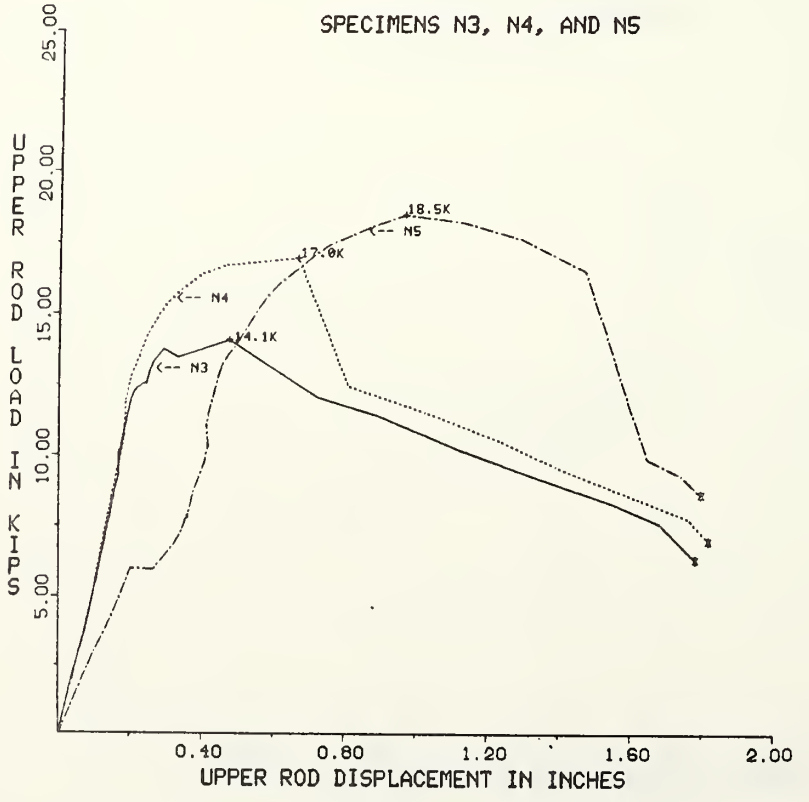

Figure A6.10-20 In-plane load vs displacement curves for specimens N3, N4, and N5.

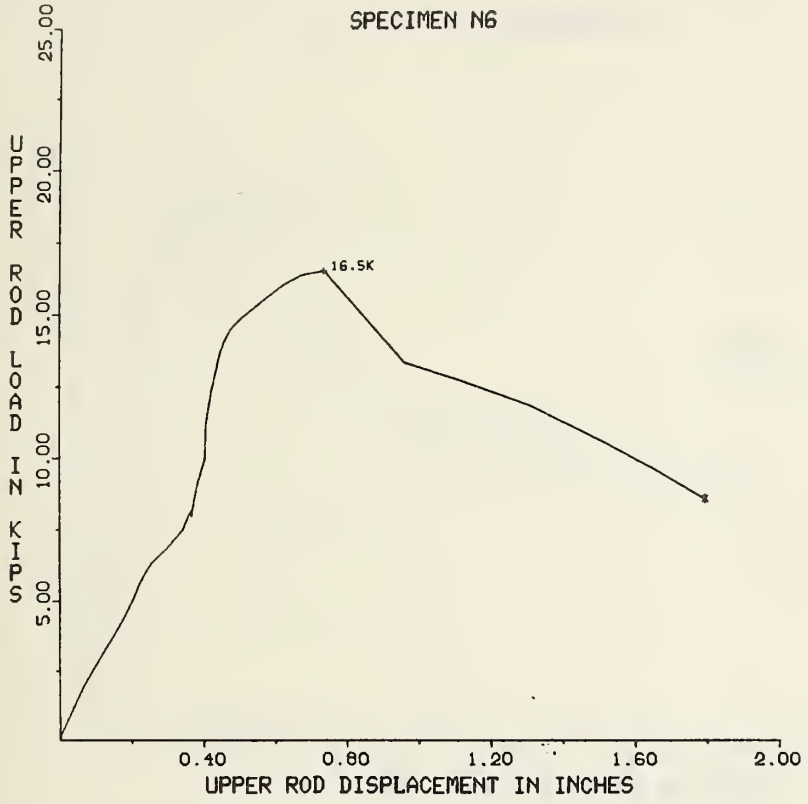

Figure A6.10-21 In-plane load vs displacement curve for specimens N6.

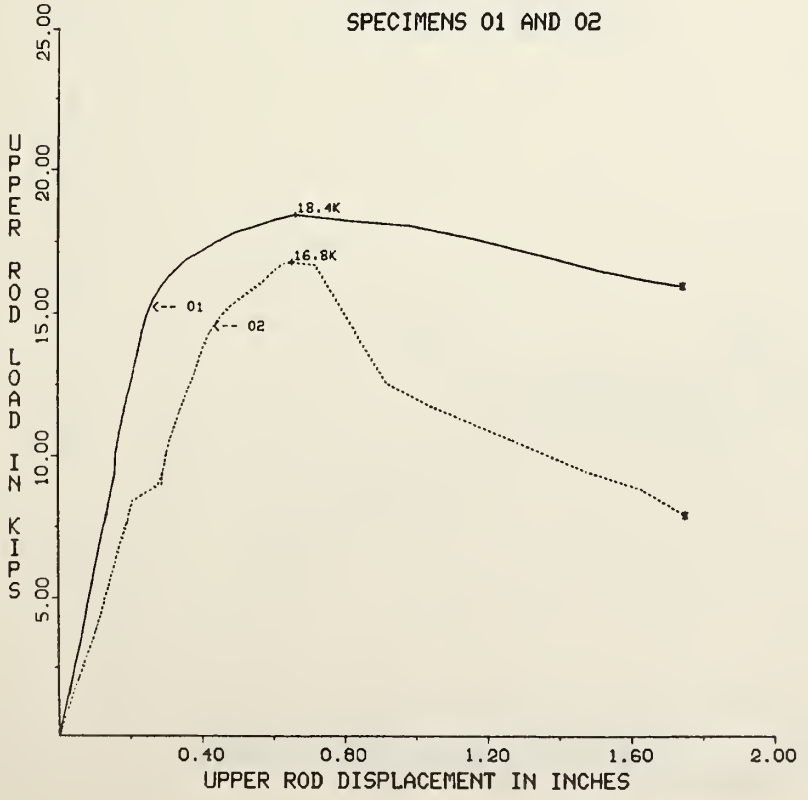

Figure A6.10-22 In-plane load vs displacement curves for specimens 01 and 02.

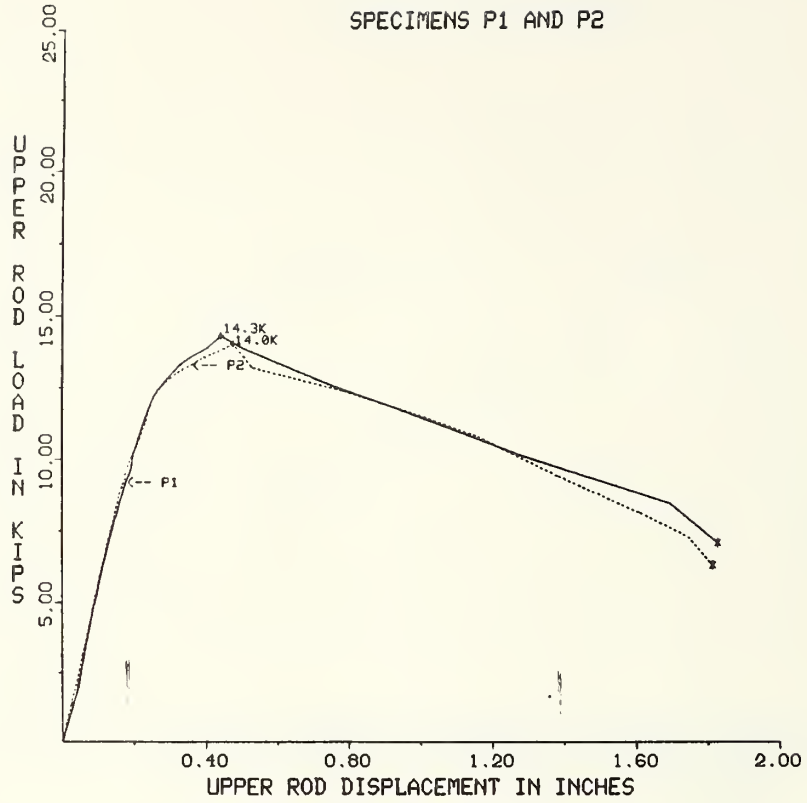

Figure A6.10-23 In-plane load vs displacement curves for specimens P1 and P2.

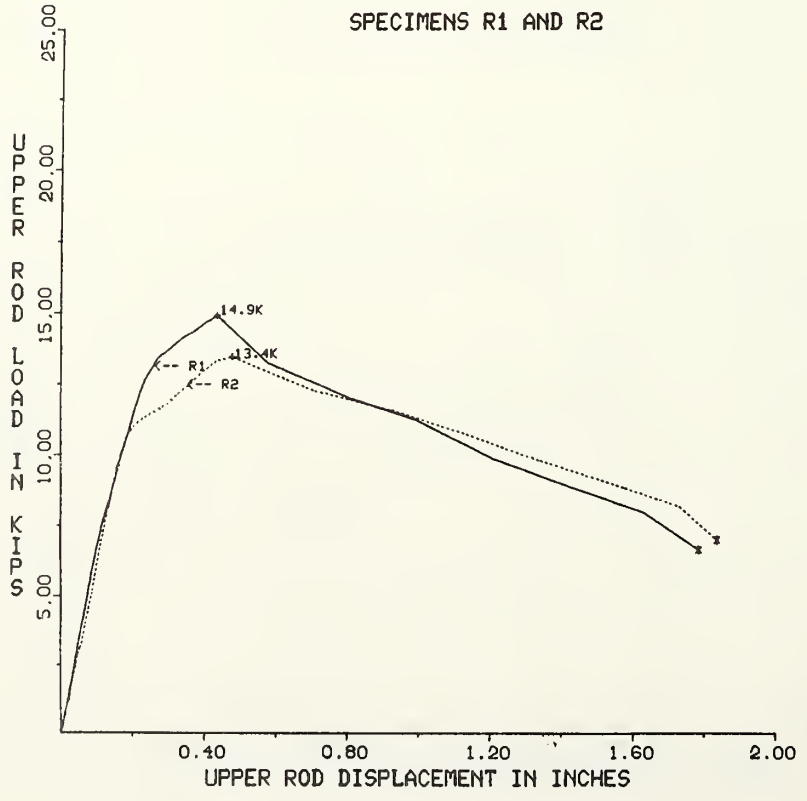

Figure A6.10-24 In-plane load vs displacement curves for specimens R1 and R2.

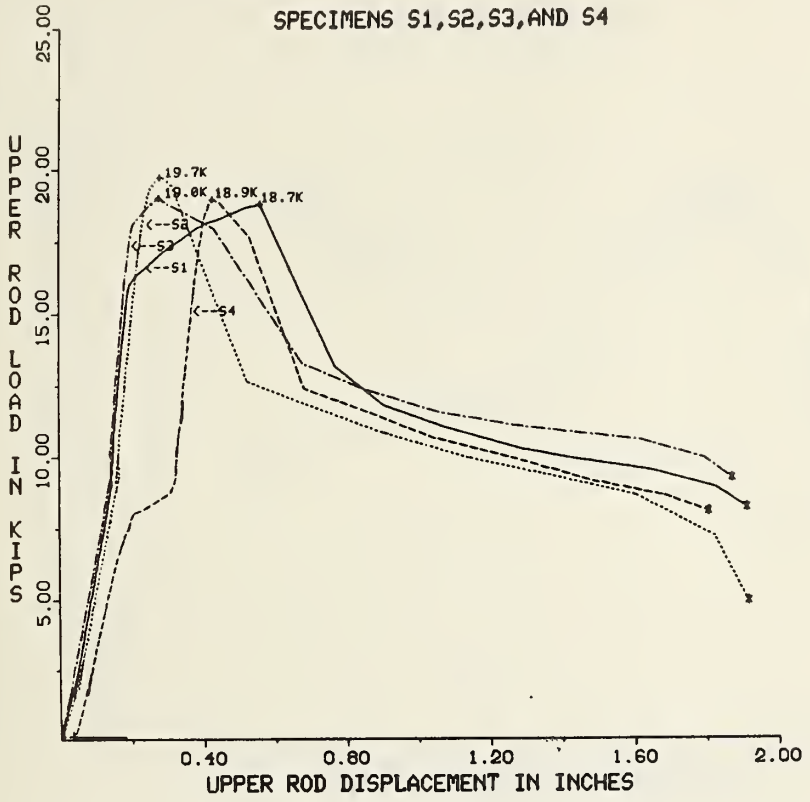

Figure A6.10-25 In-plane load vs displacement curves for specimens S1, S2, S3, and S4.

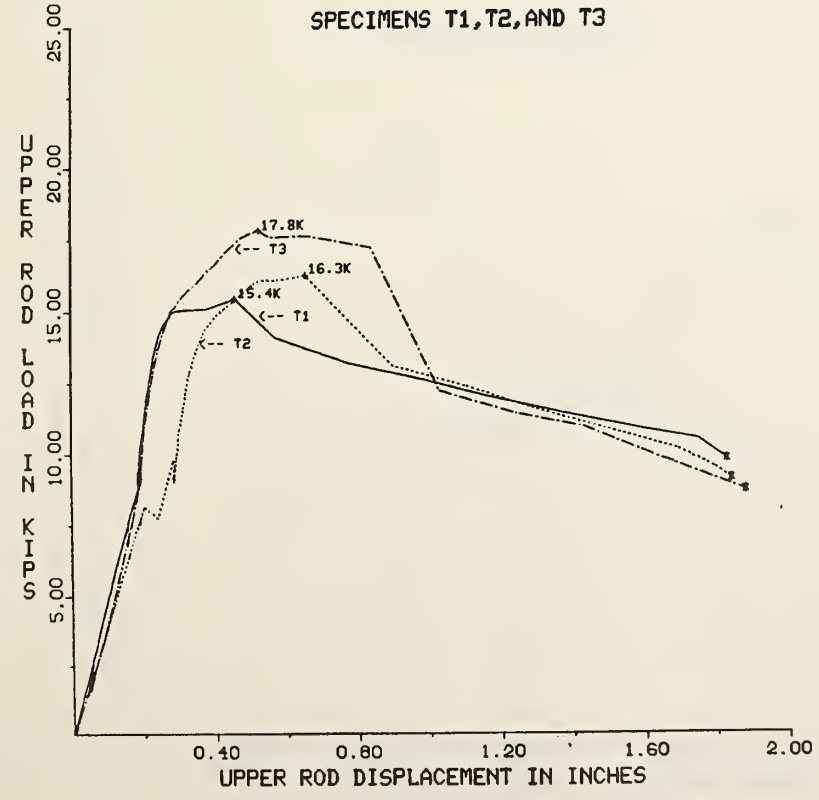

Figure A6.10-26 In-plane load vs displacement curves for specimens T1, T2, and T3.

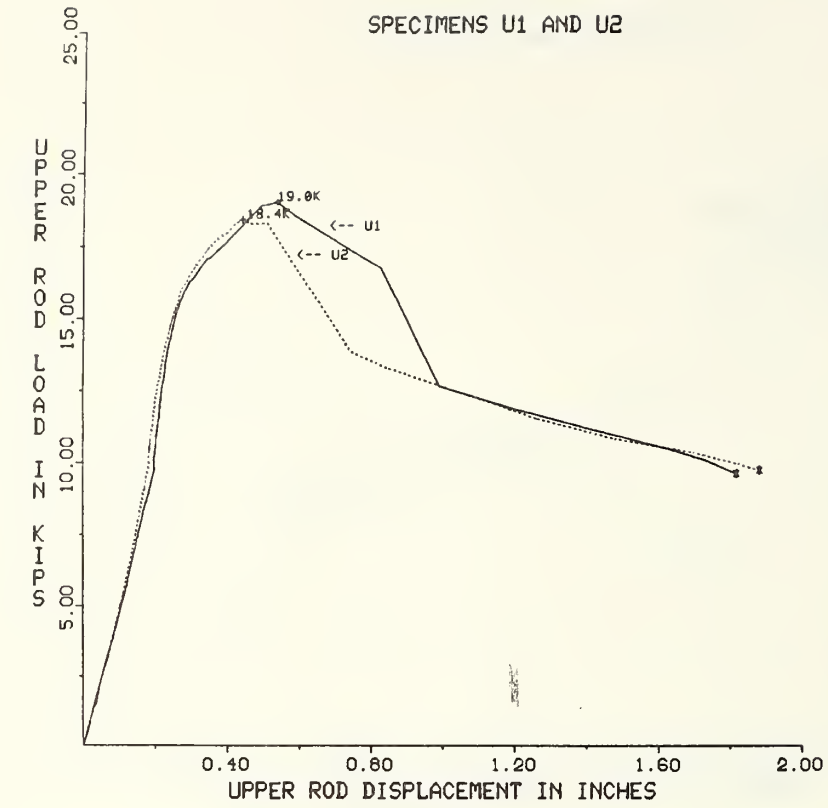

Figure A6.10-27 In-plane load vs displacement curves for specimens U1 and U2.

Figure A6.10-28 In-plane load vs displacement curves for specimens V1 and V2.

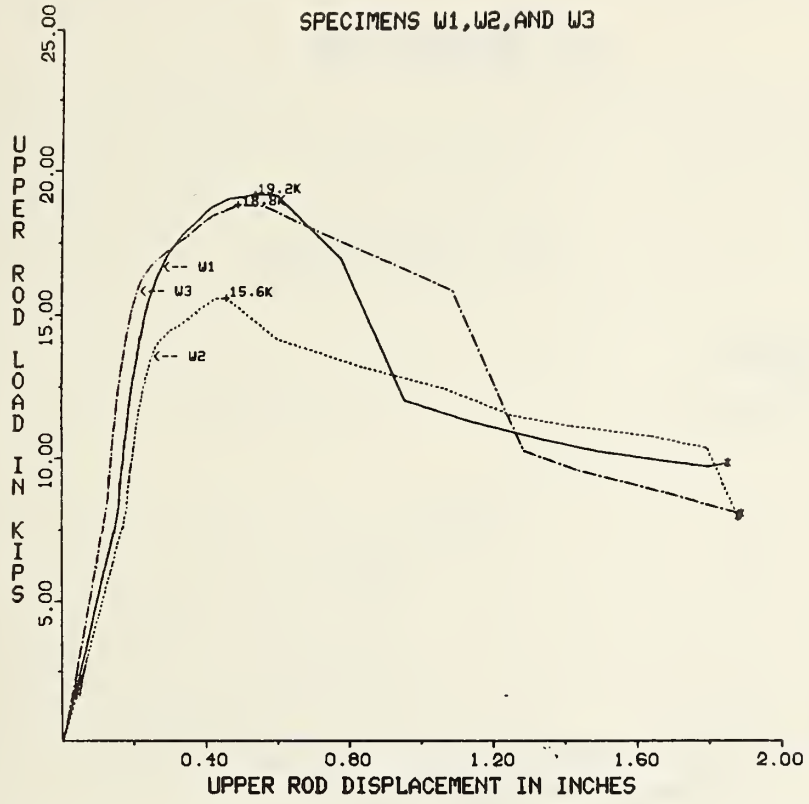

Figure A6.10-29 In-plane load vs displacement curves for specimens W1, W2, and W3.

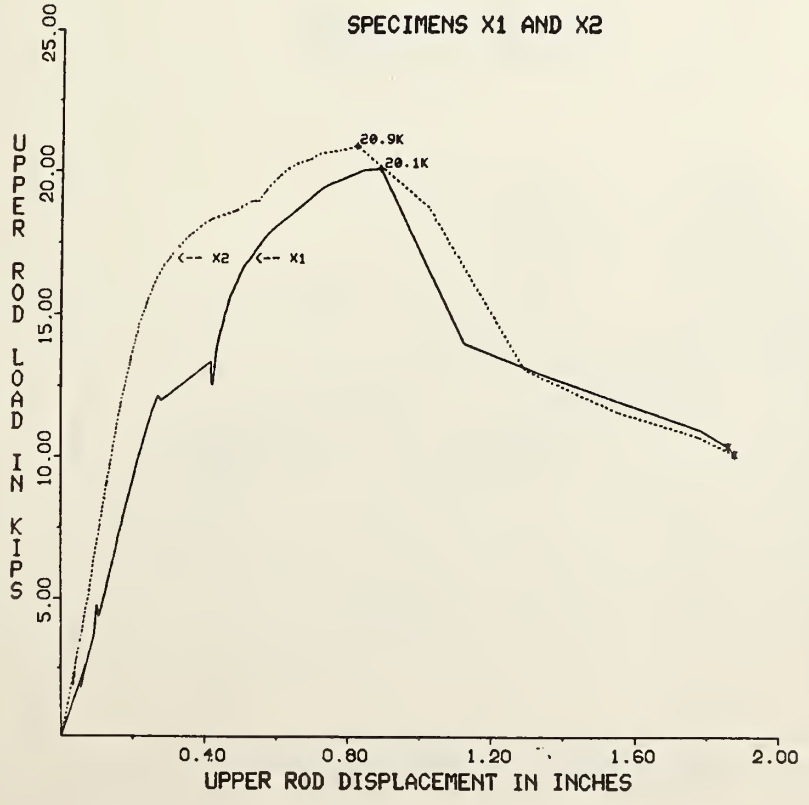

Figure A6.10-30 In-plane load vs displacement curves for specimens X1 and X2.

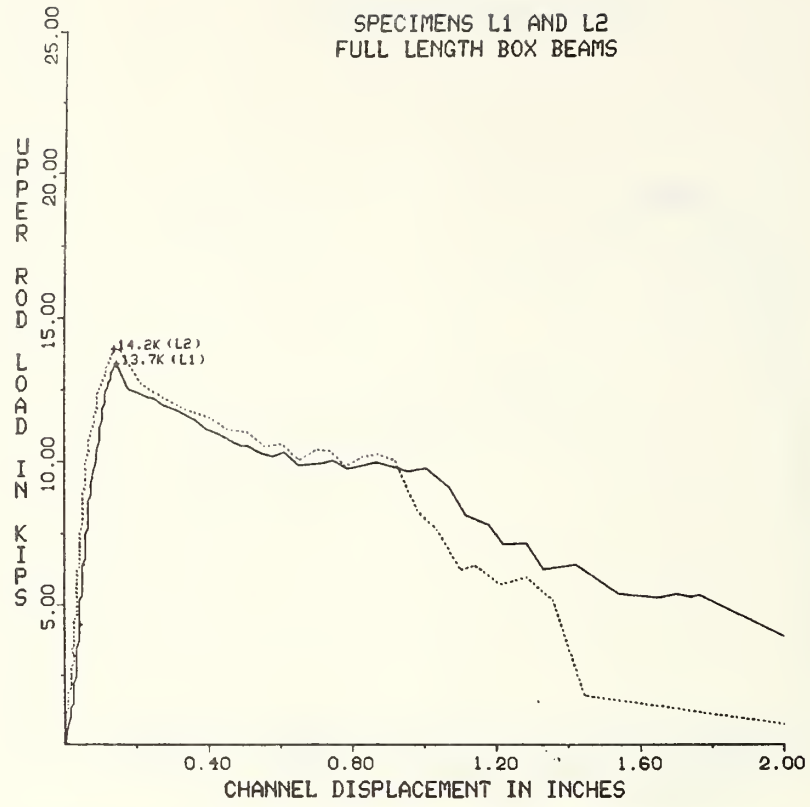

Figure A6.11-1 In-plane load vs deflection curves for specimens L1 and L2.

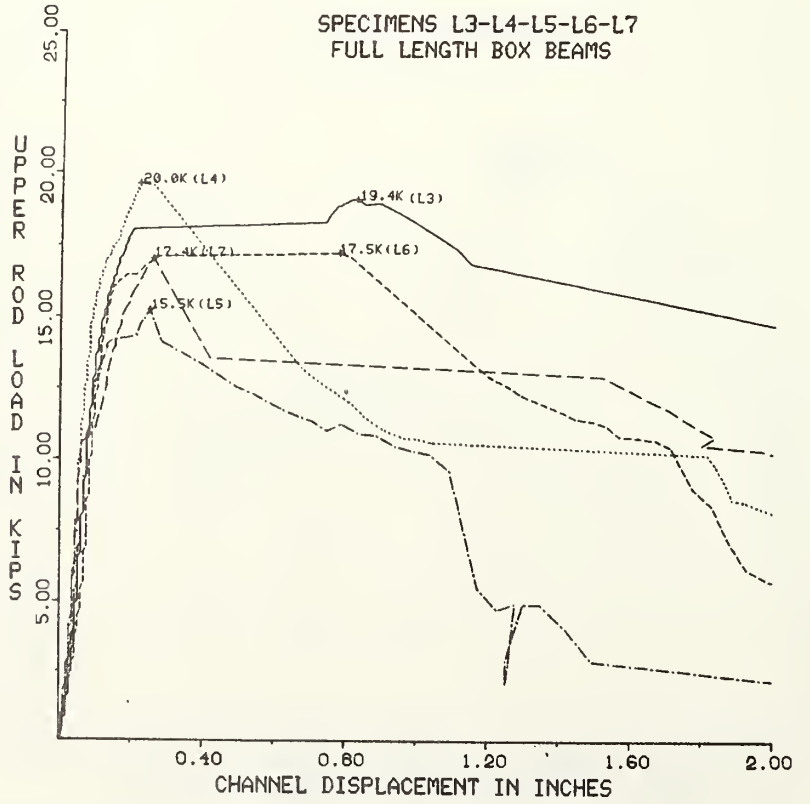

Figure A6.11-2 In-plane load vs deflection curves for specimens L3, L4, L5, L6, and L7

Sections A7.2 - A7.5

A7. NBS MATERIALS TESTING PROGRAM

A7.2 INITIAL INSPECTION

A7.2.2 Radiography

Radiographs of portions of box beam 9M used in the analysis described in section 7 of the report are produced in figure A7.2.2-1.

A7.3 MECHANICAL PROPERTIES OF STRUCTURAL STEEL AND WELDMENTS

A7.3.1 NBS Channel Specimens

Load-strain plots for tensile tests performed on NBS channel specimens are given in figures A7.3.1-1 to A7.3.1-3.

A7.3.2 Walkway Box Beams

Locations from which base metal tensile specimens were removed from box beams 9U, 8L and 9M are illustrated in figures A7.3.2-1 through A7.3.2-3. Load-strain plots for the tensile tests performed on walkway box beam specimens appear in figures A7.3.2-4 through A7.3.2-9.

A7.3.3 Walkway Hanger Rods

Locations from which tensile specimens were removed from hanger rods NBS 5A and 5B are illustrated in figure A7.3.3-1. Load-strain plots for the walkway hanger rod tests appear in figure A7.3.3-2.

A7.3.4 Walkway Box Beam Longitudinal Welds

Locations from which tensile specimens were removed from box beams 9U, 8L and 9M are illustrated in figures A7.3.2-1 through A7.3.2-3.

A7.4 METALLOGRAPHY AND HARDNESS MEASUREMENTS

A7.4.1 Box Beam Weldments

A "U" shaped transverse section through NBS weldment IC was examined for microstructure and hardness. Weldment IC was welded by the GMAW process using a mild steel electrode. The section examined, shown at low magnification in figure A7.4.1-1, included the welded flange region and part of the web region of each box beam channel. The section was metallographically polished and chemically etched to reveal the microstructure. The region of this section containing the weld is shown at higher magnification in figure A7.4.1-2. In this figure, the light region in the center represents weld metal; the darker regions on either side of the weld are the heat affected zones associated with the weld. The light regions at both sides of the figure, adjacent to the heat affected zones, are flange base metal.

Knoop microhardness measurements at a load of 500 grams force (HK_{500}) were made across the weld metal, across one of the heat affected zones, and into the base material on this same transverse section through NBS weldment IC. The indentations produced by the microhardness tests appear as a line of small, dark, elongated marks in figure A7.4.1-2. Approximately equivalent Rockwell B (HRB) hardness values, converted in accordance with ASTM E140-79 (Standard Hardness Conversion Tables for Metals) [7.1], are reported along with the HK_{500} values.

A representative region of the weld metal appears in figure A7.4.1-3. The microstructure consists primarily of bainite. Microhardness values based on 17 measurements average 205 HK_{500} (90.9 HRB) and range from 195 to 228 HK_{500} (88.5 to 95.5 HRB).

The transition region between the weld metal and the heat affected zone is shown in figure A7.4.1-4. Nothing unusual was observed at the transition. The microstructure within the heat affected zone is shown in figure A7.4.1-5. The microstructure consists of ferrite, primarily as a network in prior austenite grain boundaries, bainite, partially spheroidized carbides, and tempered martensite. Average hardness of the heat affected zone based on five measurements is 202 HK_{500} (90.2 HRB) with a range of 196 to 206 HK_{500} (89 to 91 HRB). Figure A7.4.1-6 shows the transition from the heat affected zone to the base material of the box beam. Hardness in this region averages 173 HK_{500} (83 HRB) and the hardness range is 167 to 177 HK_{500} (81 to 84 HRB).

A region representative of the base material away from the heat affected zone is shown in figure A7.4.1-7. The microstructure is relatively fine grained and consists primarily of ferrite (light) and pearlite (dark) in a normalized condition. Within the base material, the average hardness is 152 HK_{500} (75.4 HRB) and the range is 139 to 161 HK_{500} (70 to 70.9 HRB).

Two transverse sections similar to that described in the previous section on the NBS weldment were examined from each of the two box beam segments (9U and 8L) and the full length box beam (9M) obtained from the walkway debris. The locations of these sections in the box beams are indicated in figures A7.3.2-1 through A7.3.2-3. Each "U" shaped transverse section included the bottom of the beam (channel flanges and weld region) and parts of the web region of each box beam channel. To facilitate handling during metallographic preparation, parts of the channel web regions were removed from each section. The metallographic examination was concentrated in the remaining shorter "U" shaped sections, but hardness measurements were made both in the shortened sections and in the pieces that had been removed. The sections were polished metallographically and chemically etched to reveal microstructure. Knoop microhardness measurements at a load of 500 grams force (HK_{500}) were taken in the weld, heat affected zones, and adjacent base channel material of these sections. Rockwell B (HRB) hardness measurements were taken in the flange and web regions of each channel piece. Summaries of the hardness test results appear in tables A7.4.1-1 through A7.4.1-3 for sections from box beams 9U, 8L and 9M, respectively. Approximately equivalent Rockwell B (HRB) hardness values, converted in accordance with ASTM Standard E140-79, are reported along with the HK_{500} values.

The sections from box beam 9U (NBS 1), designated 1BM1 and 1BM2, are shown in figures A7.4.1-8 and A7.4.1-10, respectively. These two sections were separated by about 7 in (180 mm) as measured along the length of the beam. The weld regions of sections 1BM1 and 1BM2 are shown at higher magnification in figures A7.4.1-9 and A7.4.1-11, respectively. The depth of weld penetration is greater in section 1BM2 than in section 1BM1 and there is some misalignment of the channel flanges at the weld.

Representative regions of the weld metal from sections 1BM1 and 1BM2 are shown in figures A7.4.1-12 and A7.4.1-13, respectively. In both cases, the microstructure appears to consist of bainite. A number of inclusions are evident in section 1BM1. The average hardness of the weld in section 1BM1 (95 HRB) is slightly higher than in the weld of section 1BM2 (91 HRB) and the hardness range in the weld of section 1BM1 is greater.

There were some patches of hard material at the transition region from the weld material to the heat affected zone at both the north and south channels in section 1BM1. One such patch can be seen in figure A7.4.1-14. A similar region is shown at higher magnification in figure A7.4.1-15. The microstructure in this region appears to be fine-grained tempered martensite. Maximum hardness measured in these patches was 336 HK_{500} which is approximately equivalent to a Rockwell C hardness of 33. This value compares to a hardness of 241 HK_{500} (98 HRB) in an adjacent location of the transition region.

Hard patches were not observed in the transition region from weld to heat affected zone in section 1BM2. An area representative of this region in section 1BM2 is shown in figure A7.4.1-16.

Regions representative of the heat affected zones (HAZ) of sections 1BM1 and 1BM2 are shown in figures A7.4.1-17 and A7.4.1-18, respectively. In both cases, the microstructure appears to consist of ferrite, both as a network in prior austenite grain boundaries and as needles, bainite, partially spheroidized carbides, and tempered martensite. Hardness of the heat affected zones in section 1BM1 is somewhat greater at the south channel than at the north. At both heat affected zones, hardness decreased with distance from the weld. Hardness values in the heat affected zones of section 1BM2 were similar for both zones.

The transition regions from the heat affected zone to the base channel material appeared similar for both sections. A region representative of the transition zone in section 1BM2 is shown in figure A7.4.1-19.

Base material from both channel pieces appeared similar. A region representative of section 1BM1 is shown in figure A7.4.1-20. The microstructure consists primarily of ferrite (light) and pearlite (dark) in a normalized condition. Rockwell B hardness measurements made on both sections indicated no significant differences in hardness between the two channel pieces used to fabricate the box beam. Regions of the channel adjacent to the heat affected zones and in the web region about 0.6 to 1 in (15 to 25 mm) from the bottom of the beam were harder than elsewhere with HRB hardness averaging 81.5. The hardness of the

channel material elsewhere in the sections averaged 74.4 HRB for section 1BM1 and 74.3 HRB for section 1BM2.

The transverse sections examined from box beam 8L (NBS 2), designated 2BM1 and 2BM2, are shown in figures A7.4.1-21 and A7.4.1-23, respectively. These sections were separated by about 7 1/2 in (190 mm) as measured along the length of the beam. The regions of sections 2BM1 and 2BM2 containing the weld are shown at higher magnification in figures A7.4.1-22 and A7.4.1-24, respectively. There appears to be minor undercutting at the weld in section 2BM2 and the heat affected zone is somewhat narrower than in section 2BM1. In section 2BM1 there is a void at the base of the weldment adjacent to the gap between the channel flanges.

Regions representative of the weld metal in sections 2BM1 and 2BM2 are shown in figures A7.4.1-25 and A7.4.1-26, respectively. Overall, the microstructure in both cases appeared similar and consisted primarily of bainite. Inclusions are evident in both sections. The average hardness values for weld metal in the two sections do not differ significantly.

The transition from weld to the heat affected zone for section 2BM1 is shown in figure A7.4.1-27. There are no unusual features.

As was the case in section 1BM1 from box beam 9U, there were some hard spots at the transition from weld to the heat affected zone in section 2BM2 on the south side. The transition in section 2BM2 is shown in figure A7.4.1-28 at 200 magnifications. One of the hard regions is shown at much higher magnification (X1200) in figure A7.4.1-29. The microstructure of this region appears to be tempered martensite. The highest hardness value obtained in this region was 298 HK_{500} which is approximately equivalent to 28 Rockwell C. Away from the hard regions, hardness averaged 247 HK_{500} (99 HRB).

In the heat affected zones, the microstructure was similar in both sections 2BM1 and 2BM2. A representative region from section 2BM1 is shown in figure A7.4.1-30. The microstructure appears to consist of ferrite, both as a network in prior austenite grain boundaries and as needles, bainite, partially spheroidized carbides and tempered martensite. Hardness was 5 to 6 HRB points lower for the heat affected zones in section 2BM2 than in the weld metal. In section 2BM1, hardness was similar for both weld metal and the heat affected zone.

The transition regions from the heat affected zones to base channel material appeared similar for both sections. A region representative of this transition in section 2BM1 is shown in figure A7.4.1-31. A region representative of the base channel material in both sections is shown for section 2BM1 in figure A7.4.1-32. The microstructure of the channel material consists primarily of ferrite and pearlite in a normalized condition.

There were no significant differences in hardness between the two channel sections. As in the case of the section from box beam 9U, the channel material was somewhat harder adjacent to the heat affected zones and in the web about 0.6 to 1 in (15 to 25 mm) from the flange base than elsewhere.

The sections examined for microstructure and hardness from box beam 9M (NBS 3) are designated 3BM1 and 3BM2 and are shown in figures A7.4.1-33 and A7.4.1-35, respectively. These two sections were separated by about 7 1/2 in (190 mm) as measured along the length of the beam. The weld regions of sections 3BM1 and 3BM2 are shown at higher magnification in figures A7.4.1-34 and A7.4.1-36, respectively. The weld configuration differs considerably between the two sections. In section 3BM1, the heat affected zones penetrate to a point slightly greater than half the flange thickness, whereas the heat affected zones in section 3BM2 penetrate all the way through the flange.

Representative regions of the weld from sections 3BM1 and 3BM2 are shown in figures A7.4.1-37 and A7.4.1-38, respectively. In both cases, the microstructure appears to consist primarily of bainite. More inclusions are evident in section 3BM1 than in section 3BM2. The average hardness of the weld was essentially the same for both sections, being somewhat lower than that of the welds at the sections from the other two walkway box beams.

Nothing unusual was observed at the transition from the weld to the heat affected zones in either section. None of the harder regions found in the transition regions of sections 1BM1 and 2BM2 were in evidence. A region representative of these transition regions in section 3BM2 is shown in figure A7.4.1-39.

The microstructure and hardness of the heat affected zones in both section 3BM1 and 3BM2 were similar. In both cases, the microstructure consists of ferrite both as a network in prior austenite grain boundaries and as needles, bainite, partially spheroidized carbides and some tempered martensite. Hardness in the heat affected zones was similar to that of the weld. A region representative of the heat affected zone in section 3BM1 is shown in figure A7.4.1-40.

The transition from the heat affected zone to the base channel material appeared similar in both sections. A region representative of the transition zone in section 3BM2 is shown in figure A7.4.1-41.

The base material of both channel pieces of the box beam appeared similar in microstructure in both sections 3BM1 and 3BM2. In both cases, the microstructure consists of ferrite and pearlite in a normalized condition. A region representative of the channel material is shown in figure A7.4.1-42. Hardness of both channels was also similar.

In summary, the walkway and NBS box beam structural steel weldment microstructure and hardness are comparable and normal.

A7.4.2 Walkway Hanger Rods

Transverse and longitudinal sections from each of the walkway hanger rod segments obtained from the debris (NBS 5A and 5B) were examined metallographically. The locations of these sections in the hanger rods are shown in figure A7.3.3-1. A representative region showing the etched microstructure of the transverse section from hanger rod NBS 5A is shown in figure A7.4.2-1. The

microstructure consists of ferrite (light) and pearlite (dark) in a reasonably fine grained (ASTM grain size 9) normalized structure.

The representative microstructure of the transverse section from hanger rod NBS 5B is shown in figure A7.4.2-2. The microstructure again consists of ferrite (light) and pearlite (dark) in the normalized condition. This microstructure is coarser (ASTM grain size 7-1/2 to 8) than that of hanger rod NBS 5A, and there appears to be more pearlite present than in hanger rod NBS 5A.

Longitudinal sections through each hanger rod segment revealed the material of both to be fully normalized with equiaxed grains. Regions representative of the longitudinal microstructures are shown in figure A7.4.2-3 for rod segment NBS 5A and in figure A7.4.2-4 for rod segment NBS 5B.

Rockwell B (HRB) hardness measurements were made on each of the transverse sections examined for microstructure. Twelve measurements were made on each section. The average hardness value for the finer grained hanger rod NBS 5A material was HRB 74.5 with a range of HRB 72-76. The average hardness value for hanger rod NBS 5B material was HRB 68.5 with a range of HRB 66 to 71.5. In the section from hanger rod NBS 5B, there was a slight hardness gradient with hardness decreasing from the outside toward the center.

A7.4.3 Washers

Hardness measurements were made on NBS washers and on washers obtained from the walkway debris. A metallographic examination was performed on sections through a hanger rod washer obtained from the walkway debris at location 9MW and through one of the NBS hardened washers.

Rockwell C (HRC) hardness measurements were made on the surfaces of four washers obtained from the walkway debris. The results of these measurements are given in table A7.4.3-1. It is apparent from these results that the washers obtained from the walkway were hardened washers.

Rockwell C hardness measurements were made on the surface of one NBS hard washer, and Rockwell B (HRB) hardness measurements were made on the surface of one unplated regular grade washer. The results of these measurements are also given in table A7.4.3-1.

Knoop microhardness measurements at a load of 500 grams force (HK_{500}) were made on a cross section through a washer from the walkway debris at location 9MW after it had been used in an NBS full length test on box beam 9M. During the test, the washer fractured into five pieces. A microhardness traverse was made through the thickness of the washer on the section examined. The washer thickness was approximately 0.075 in (1.80 mm). Average hardness from 16 measurements across the section was 459 HK_{500} which is approximately equivalent to 44.3 HRC and the hardness range was 422 to 514 HK_{500} (41.5 to 48.5 HRC). The highest values were near the center of the section and the lowest values were near the surface of the washer. The microstructure of the washer from location 9MW is shown in figure A7.4.3-1. There is a very small apparent decarburized

layer at the surface (light area at the top in the figure). Tempered martensite is the primary constituent of the microstructure.

A similar microhardness traverse on a section through one of the NBS hard washers was made. Hardness values in this section, excluding the decarburized layer at the surface, averaged 431 HK_{500} (42.5 HRC) and ranged from 401 to 422 HK_{500} (40 to 43.5 HRC). Measured hardness in the decarburized layer was as low as 247 HK_{500} (99 HRB). The microstructure of the NBS hard washer is shown in figure A7.4.3-2. The decarburized layer at the surface appears light in the figure. Tempered martensite is the primary constituent in the microstructure.

A7.5 CHEMICAL ANALYSIS

Five specimens from the walkway box beam longitudinal welds (four exterior welds and one interior tack weld) and weld specimens from four NBS box beam replicas were analyzed for chemical composition by emission spectrometry. Also analyzed for chemical composition were two samples of hanger rod material removed from the walkway debris.

A 3/4 mm vacuum spectrometer with an adjustable waveform excitation source was used for the analysis. The instrumental analytical curves were constructed using NBS SRMs 1261, 1262, 1263, 1264 and 1265 plus other selected reference materials. All specimens were surfaced using 50 grit Al_2O_3 sanding disks. In order to confine the analytical discharge to the weld area, a boron nitride disk with a 0.157 in (4 mm) opening was used in the excitation stand.

The specimen identification numbers and origins are listed in table A7.5-1. Actual locations of specimens within the walkway box beam and hanger rod segments are described in figures A7.3.2-1 through A7.3.2-3 and in figure A7.3.3-1. Normal laboratory routines used for SRM homogeneity testing were used in the analysis. Program outputs included averages, standard deviations and a pictorial presentation (box plots) of the individual values for those elements normally considered the most important in ferrous analysis. Each value reported in the tables of this section is an average of four exposures.

A7.5.1 Box Beam Longitudinal Welds

Results of the analysis of longitudinal weld specimens obtained from segments of the walkway box beams are listed in table A7.5.1-1. In table A7.5.1-2, the results obtained from the four weld specimens removed from NBS box beam replicas are presented. In each case the tables include analytical values for the base metal in the flange on either side of the longitudinal weld seam.

It is concluded that of the four NBS weld specimens analysed, specimen M2 (flux cored electrode) most closely corresponds to the weld material in the walkway box beam longitudinal welds. This is based primarily on the comparable values for manganese, silicon and titanium. While this comparison does not rule out the possibility of other types of electrodes being used in the fabrication of the walkway box beams, it is in agreement with information provided by the

fabricator's legal counsel regarding welding procedure as noted in chapter 6 of this report.

A7.5.2 Walkway Box Beam Interior Tack Weld

Results of the analysis of the interior tack weld specimen removed from box beam 8L (NBS 2) are listed in table A7.5.2-1. The analysis of this weld is comparable to the four walkway box beam welds discussed in section A7.5.1, and it is concluded that exterior and interior welds were made using the same type of electrode.

A7.5.3 Walkway Hanger Rod Specimens

The chemical analysis of two hanger rod specimens (one specimen from each of two segments designated NBS 5A and NBS 5B) is presented in table A7.5.3-1. The analysis clearly shows that the two hanger rod segments are from different heats since nine elements have significantly different concentrations. In addition, the sulfur value in specimen 5AC (NBS 5A) shows this element at or just above the limit specified for ASTM Grade A36 steel. Further analysis of this material by a gasometric method showed the sulfur value to be within specification with levels of 0.046 ± 0.001 for rod 5A and 0.033 ± 0.001 for rod 5B as reported in table A7.5.3-1.

Table A7.4.1-1 Hardness Test Results from Transverse Sections Through Box Beam 9U (NBS 1)

HK_{500} (HRB) Hardness Numbers

Region of Section	Section 1BM1			Section 1BM2		
	Number of Measurements	Average	Range	Number of Measurements	Average	Range
Weld Metal	10	227(95.2)	200-246(90-98)	13	208(91.2)	201-222(90-94
Transition Zone Between Weld & HAZ, South Side						
Hard Spot	3	324[31.5](a)	306-336[29-33](a)			
Away from Hard Spot	1	238(97.5)				
HAZ						
South	8	219(93.7)	200-241(90-98)	3	196(88.6)	189-204(87-90
North	5	193(88.3)	179-201(85-90)	2	199(89.5)	198-200(89-90
Channel Adjacent to HAZ						
South	5	174(85)	173-176(83-84)	4	172(82.5)	167-174(81-83
North	4	183(83.7)	173-191(83-88)	5	178(84.4)	171-186(82-86
Direct HRB Measurements Flange adjacent to HAZ and web about 0.6 to 1 in from base of flange	5	81	80-83	4	82.1	81.5-83
Elsewhere in flange and web						
South	22	74.5	72-77.5	21	75.1	73-79.5
North	21	74.3	72-76	21	73.4	70.5-77

(a) Values in brackets are HRC hardness numbers

1 in = 25.4 mm

Table A7.4.1-2 Hardness Test Results from Transverse Sections Through Box Beam 8L (NBS 2)

HK_{500} (HRB) Hardness Numbers

Region of Section	Section 2BM1			Section 2BM2		
	Number of Measurements	Average	Range	Number of Measurements	Average	Range
Weld Metal	12	210(91.8)	199-230(89.5-96)	8	223(94.3)	211-234(92-96.5
Transition Zone Between Weld & HAZ, South Side						
Hard Spot				1	298[28][a]	
Away from Hard Spot				2	247(99)	241-253(98-100)
HAZ						
South	2	209(91.8)	205-213(91-92.5)	3	208(89)	196-227(89-95)
North	4	196(88.8)	177-212(84-92)	2	194(88.5)	187-201(87-90)
Channel Adjacent to HAZ						
South	5	178(84.4)	173-188(83-87)	5	171(82)	161-191(79-88)
North	5	167(81.1)	156-180(77.5-85)	4	166(80.5)	158-180(78-85)
Direct HRB Measurements Flange adjacent to HAZ and web about 0.6 to 1 in from base of flange	8	81.1	79.5-82.5	5	81.9	80.5-84
Elsewhere in flange and web						
South	23	75.3	73-79	24	75.3	73.5-79
North	21	74.2	70.5-76	22	75.5	73.5-79

(a) Values in brackets are HRC hardness numbers

1 in = 25.4 mm

Table A7.4.1-3 Hardness Test Results from Transverse Sections Through Box Beam 9M (NBS 3)

HK_{500} (HRB) Hardness Numbers

Region of Section	Section 3BM1			Section 3BM2		
	Number of Measurements	Average	Range	Number of Measurements	Average	Range
Weld Metal	21	188(87)	162-210(79-92)	17	190(87.2)	153-203(76-90.5
HAZ North	7	191(87.6)	174-201(83-90)			
HAZ South				12	186(86.5)	171-201(82-90)
Channel Adjacent to HAZ, North	4	173(82.6)	162-180(79-85)			
Channel Adjacent to HAZ, South				6	170(81.9)	159-173(78-83)
Direct HRB Measurements Flange adjacent to HAZ and web about 0.6 to 1 in from base of flange	5	79.6	78-82	3	80.7	79-82
Elsewhere in flange and web	22	74.4	73-77.5	22	73.3	70-76

1 in = 25.4 mm

Table A7.4.4-1 Results of Washer Hardness Tests

Washer Identification	Number of Measurements	Hardness			
		HRC		HRB	
		Average	Range	Average	Range
8UE Top	8	40.2	39.0-41.0		
8LW Top	8	43.0	40.0-45.0		
9ME Top	8	37.5	34.5-40.5		
9MW Top	8	44.0	42.5-45.0		
NBS Hardened	5	39.6	38.5-41.9		
NBS Regular Grade	5			60.7	58.9-61.3

Table A7.5-1 Origin of Specimens Analyzed for Chemical Composition

Specimen Identification	Origin
1BX4	Bottom flange of walkway box beam 9U (NBS 1)
2BX1	Bottom flange of walkway box beam 8L (NBS 2)
3BX1	Bottom flange of walkway box beam 9M (NBS 3)
2TFX4	Top flange of walkway box beam 9M (NBS 3)
B2	NBS box beam replica B2. E7018 electrode
C3	NBS box beam replica C3. E7014 electrode
M2	NBS box beam replica M2. Flux cored electrode
N6	NBS box beam replica N6. Mild steel electrode
2C	Interior tack weld, bottom flange, walkway box beam 8L (NBS 2)
5AC	Fourth floor to ceiling walkway hanger rod 8E (NBS 5A)
5AB	Second to fourth floor walkway hanger rod (NBS 5B)

Table A7.5.1-1 Chemical Analysis of Walkway Box Beam Longitudinal Welds

Analytical Values--Percent by Weight

Element	Specimen Identification Number											
	1BX4			2BX1			3BX1			2TFX4		
	base	weld	base	base	weld	base	base	weld	base	base	weld	base
Carbon	.181	.121	.185	.183	.117	.185	.184	.169	.185	.180	.131	.188
	.187	.123	.184	.186	.118	.183	.183	.140	.188	.181	.121	.184
Phosphorus	.017	.012	.016	.017	.012	.016	.016	.013	.016	.016	.012	.017
	.017	.011	.017	.017	.012	.017	.017	.011	.018	.017	.013	.017
Sulfur	.016	.019	.016	.016	.020	.017	.016	.021	.016	.016	.017	.016
	.016	.019	.016	.016	.019	.015	.016	.019	.016	.015	.017	.016
Manganese	.672	.946	.726	.707	.992	.715	.727	1.061	.671	.703	1.013	.721
	.699	.991	.764	.741	1.028	.748	.764	1.118	.710	.740	1.143	.749
Silicon	.181	.370	.191	.194	.413	.196	.191	.480	.179	.191	.413	.197
	.183	.382	.196	.197	.415	.199	.196	.465	.187	.199	.480	.201
Nickel	.010	.009	.010	.010	.009	.010	.010	.009	.010	.010	.009	.010
	.011	.010	.011	.011	.009	.011	.011	.010	.011	.011	.009	.011
Chromium	.017	.020	.018	.017	.020	.018	.018	.021	.018	.018	.021	.018
	.019	.021	.019	.020	.021	.019	.019	.023	.019	.019	.023	.019
Vanadium	.002	.005	.002	.002	.005	.002	.002	.006	.002	.002	.005	.002
	.002	.005	.003	.002	.006	.002	.002	.006	.002	.002	.006	.002
Titanium	.001	.010	.001	.001	.011	.001	.001	.012	.001	.001	.011	.001
	.001	.010	.001	.001	.011	.001	.001	.012	.001	.001	.014	.001
Molybdenum	.006	.005	.006	.006	.005	.006	.006	.007	.006	.006	.005	.006
	.006	.005	.006	.006	.005	.006	.006	.005	.006	.006	.005	.006
Copper	.012	.017	.012	.013	.015	.012	.012	.013	.012	.011	.014	.013
	.013	.016	.013	.013	.015	.012	.013	.015	.013	.013	.020	.016
Cobalt	.006	.005	.006	.006	.005	.006	.006	.007	.006	.005	.004	.006
	.005	.004	.005	.005	.004	.005	.005	.005	.005	.005	.005	.005
Aluminum	.001	<.001	.001	.001	<.001	.001	.001	.001	<.001	.001	<.001	.001
	<.001	<.001	.001	.001	<.001	<.001	.001	<.001	<.001	.001	.001	.001
Niobium	<.001	.002	.001	<.001	.002	.001	.001	.001	<.001	<.001	.002	.001
	.001	.003	.001	.001	.003	.001	.001	.003	.002	.001	.003	.001
Zirconium	.001	.002	.001	.001	.001	.001	.001	.001	.001	.001	.001	.001
	.001	.002	.001	.001	.002	.001	.001	.002	.001	.001	.002	.001

Table A7.5.1-2 Chemical Analysis of NBS Box Beam Longitudinal Welds

Analytical Values--Percent by Weight

Element	Specimen Identification Number											
	B2			C3			M2			N6		
	base	weld	base	base	weld	base	base	weld	base	base	weld	base
Carbon	.181	.093	.182	.182	.119	.183	.179	.124	.181	.182	.123	.182
	.181	.097	.183	.180	.117	.181	.179	.123	.178	.180	.123	.180
Phosphorus	.012	.011	.012	.013	.014	.012	.012	.008	.012	.012	.011	.012
	.013	.009	.013	.013	.014	.013	.013	.008	.012	.013	.010	.011
Sulfur	.022	.022	.023	.023	.024	.022	.022	.021	.022	.023	.023	.023
	.022	.022	.023	.023	.024	.022	.023	.021	.021	.022	.023	.022
Manganese	.782	.588	.784	.786	.426	.780	.777	1.109	.782	.789	.590	.787
	.806	.615	.813	.810	.443	.812	.809	1.178	.810	.806	.647	.806
Silicon	.208	.266	.207	.209	.270	.207	.210	.437	.212	.214	.193	.212
	.210	.249	.210	.210	.272	.210	.215	.450	.213	.214	.210	.213
Nickel	.010	.010	.010	.010	.039	.010	.010	.011	.010	.010	.010	.011
	.011	.011	.011	.011	.040	.011	.011	.011	.011	.011	.010	.011
Chromium	.040	.030	.041	.040	.030	.040	.040	.035	.039	.040	.028	.041
	.041	.032	.043	.043	.032	.042	.041	.037	.042	.041	.032	.041
Vanadium	.001	.007	.001	.001	.005	.001	.001	.004	.001	.001	.001	.001
	.001	.007	.002	.002	.006	.002	.001	.005	.001	.001	.001	.001
Titanium	.001	.005	.001	.001	.013	.001	.001	.010	.001	.001	.001	.001
	.001	.005	.001	.001	.014	.001	.001	.011	.001	.001	.001	.001
Molybdenum	.005	.005	.005	.005	.005	.005	.005	.005	.005	.005	.004	.005
	.005	.005	.005	.005	.005	.005	.005	.004	.005	.004	.004	.005
Copper	.010	.009	.010	.010	.010	.010	.010	.013	.010	.010	.098	.011
	.013	.011	.012	.010	.014	.011	.010	.014	.011	.010	.091	.011
Cobalt	.004	.004	.003	.004	.006	.003	.003	.004	.003	.004	.004	.004
	.003	.003	.003	.003	.006	.003	.003	.003	.003	.003	.003	.003
Aluminum	.006	.001	.007	.006	.001	.006	.007	.002	.007	.006	.001	.007
	.006	.001	.006	.006	.001	.006	.006	.002	.006	.006	.002	.008
Niobium	.001	.001	.001	.001	.004	.001	.001	.003	.001	.001	.001	.001
	.001	.002	.002	.002	.005	.002	.001	.004	.002	.001	.002	.002
Zirconium	.001	.001	.001	.001	.001	.001	.001	.002	.001	.001	.001	.001
	.001	.001	.001	.001	.002	.001	.001	.002	.001	.001	.002	.001

Table A7.5.2-1 Chemical Analysis of Walkway Box Beam Interior Tack Weld

Analytical Values--Percent by Weight

Specimen Identification Number

Element	2C		
	base	weld	base
Carbon	.184	.091	.184
	.184	.095	.181
Phosphorus	.017	.012	.016
	.018	.013	.017
Sulfur	.016	.018	.015
	.017	.018	.015
Manganese	.711	1.096	.719
	.722	1.086	.722
Silicon	.193	.452	.198
	.195	.442	.197
Nickel	.011	.010	.010
	.011	.009	.010
Chromium	.018	.023	.018
	.018	.021	.018
Vanadium	.002	.006	.002
	.002	.006	.002
Titanium	.001	.014	.001
	.001	.014	.001
Molybdenum	.005	.004	.005
	.005	.004	.005
Copper	.012	.016	.012
	.012	.016	.013
Cobalt	.005	.004	.005
	.005	.005	.005
Aluminum	.001	.001	.001
	.001	.001	.001
Niobium	.001	.003	.001
	.001	.003	.001
Zirconium	.001	.002	.001
	.001	.001	.001

Table A7.5.3-1 Chemical Analysis of Walkway Hanger Rod Specimens

Analytical Values--Percent by Weight

Specimen Identification Number

Element	5AC	5BC	5AX1*	5BX*
Carbon	.168 .168	.200 .197	.159	.200
Phosphorus	.037 .038	.010 .009		
Sulfur	.050 .052	.035 .035	.046	.033
Manganese	.510 .527	.672 .696		
Silicon	.187 .185	.038 .039		
Nickel	.094 .098	.053 .055		
Chromium	.106 .110	.115 .117		
Vanadium	.001 .001	.001 .001		
Titanium	.001 .001	.002 .002		
Molybdenum	.009 .009	.009 .009		
Copper	.330 .338	.112 .114		
Cobalt	.008 .008	.007 .007		
Aluminum	.001 .001	.003 .005		
Niobium	.001 .002	.001 .001		
Zirconium	.001 .002	.001 .001		

* Gasometric method

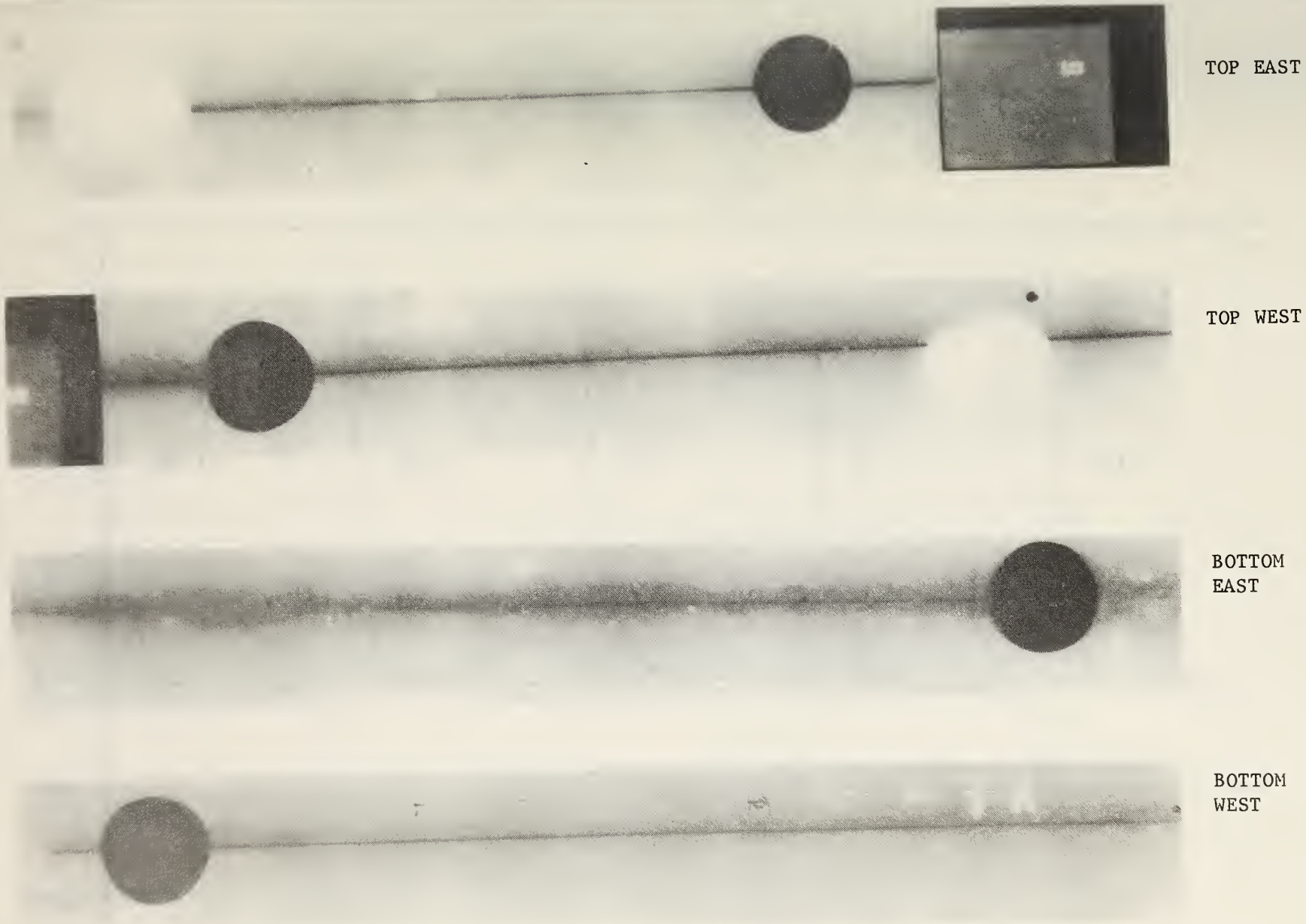

Figure A7.2.2-1 Radiographs of portions of box beam 9M used in the analysis described in section 7.2 of the report.

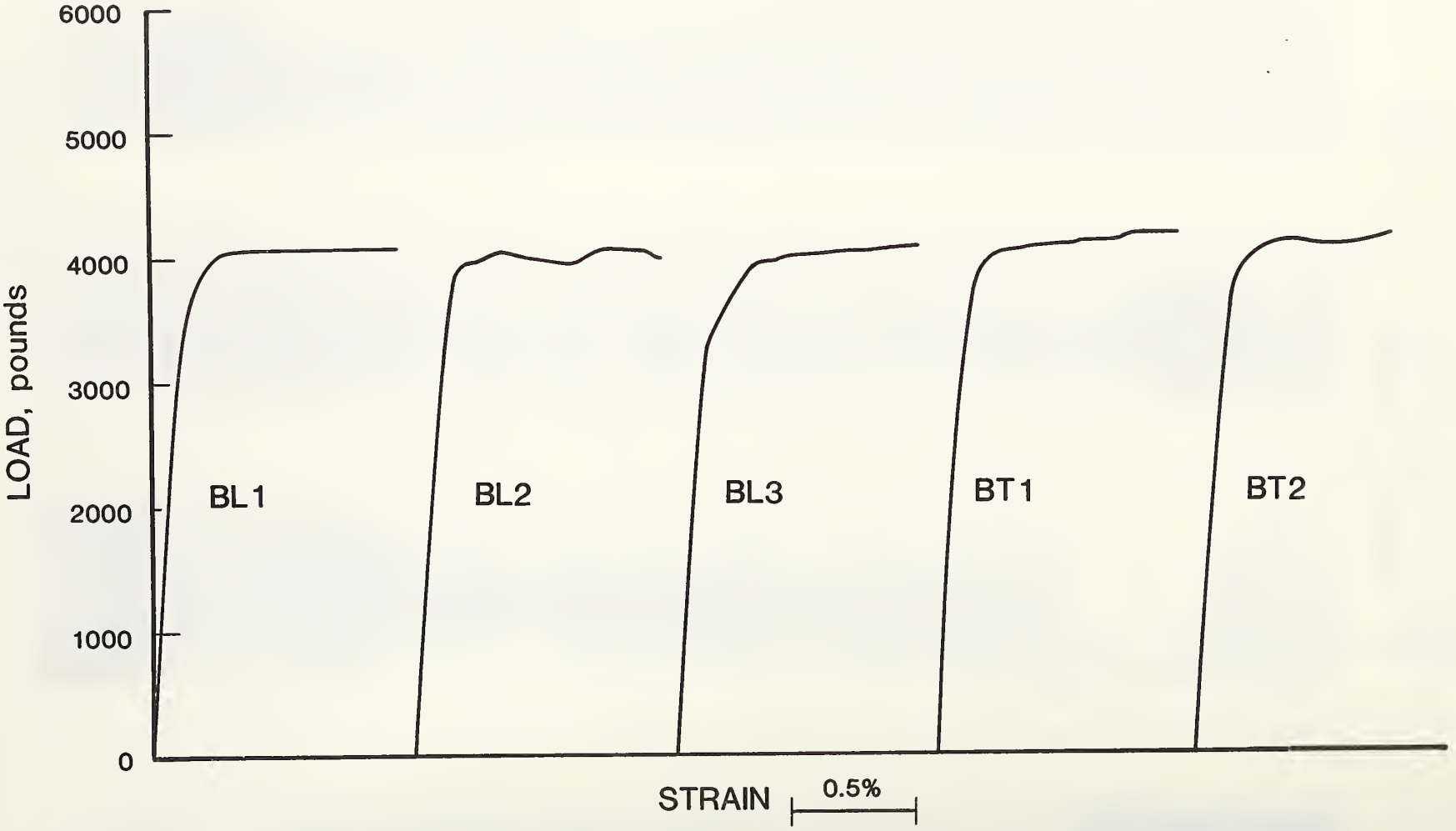

Figure A7.3.1-1 Load-strain plots for NBS channel specimens BL1, BL2, BL3, BT1, BT2.

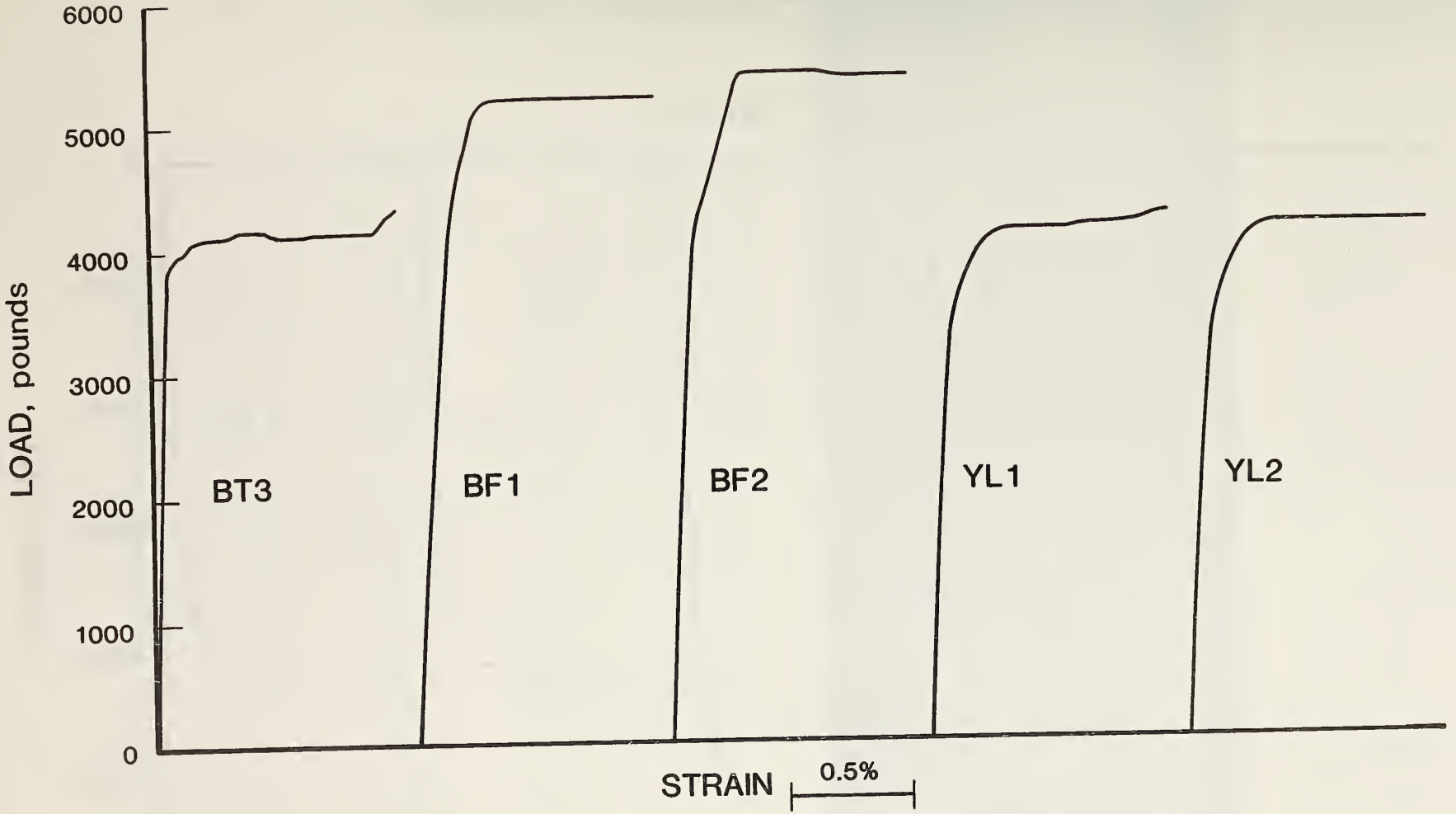

Figure A7.3.1-2 Load-strain plots for NBS channel specimens BT3, BF1, BF2, YL1, YL2.

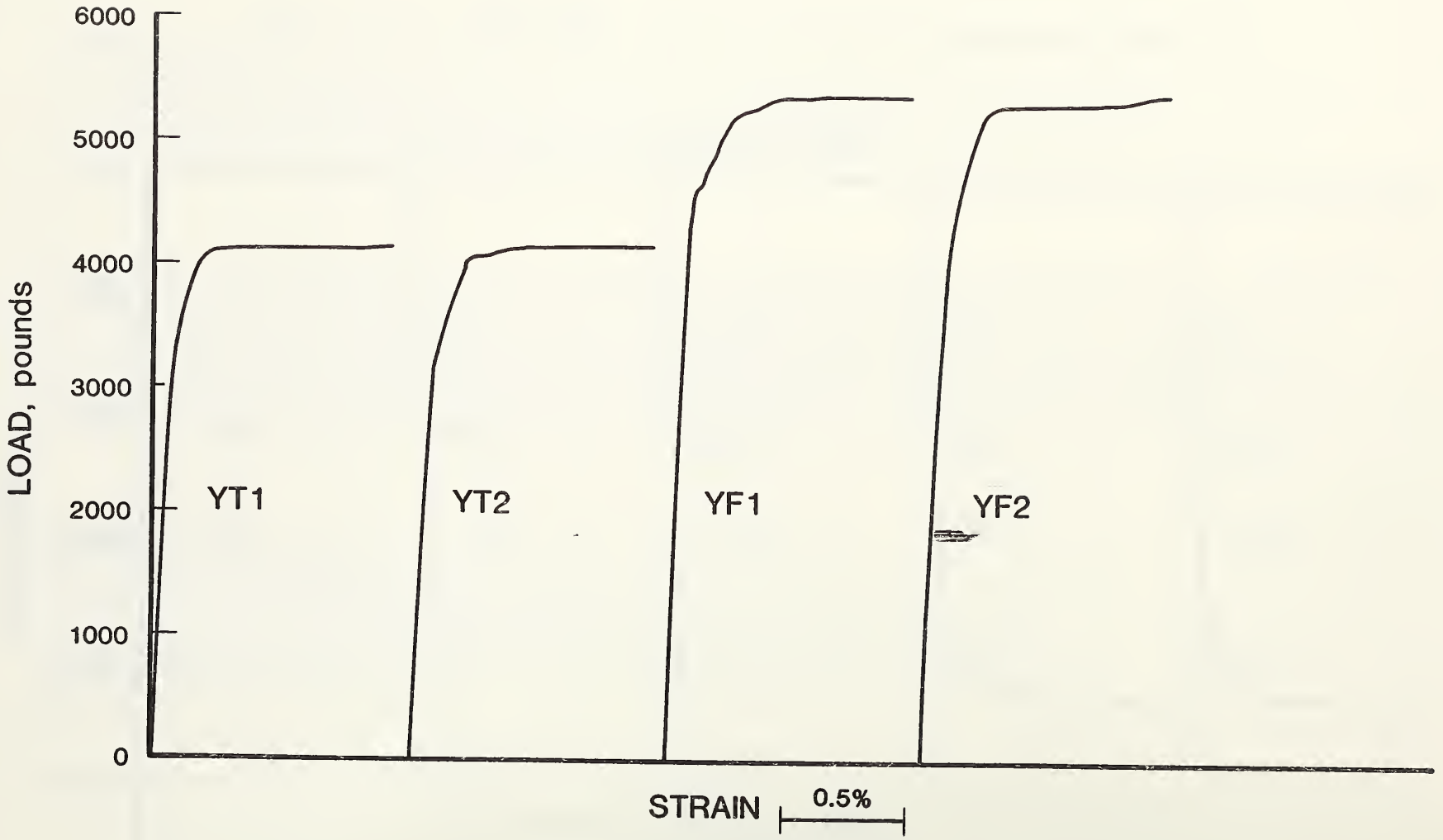

Figure A7.3.1-3 Load-strain plots for NBS channel specimens YT1, YT2, YF1, YF2.

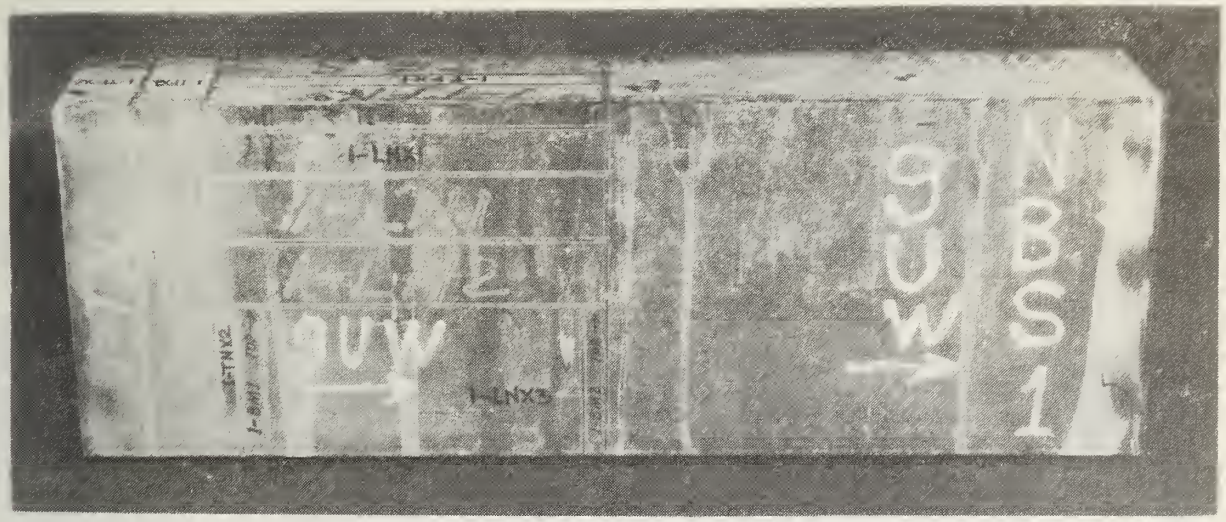

a. North face of box beam segment 9U (NBS 1).

Figure A7.3.2-1 Location of test specimens from box beam segment 9U obtained from the walkway debris.

a. North face:
   Longitudinal web tensile test specimens 1-LN1, 1-LN2
   Transverse web tensile test specimens 1-TN1, 1-TN2
   Parts of metallographic specimens 1-BM1, 1-BM2

b. Bottom:
   Parts of metallographic specimens 1-BM1, 1-BM2
   Transverse tensile test specimens across the weld 1-BX3W2, 1-BX3W4
   Chemical analysis specimen 1-BX4

c. South face:
   Longitudinal web tensile test specimens 1-LS1, 1-LS2
   Transverse web tensile test specimens 1-TS1, 1-TS2
   Parts of metallographic specimens 1-BM1, 1-BM2

d. Top:
   Longitudinal flange tensile test specimens 1-TFN, 1-TFS

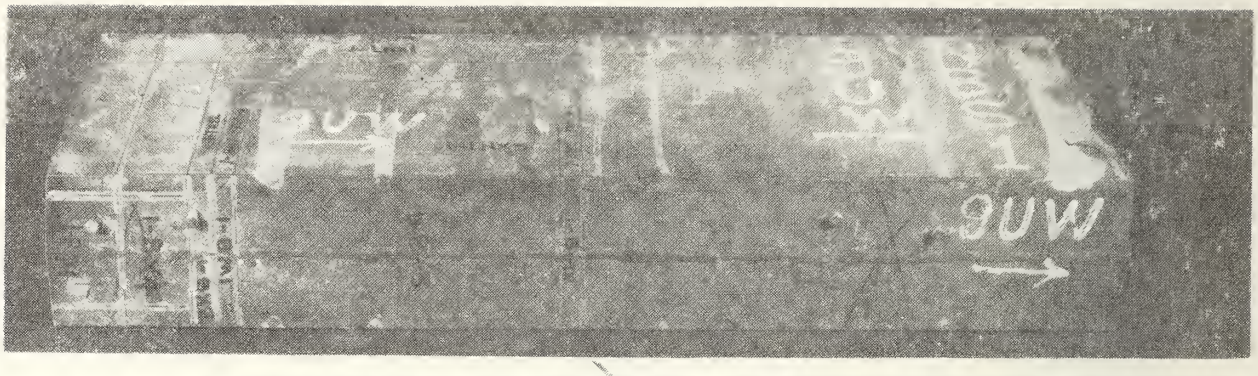

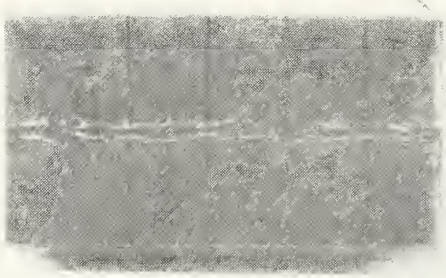

b. Bottom of box beam segment 9U (NBS 1).

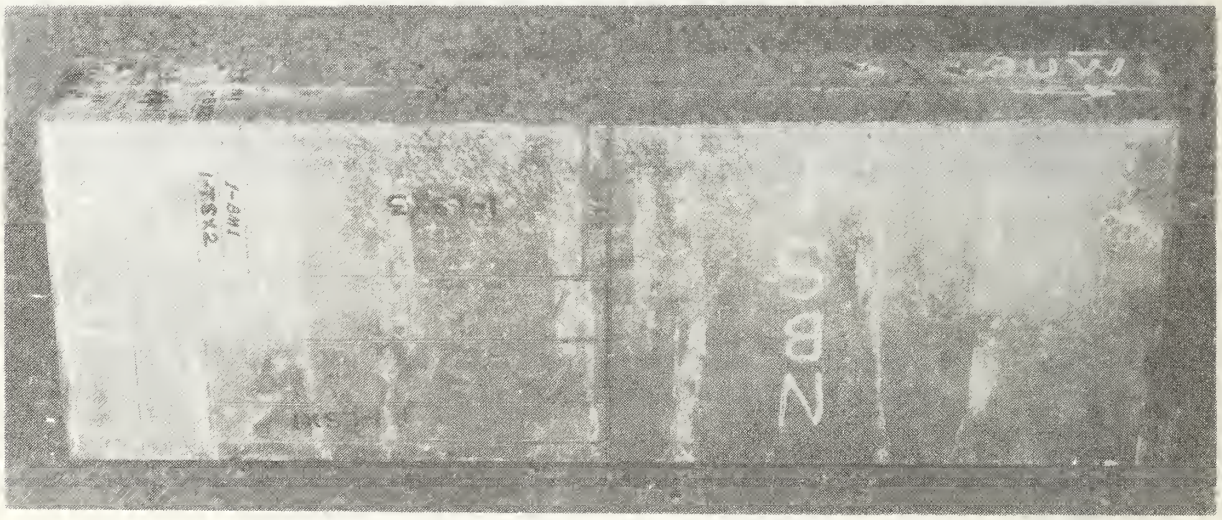

c. South face of box beam segment 9U (NBS 1).

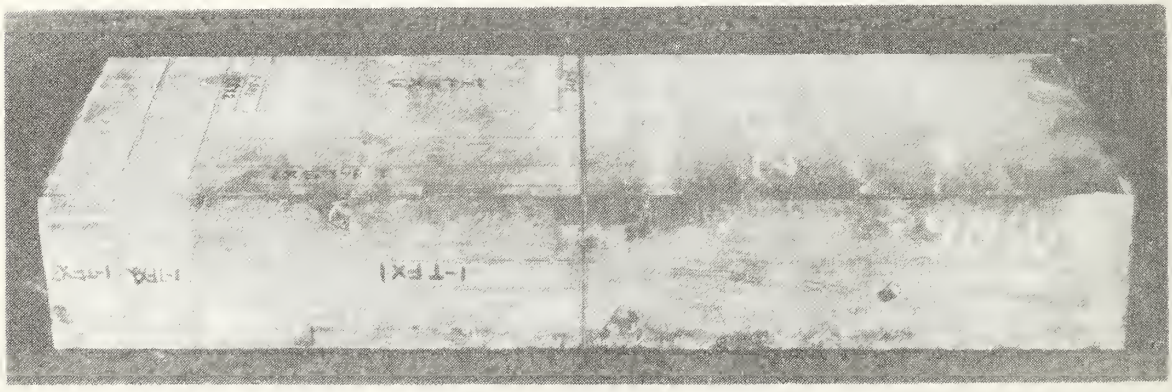

d. Top of box beam segment 9U (NBS 1).

Figure A7.3.2-1

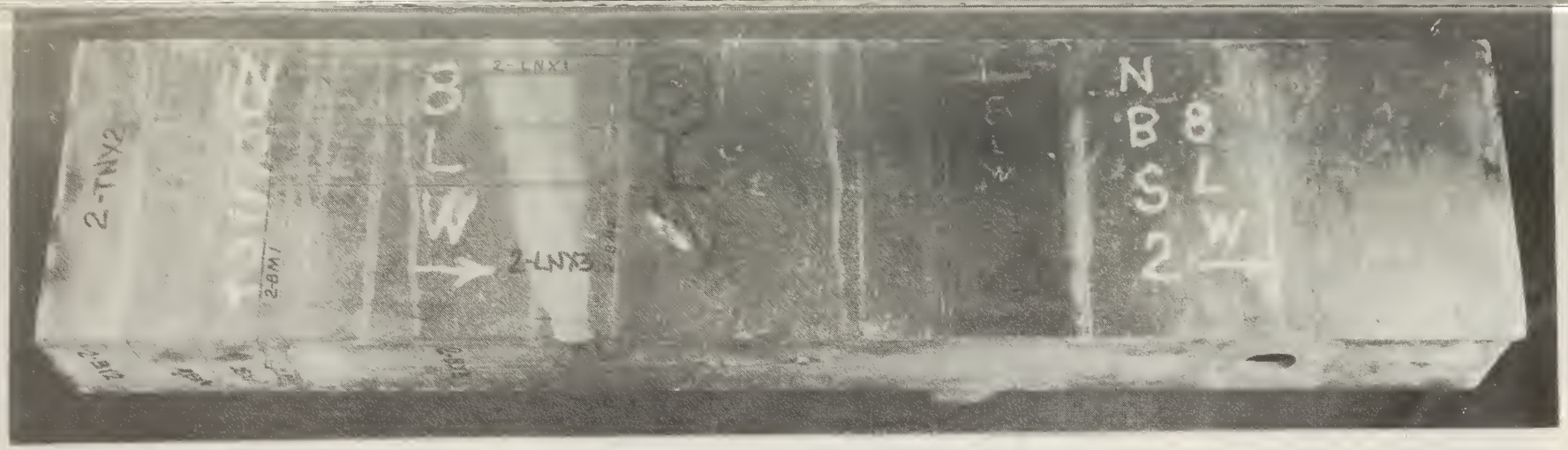

a. North face of box beam segment 8L (NBS 2).

Figure A7.3.2-2 Location of test specimens from box beam segment 8L obtained from the walkway debris.

a. North face:
   Longitudinal web tensile test specimens 2-LN1, 2-LN2
   Transverse web tensile test specimens 2-TN1, 2-TN2
   Parts of metallographic specimens 2-BM1, 2-BM2

b. Bottom:
   Parts of metallographic specimens 2-BM1, 2-BM2
   Transverse tensile test specimens across the weld 2-BX3W2, 2-BX3W4
   Chemical analysis specimen 2-BX1

c. South face:
   Longitudinal web tensile test specimens 2-LS1, 2-LS2
   Transverse web tensile test specimens 2-TS1, 2-TS2
   Parts of metallographic specimens 2-BM1, 2-BM2

d. Top:
   Longitudinal flange tensile test specimens 2-TFN, 2-TFS
   Metallographic specimen 2-TFX1
   Chemical analysis specimen 2-TFX4

e. Bottom interior:
   Chemical analysis specimen 2C of interior tack weld

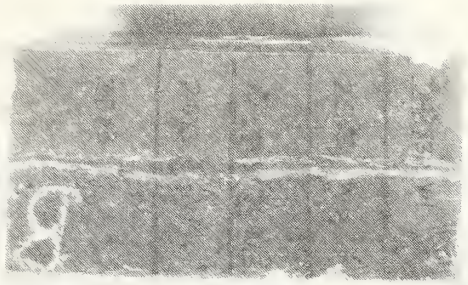

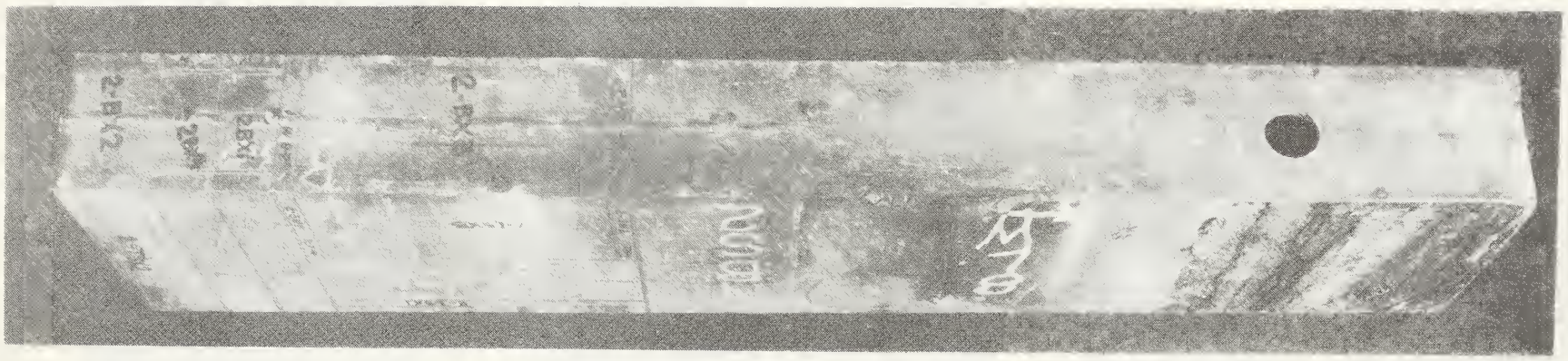

b. Bottom of box beam segment 8L (NBS 2).

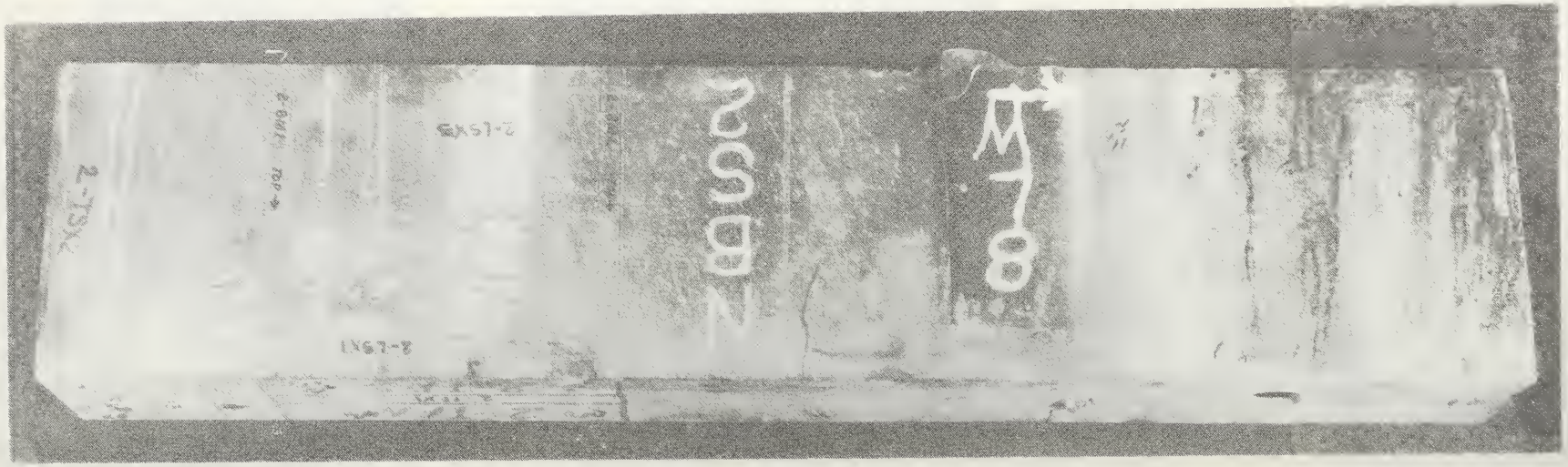

c. South face of box beam segment 8L (NBS 2).

Figure A7.3.2-2

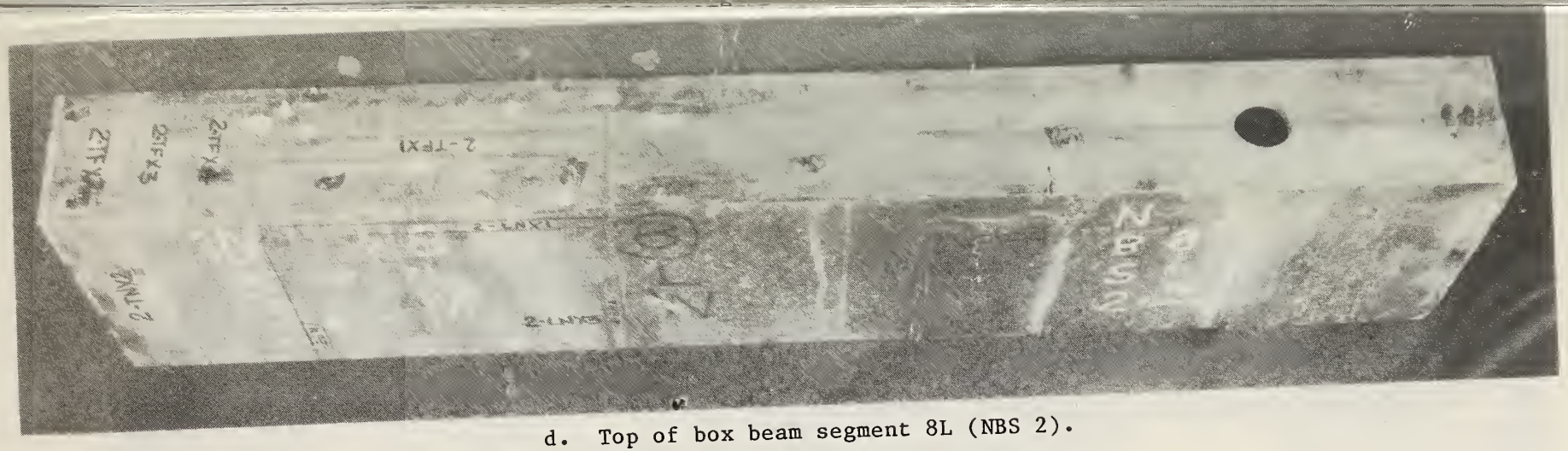

d. Top of box beam segment 8L (NBS 2).

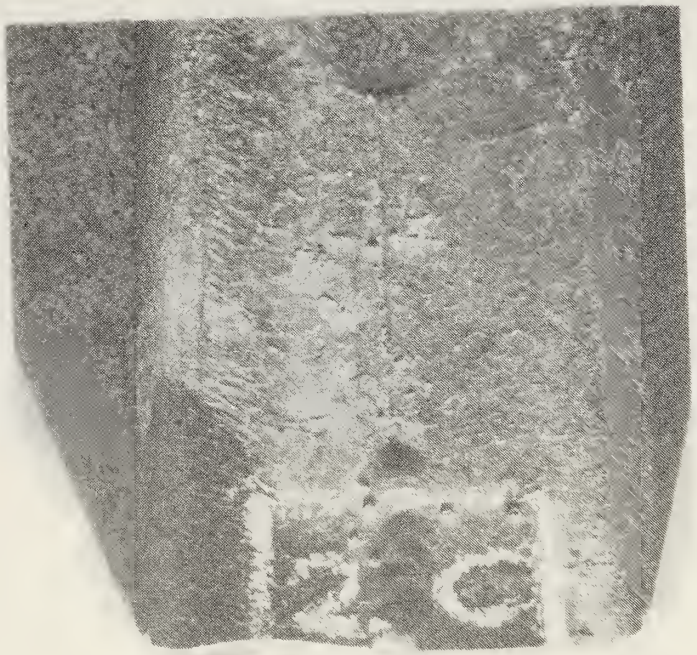

e. Bottom interior of box beam segment 8L (NBS 2).

Figure A7.3.2-2

Figure A7.3.2-3 Location of test specimens from box beam segment NBS 3-5 from box beam 9M obtained from the walkway debris.

a. North face:
   Longitudinal web tensile test specimens 3-LN1, 3-LN2
   Transverse web tensile test specimens 3-TN1, 3-TN2
   Parts of metallographic specimens 3-BM1, 3-BM2

b. Bottom:
   b.1: Parts of metallographic specimens 3-BM1, 3-BM2
   Transverse tensile test specimens across the weld 3-BW1, 3-BW4
   Chemical analysis specimen 3-BX1
   Fractographic analysis specimen 3-DBB-2

   b.2: Fractographic analysis specimen 3-DBB-1

c. South face:
   Longitudinal web tensile test specimens 3-LS1, 3-LS2
   Transverse web tensile test specimens 3-TS1, 3-TS2
   Parts of metallographic specimens 3-BM1, 3-BM2

d. Top:
   Longitudinal flange tensile test specimens 3-TFN, 3-TFS

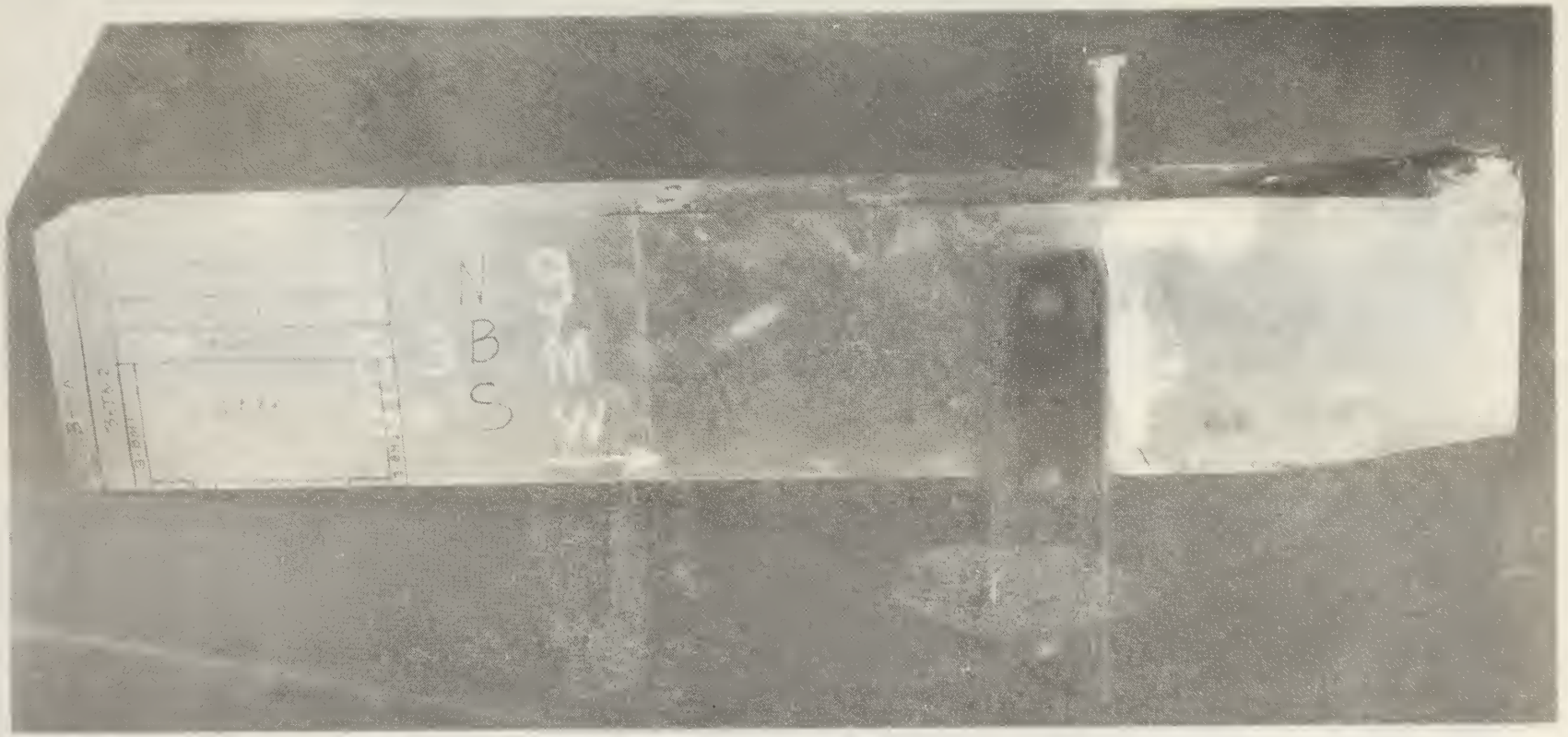

a. North face of box beam segment 9M (NBS 3-5).

Figure A7.3.2-3

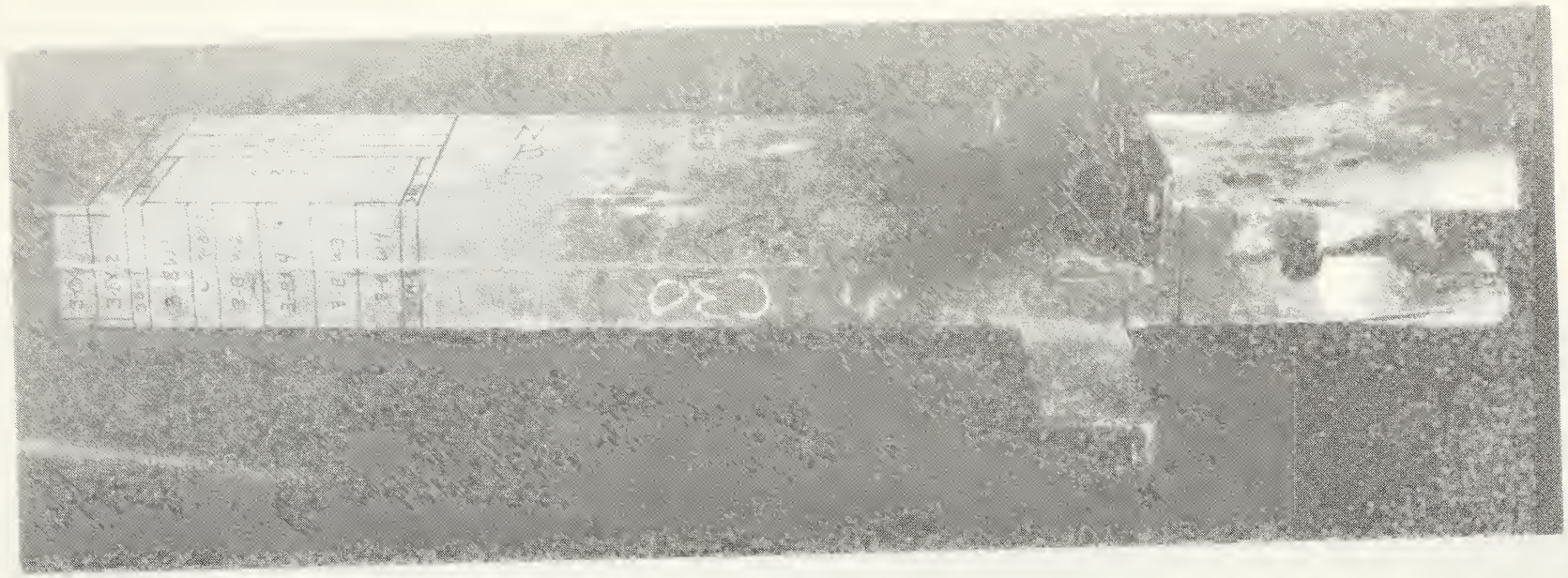

b1

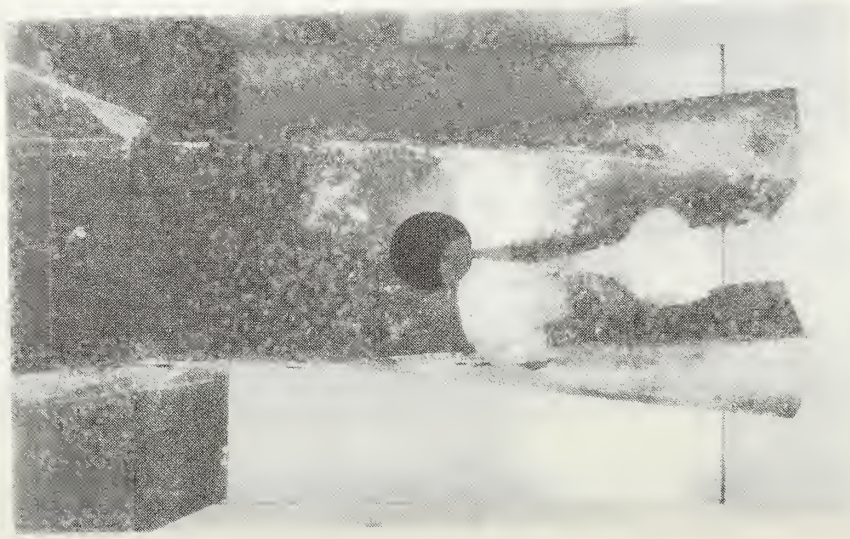

b2

b. Bottom of box beam segment 9M (NBS 3-5).

Figure A7.3.2-3

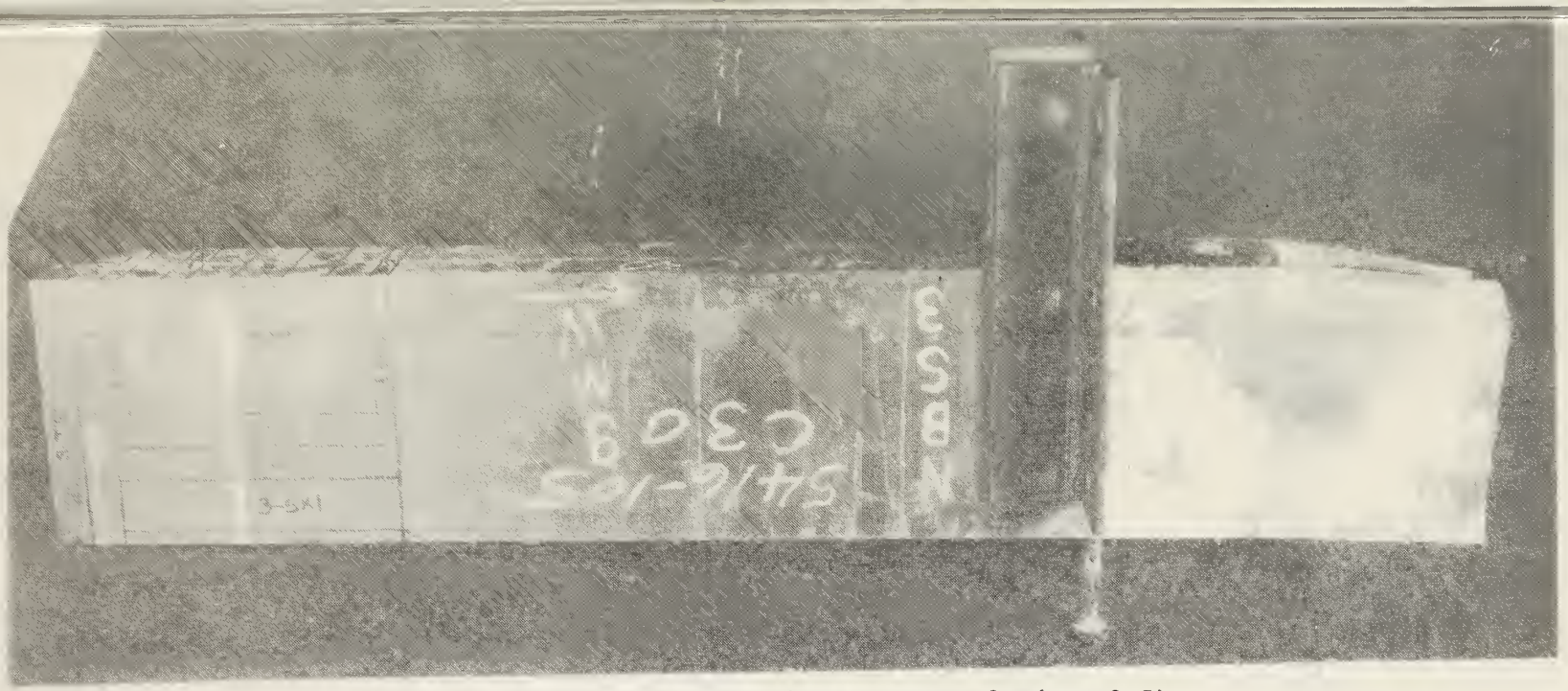

c. South face of box beam segment 9M (NBS 3-5).

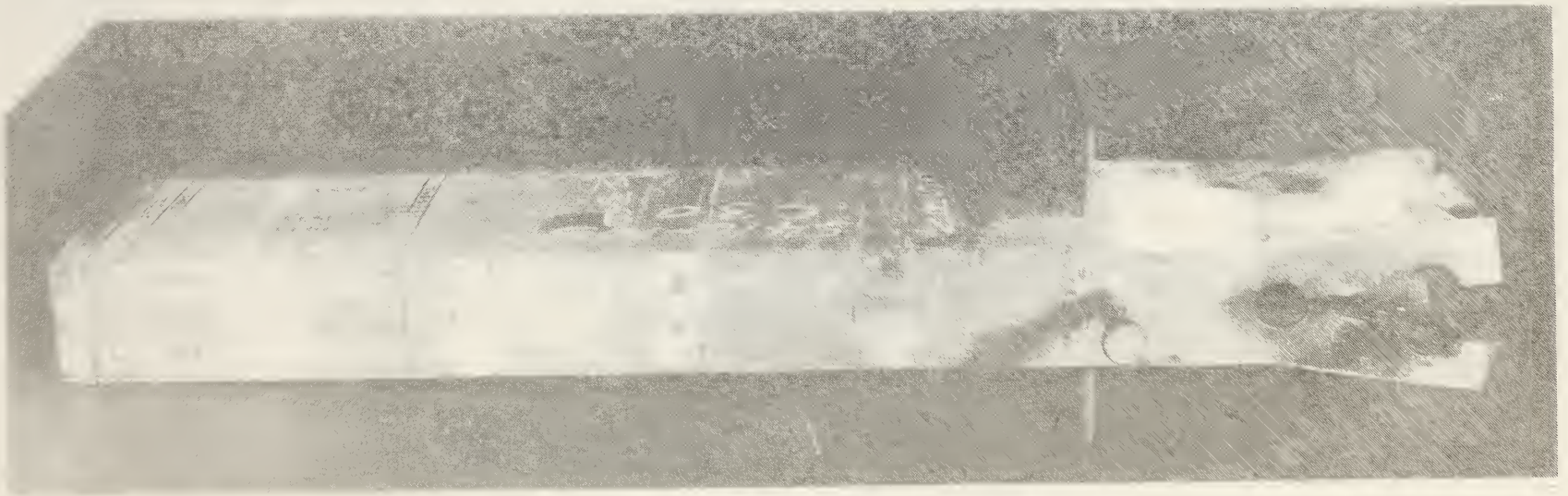

d. Top of box beam segment 9M (NBS 3-5).

Figure A7.3.2-3

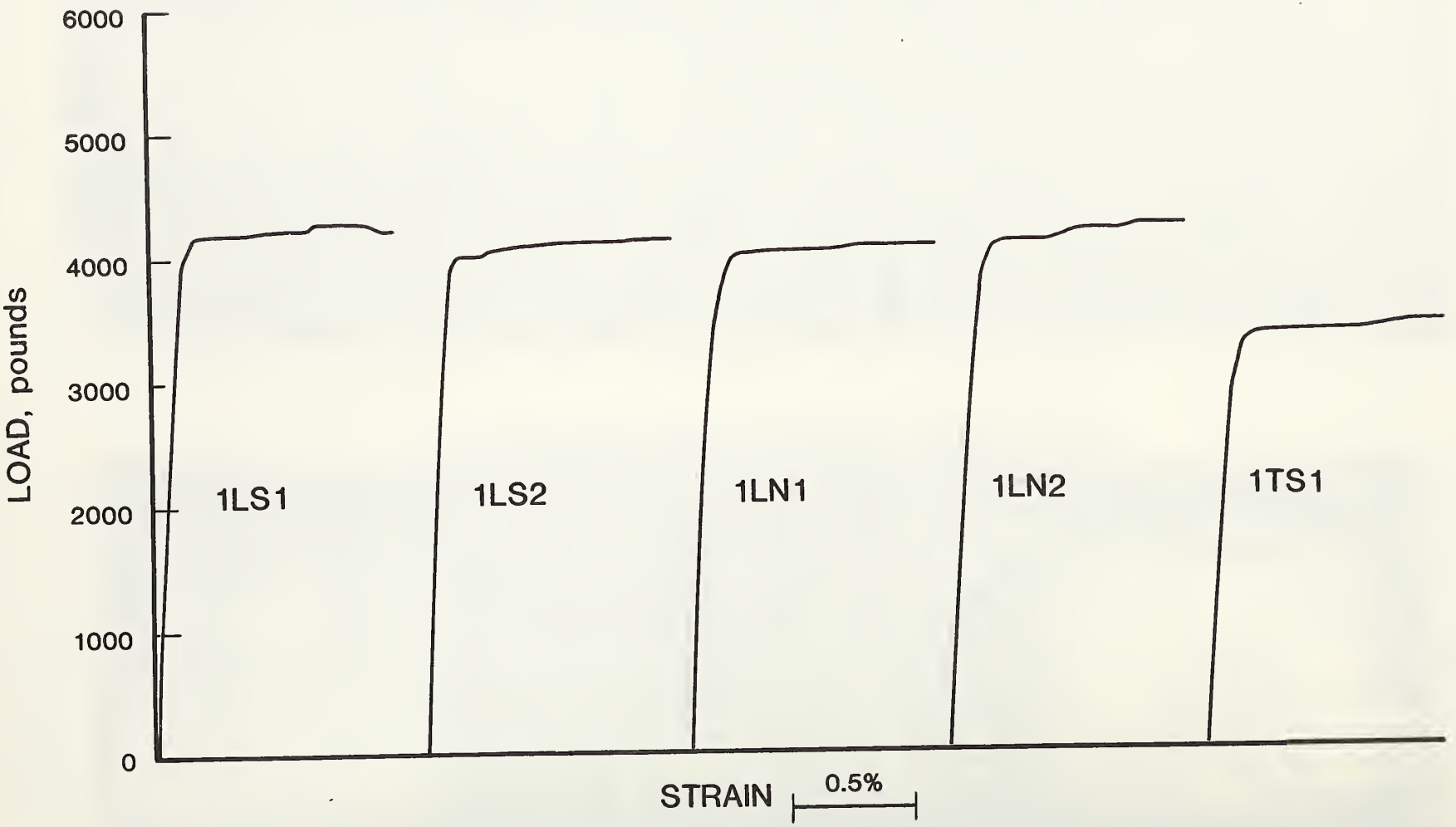

Figure A7.3.2-4 Load-strain plots for walkway box beam specimens 1-LS1, 1-LS2, 1-LN1, 1-LN2, 1-TS1.

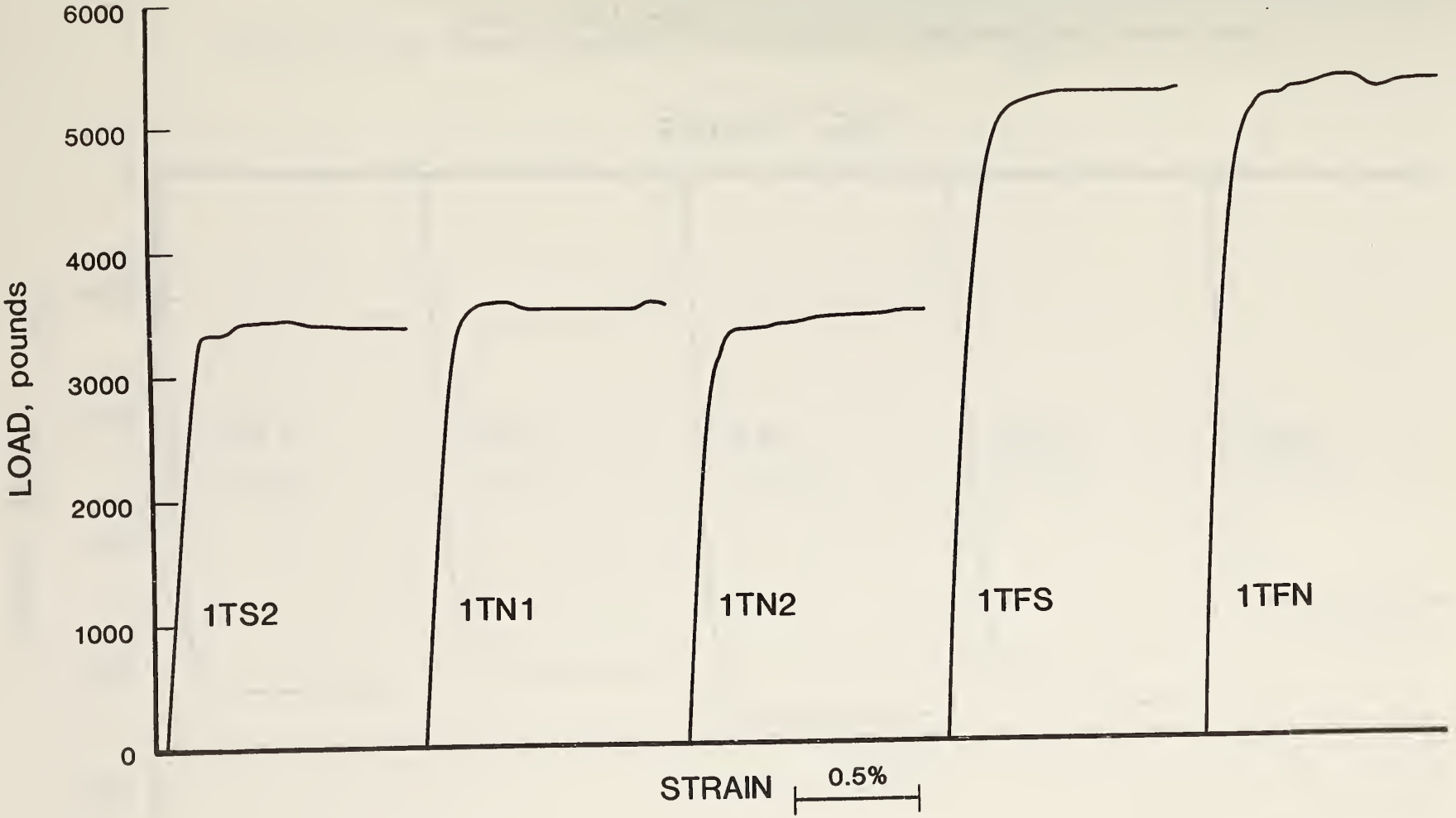

Figure A7.3.2-5 Load-strain plots for walkway box beam specimens 1-TS2, 1-TN1, 1-TN2, 1-TFS, 1-TFN.

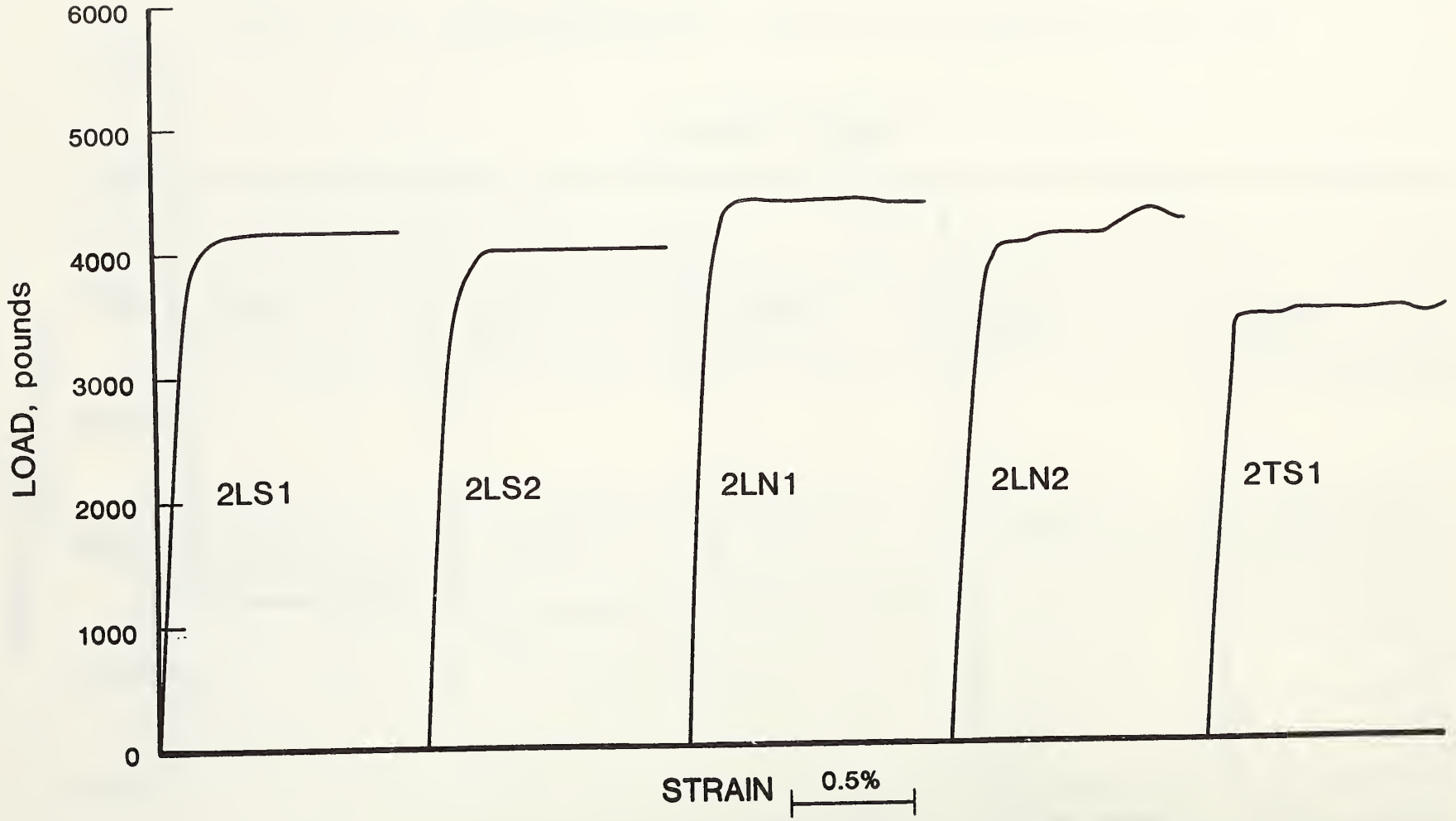

Figure A7.3.2-6 Load-strain plots for walkway box beam specimens 2-LS1, 2-LS2, 2-LN1, 2-LN2, 2-TS1.

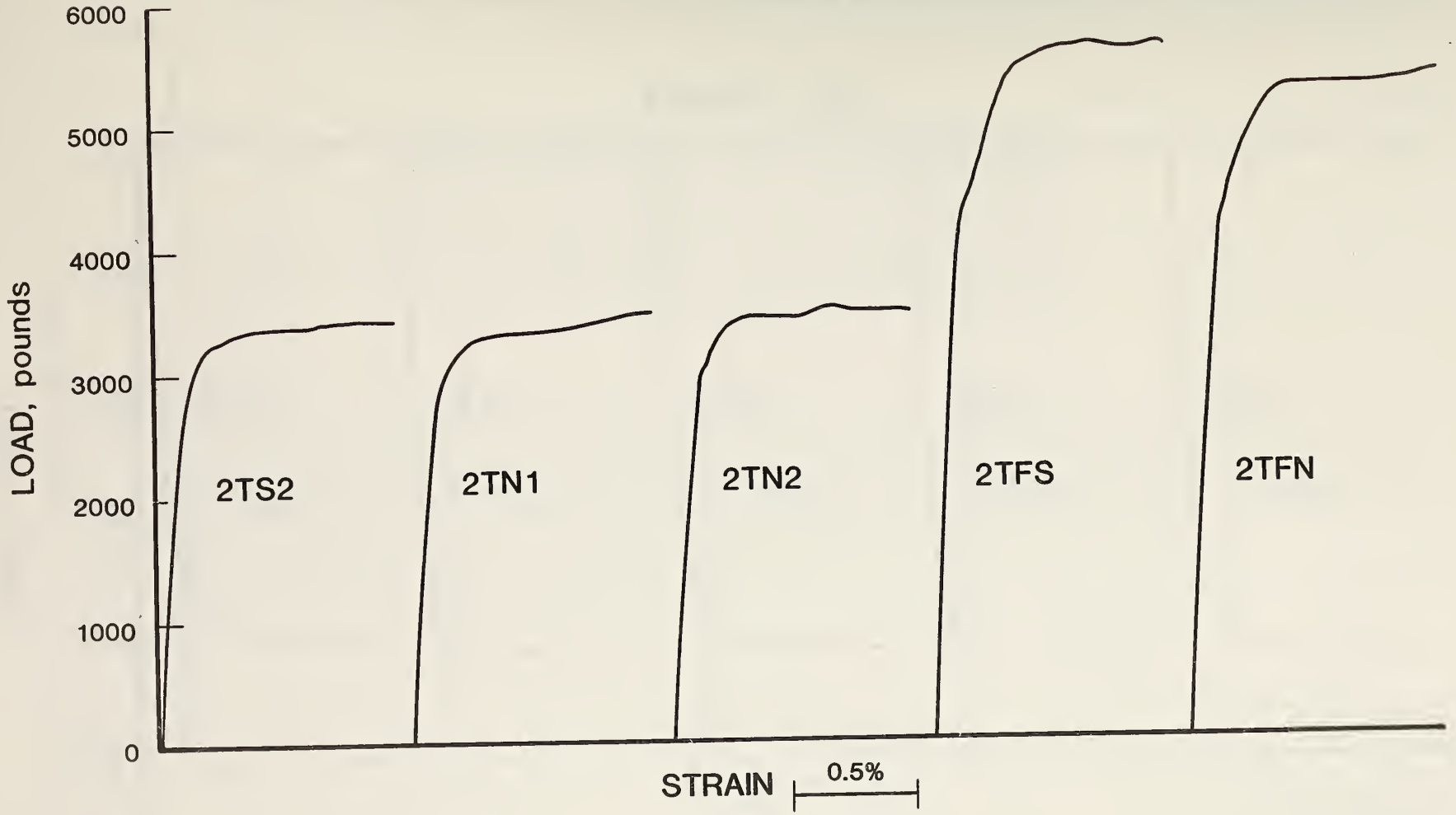

Figure A7.3.2-7 Load-strain plots for walkway box beam specimens 2-TS2, 2-TN1, 2-TN2, 2-TFS, 2-TFN.

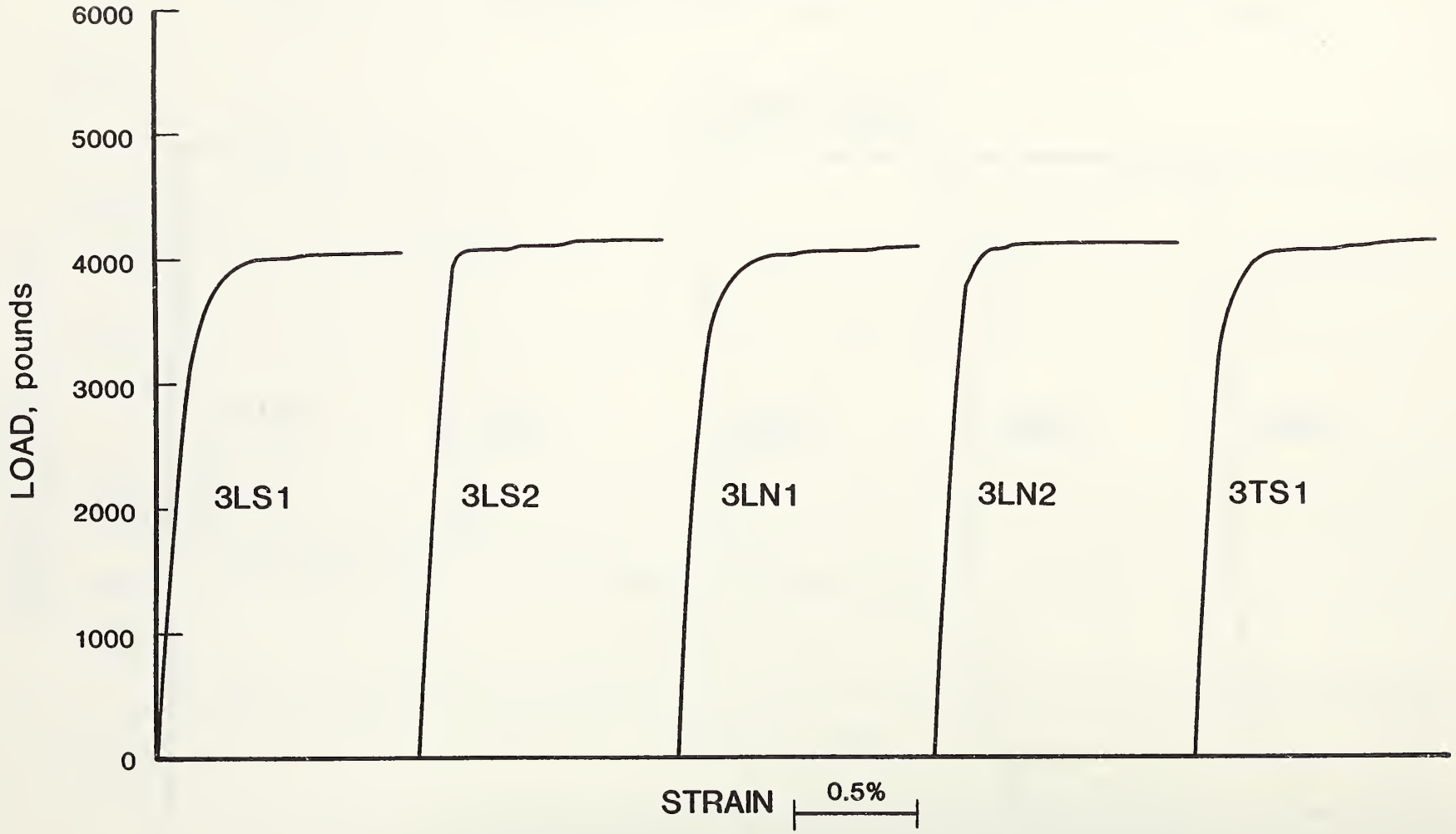

Figure A7.3.2-8 Load-strain plots for walkway box beam specimens 3-LS1, 3-LS2, 3-LN1, 3-LN2, 3-TS1.

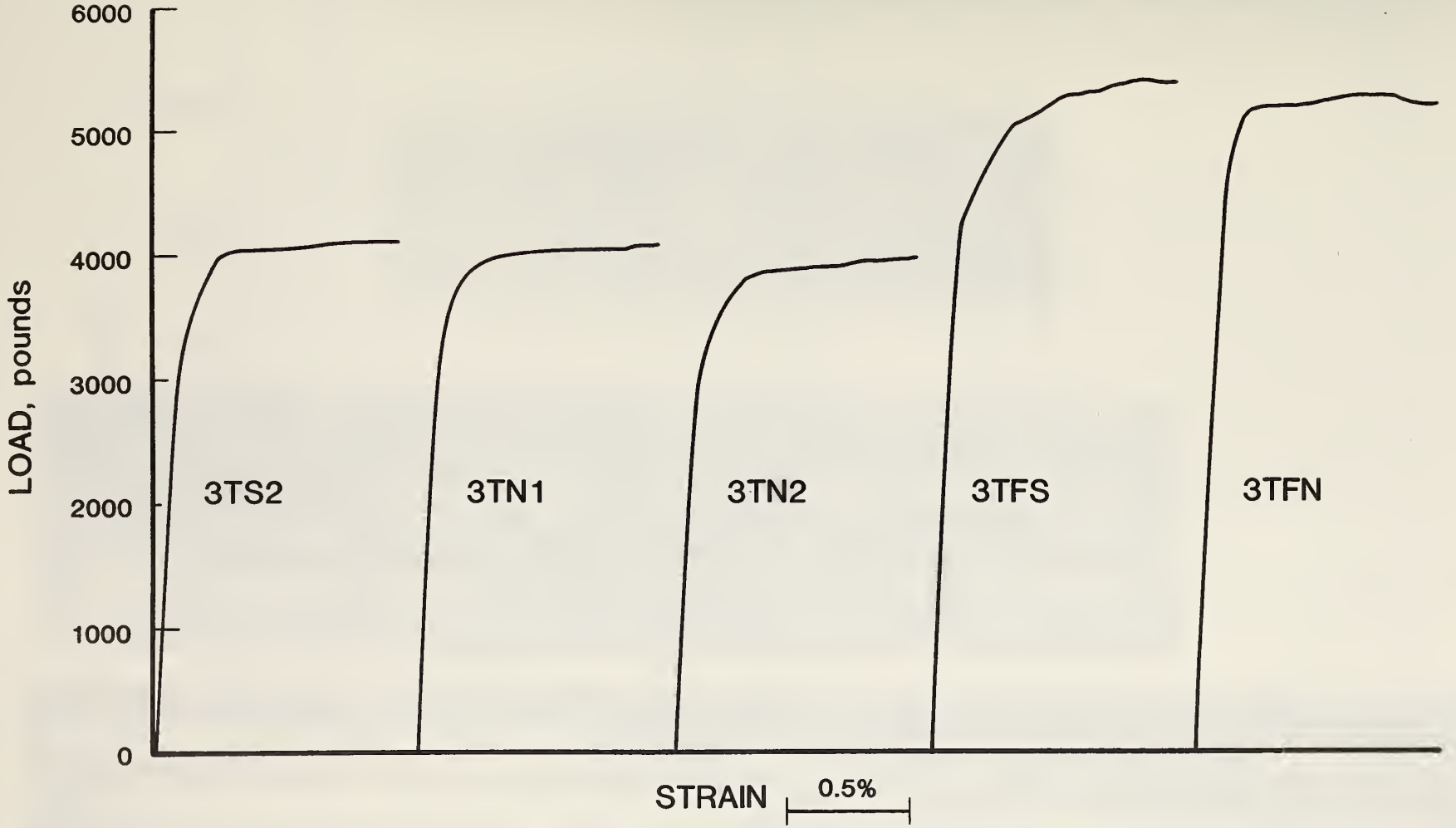

Figure A7.3.2-9 Load-strain plots for walkway box beam specimens 3-TS2, 3-TN1, 3-TN2, 3-TFS, 3-TFN.

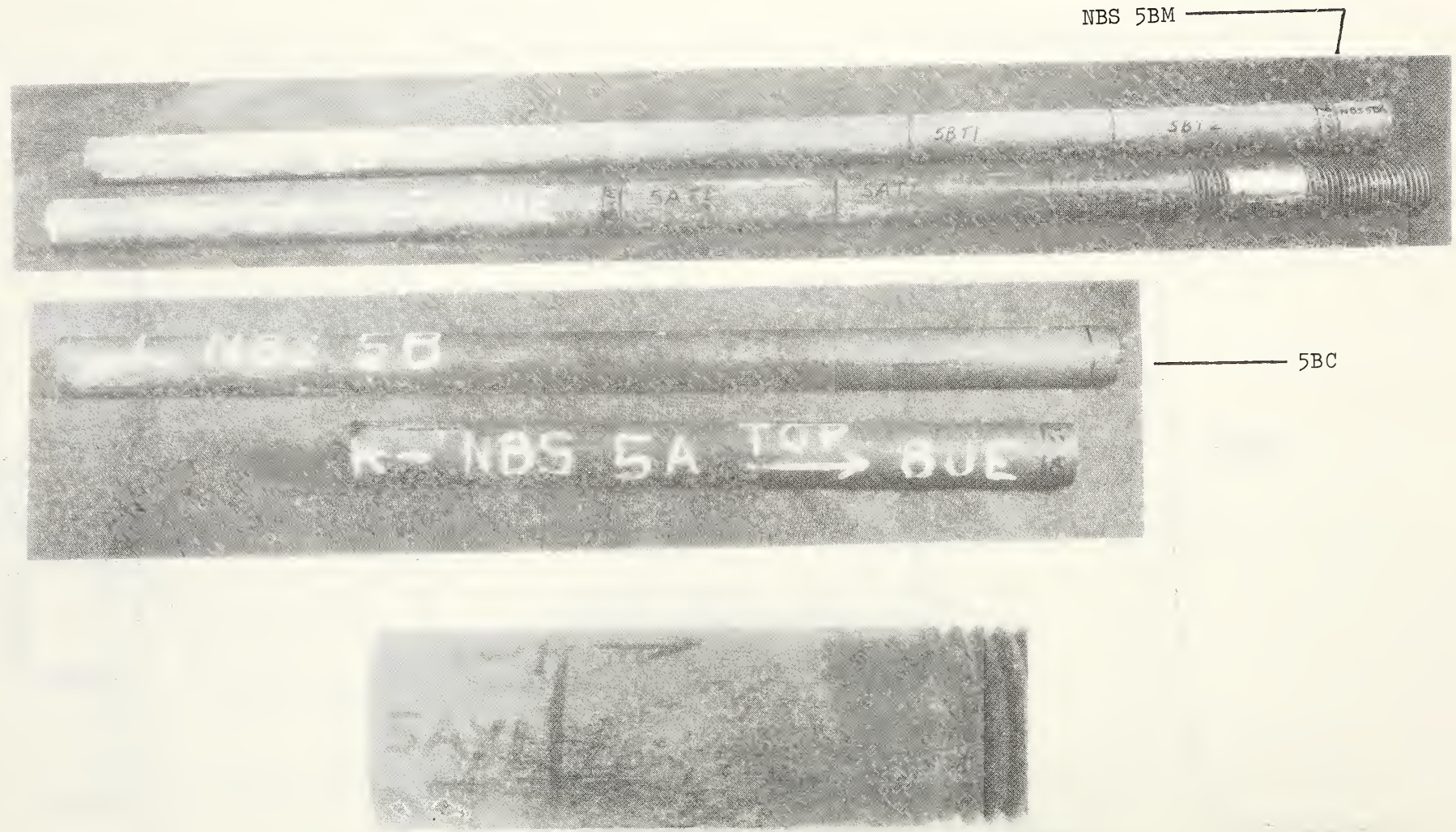

Figure A7.3.3-1. Location of test specimens from hanger rod segments NBS 5A and NBS 5B obtained from the walkway debris.

Longitudinal tensile test specimens 5AT1, 5AT2, 5BT1, 5BT2
Metallographic specimens 5AM, 5BM
Chemical analysis specimens 5AC, 5BC, 5AX1, NBS 5BX

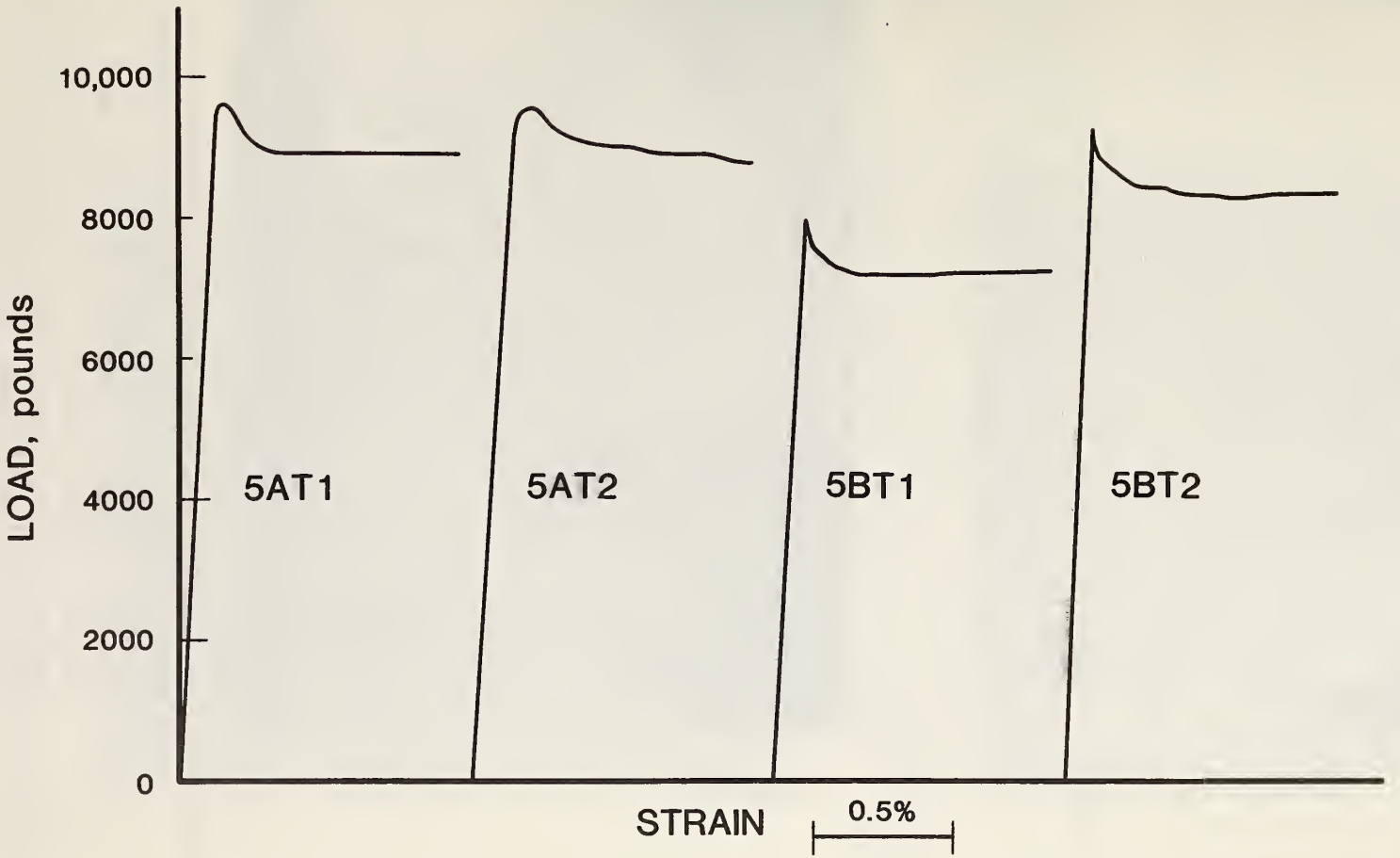

Figure A7.3.3-2 Load-strain plots for walkway hanger rod specimens 5AT1, 5AT2, 5BT1, 5BT2.

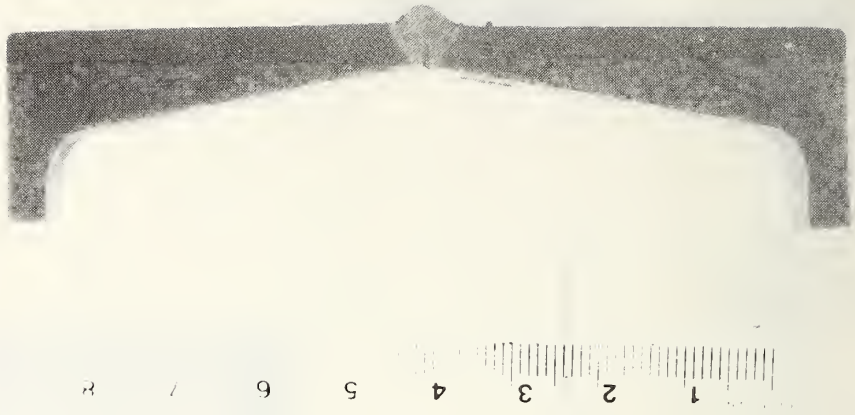

Figure A7.4.1-1 Transverse section through NBS weldment IC welded by the GMAW process using mild steel welding rod. The weld is in the center connecting flange parts of the two channel segments. Parts of the web regions of each channel are also included in the section. Etchant: two percent nital ~X1

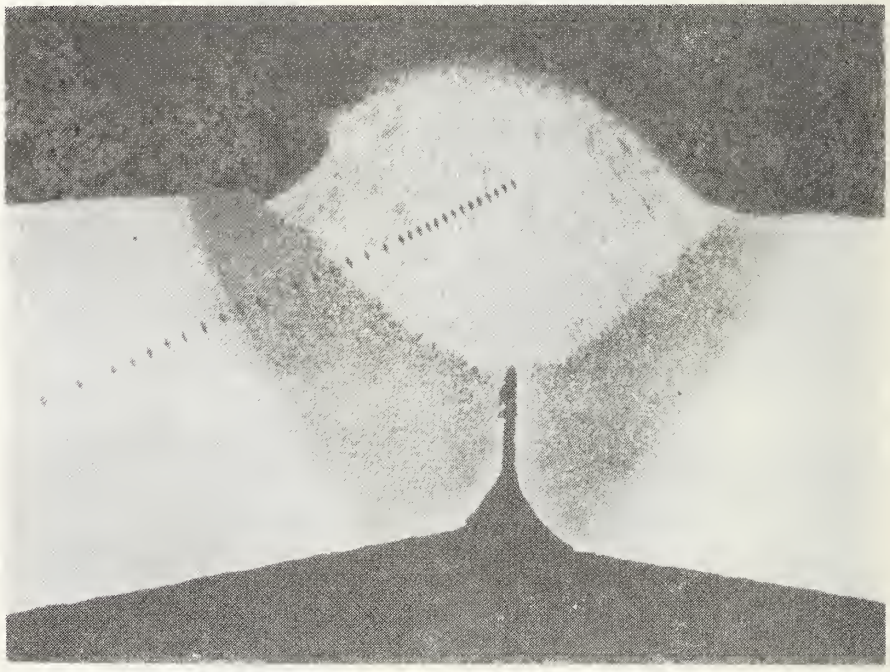

Figure A7.4.1-2. Part of the transverse section shown above, but a higher magnification. The light region in the center is weld metal. The dark regions adjacent to the weld metal are the heat affected zones. The light regions to the left and right in the photograph represent base flange regions of the channel segments. The line of small dark, elongated marks is the result of microhardness measurements. Etchant: two percent nital. X8.5

Figure A7.4.1-3 Microstructure representative of the weld metal in transverse section through NBS weldment IC. The microstructure appears to consist primarily of bainite. Etchant: two percent nital. X200

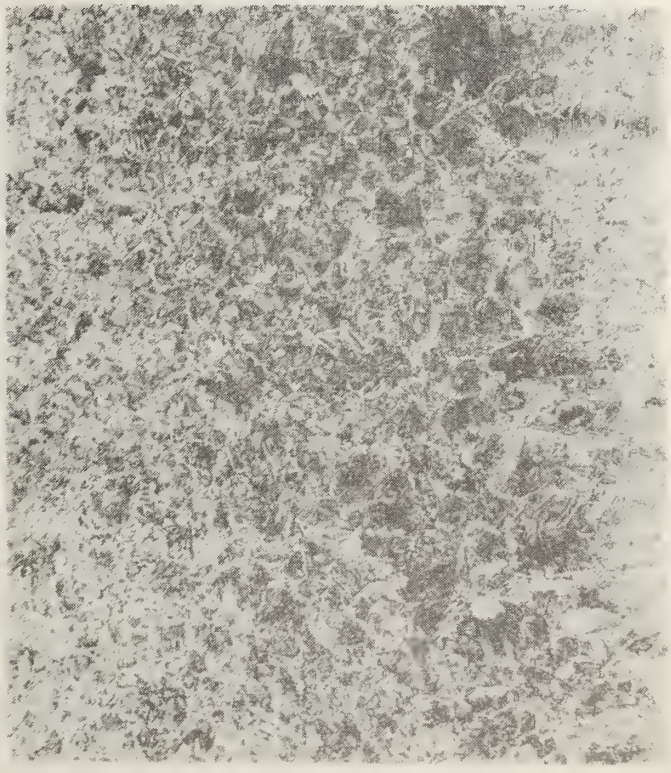

Figure A7.4.1-4 Transition region from weld metal (right) to heat affected zone (left) in transverse section through NBS weldment IC. Etchant: two percent nital. X200

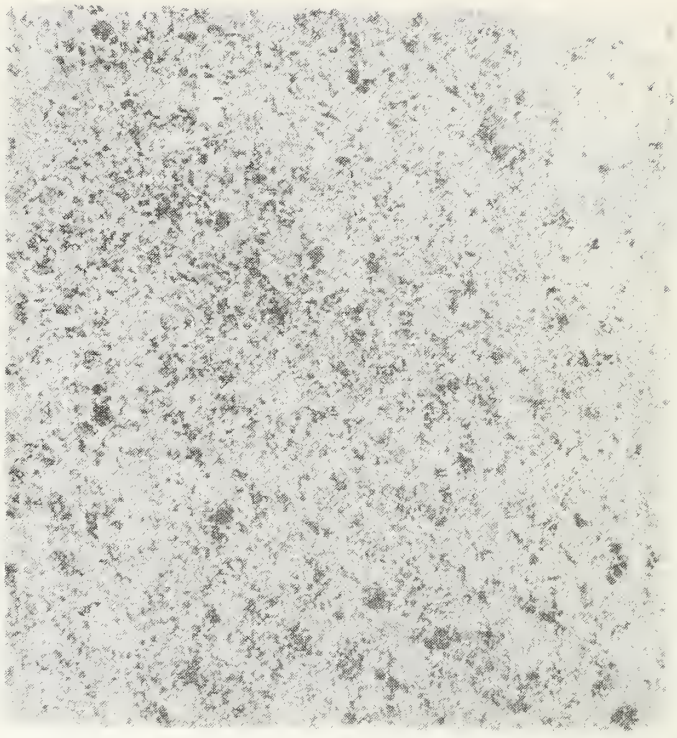

Figure A7.4.1-5 Representative microstructure of the heat affected zone in transverse section through NBS weldment IC. The microstructure consists of ferrite, primarily as a network in prior austenite grain boundaries, bainite, partially spheroidized carbides, and tempered martensite. Etchant: two percent nital. X200

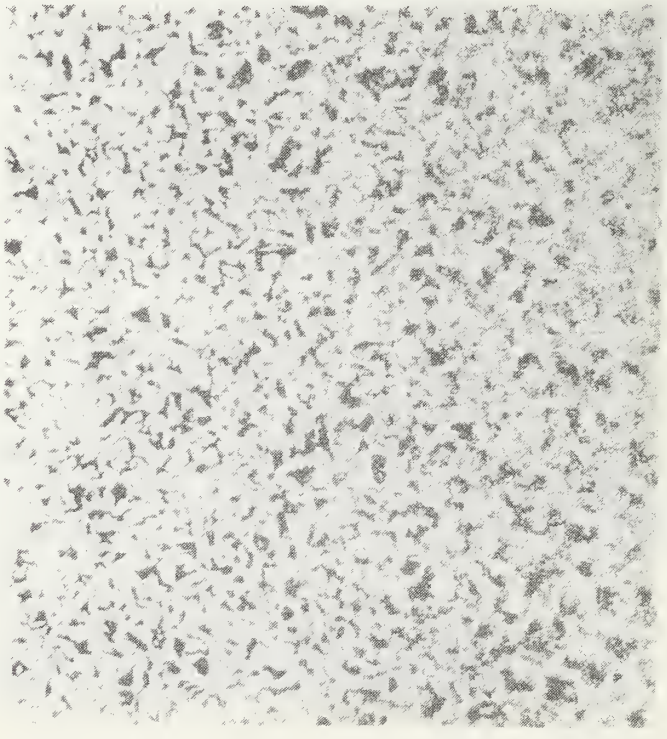

Figure A7.4.1-6 Microstructure representative of the transition region from the heat affected zone (right) to base channel material (left) in NBS weldment IC. Etchant: two percent nital. X200

Figure A7.4.1-7 Microstructure representative of the base channel material from NBS weldment IC. The microstructure consists of relatively fine grained ferrite (light) and pearlite (dark) in a normalized condition. Etchant: two percent nital. X200

Figure A7.4.1-8 Transverse section 1BM1 through the bottom of walkway box beam 9U (NBS 1). The north channel of the box beam is to the left and the south channel is to the right. The weld connecting the flanges of the two channels used to fabricate the box beam is in the center. Parts of the web regions of each channel had been removed before this photograph was taken. The indentations appearing on the surface of the section are the result of hardness measurements.
Etchant: two percent nital. ~X1

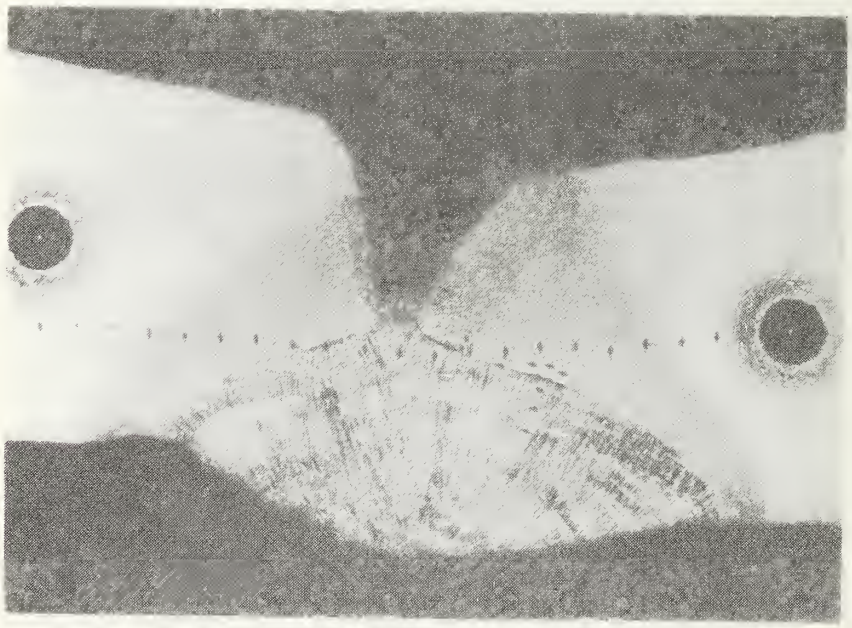

Figure A7.4.1-9 Part of the transverse section shown in figure A7.4.1-8, but at higher magnification. The region at the bottom center is weld metal. The dark gray regions on either side of the weld metal are the heat affected zones associated with the weld. The lighter regions at either side of the figure beyond the heat affected zone are base channel material.
Etchant: two percent nital. X8.5

Figure A7.4.1-10 Transverse section 1BM2 through the bottom of walkway box beam 9U (NBS 1). The north channel of the box beam is to the left and the south channel is to the right. The weld connecting the flanges of the two channels used to fabricate the box beam is in the center. Parts of the web regions of each channel had been removed before this photograph was taken. The indentations appearing on the surface of the section are the result of hardness measurements. Etchant: two percent nital. ~X1

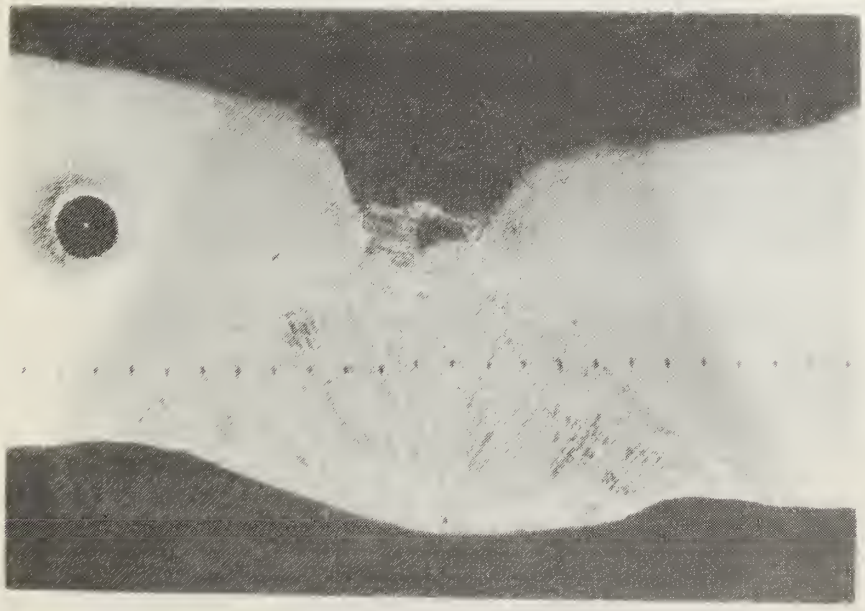

Figure A7.4.1-11 Part of the transverse section shown in figure A7.4.1-10, but at higher magnification. The region at the bottom center is weld metal. The dark gray regions on either side of the weld metal are the heat affected zones associated with the weld. The lighter regions on either side of the photomacrograph are base channel material. Etchant: two percent nital. X8.5

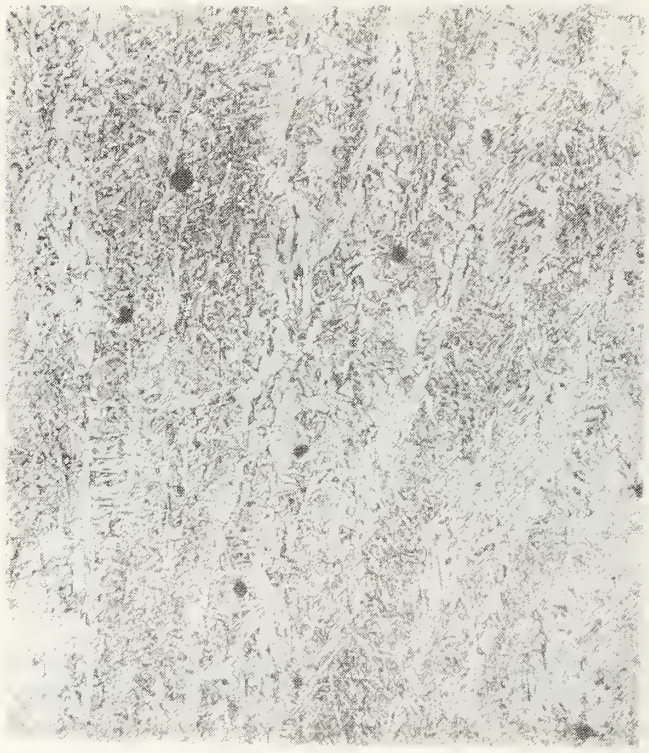

Figure A7.4.1-12 Representative microstructure of the weld metal in transverse section 1BM1 through box beam 9U (NBS 1). The microstructure consists primarily of bainite. Some inclusions are evident. Etchant: two percent nital. X200

Figure A7.4.1-13 Representative microstructure of the weld metal in transverse section 1BM2 through box beam 9U (NBS 1). The microstructure consists primarily of bainite. Etchant: two percent nital. X200

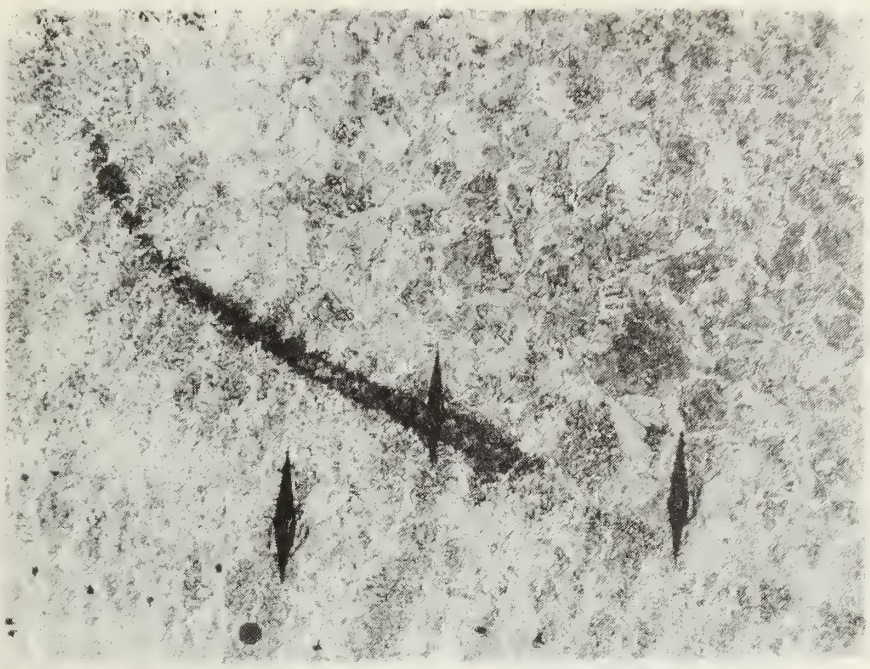

Figure A7.4.1-14 Patch of hard material (dark streak) at the transition from weld metal (top right) to the heat affected zone (bottom left) in section 1BM1. The elongated dark areas are hardness impressions. Etchant: two percent nital. X100

Figure A7.4.1-15 Hard area similar to that shown above, but at higher magnification. The hard area is in the center running from side to side. The microstructure appears to consist of fine grained tempered martensite. Parts of two hardness impressions can be seen at either side of the figure. Etchant: two percent nital. X800

Figure 7.4.1-16 Transition zone from weld metal (right) to heat affected zone (left) in section 1BM2. Some inclusions can be seen. Etchant: two percent nital. X200

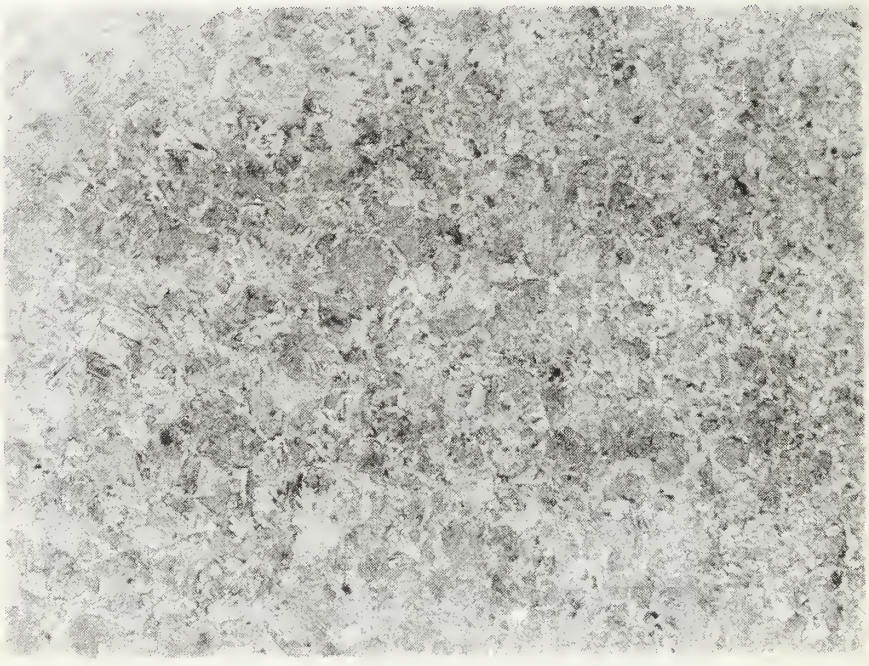

Figure A7.4.1-17 Region representative of the heat affected zone in section 1BM1. The microstructure appears to consist of ferrite, both as a network in prior austenite grains and as needles, bainite, partially sheroidized carbides, and tempered martensite. Etchant: two percent nital. X200

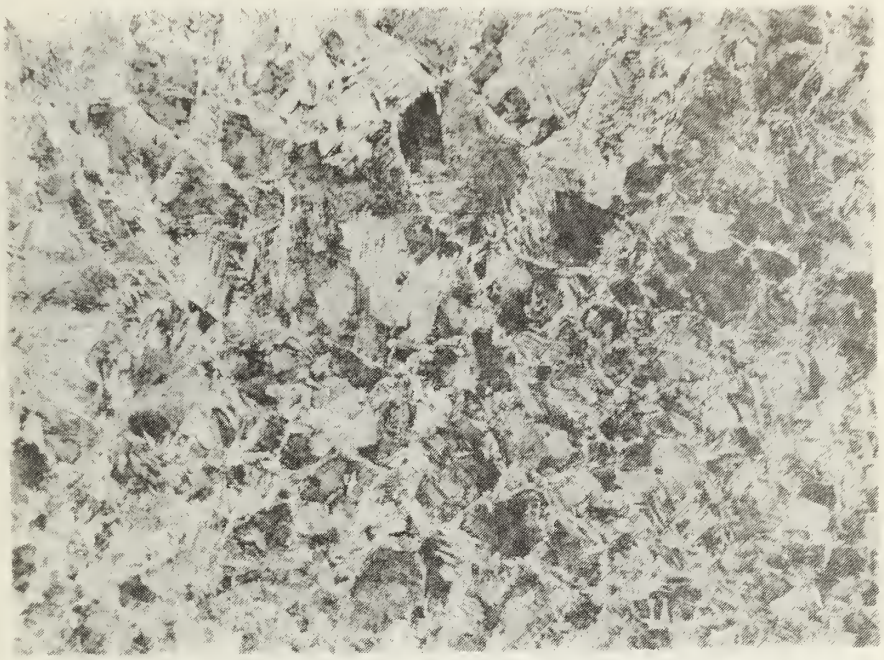

Figure 7.4.1-18 Region representative of the heat affected zone in section 1BM2. The microstructure appears to consist of ferrite, both as a network in prior austenite grains and as needles, bainite, partially spheroidized carbides, and tempered martensite. Etchant: two percent nital. X200

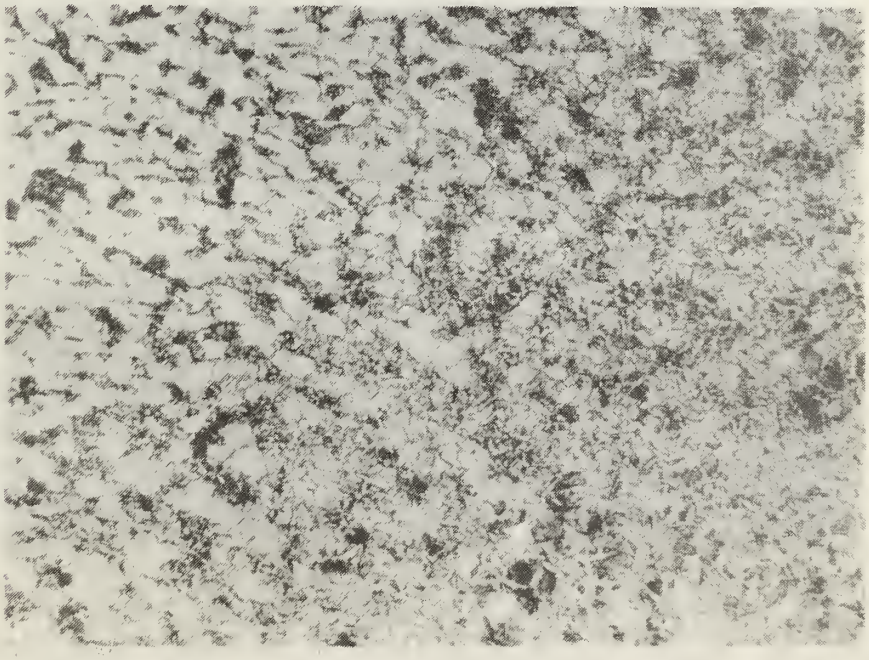

Figure A7.4.1-19 Transition from heat affected zone (right) to base channel material (left) in section 1BM2. Etchant: two percent nital. X200

Figure A7.4.1-20 Region representative of base channel material in section 1BM1. The microstructure consists primarily of ferrite (light) and pearlite (dark) in the normalized condition. Etchant: two percent nital. X200

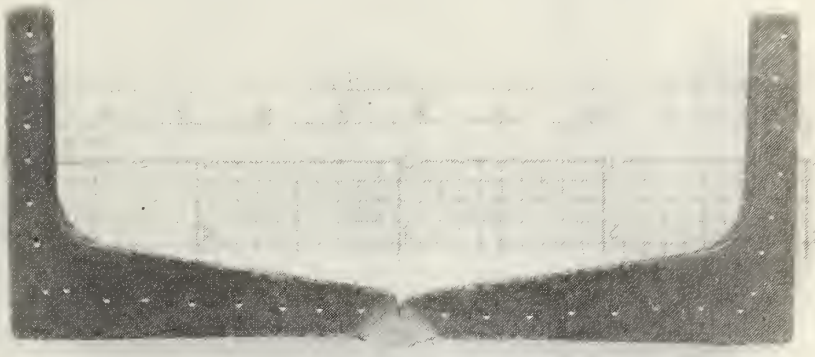

Figure A7.4.1-21 Transverse section 2BM1 through bottom of walkway box beam 8L (NBS 2). The north channel of the box beam is to the left and the south channel is to the right. The weld connecting the flanges of the two channels used to fabricate the box beam is in the center. Parts of the web regions of each channel had been removed before this photograph was taken. The indentations appearing on the surface of the section are the result of hardness measurements. Etchant: two percent nital. ~X1

Figure A7.4.1-22 Part of the transverse section shown in figure A7.4.1-21, but at higher magnification. The region at the bottom center is weld metal. The dark gray regions on either side of the weld metal are the heat affected zones associated with the weld. The lighter regions on either side of the figure beyond the heat affected zones are base channel material. Etchant: two percent nital. X8.5

Figure A7.4.1-23 Transverse section 2BM2 through bottom of walkway box beam 8L (NBS 2). The north channel of the box beam is to the left and the south channel is to the right. The weld connecting the flanges of the two channels used to fabricate the box beam is in the center. Parts of the web regions of each channel had been removed before this photograph was taken. The indentations appearing on the surface of the section are the result of hardness measurements. Etchant: two percent nital. X1

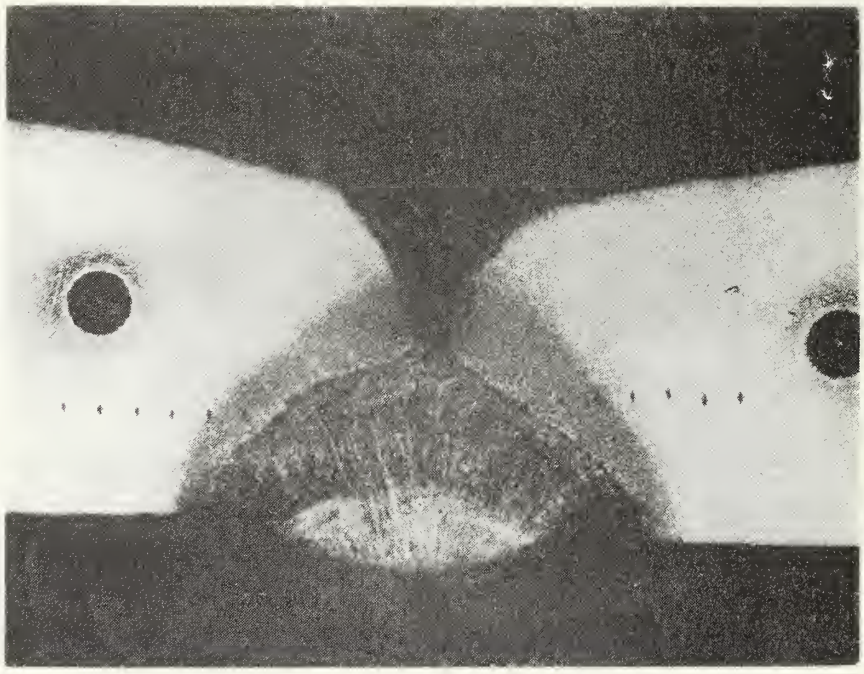

Figure A7.4.1-24 Part of the transverse section shown in figure A7.4.1-23, but at higher magnification. The region at the bottom center is weld metal. The gray regions on either side of the weld metal are the heat affected zones associated with the weld. The lighter regions on either side of the figure beyond the heat affected zones are base channel material. Etchant: two percent nital. X8.5

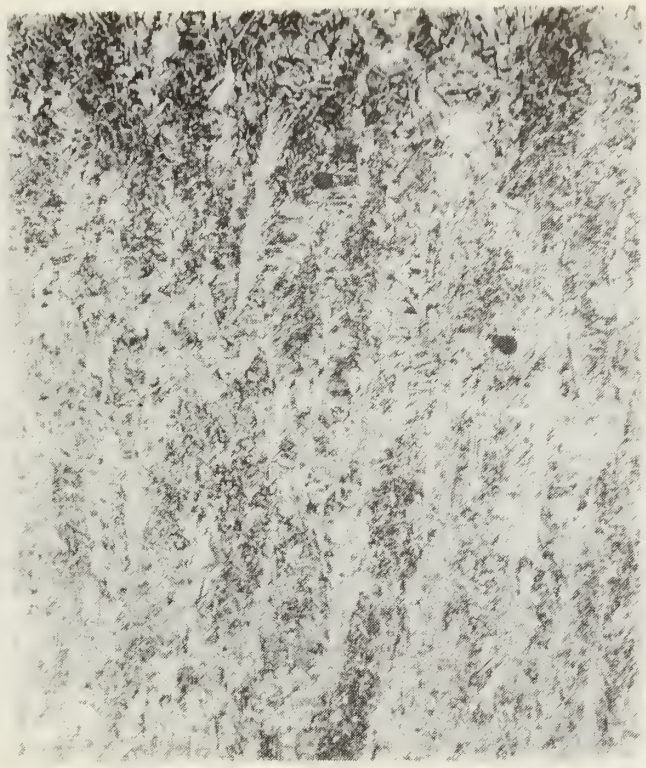

Figure A7.4.1-25 Representative microstructure of the weld metal in transverse section 2BM1 through box beam 8L (NBS 2). The microstructure appears to consist primarily of bainite. Some inclusions are evident. Etchant: two percent nital. X200

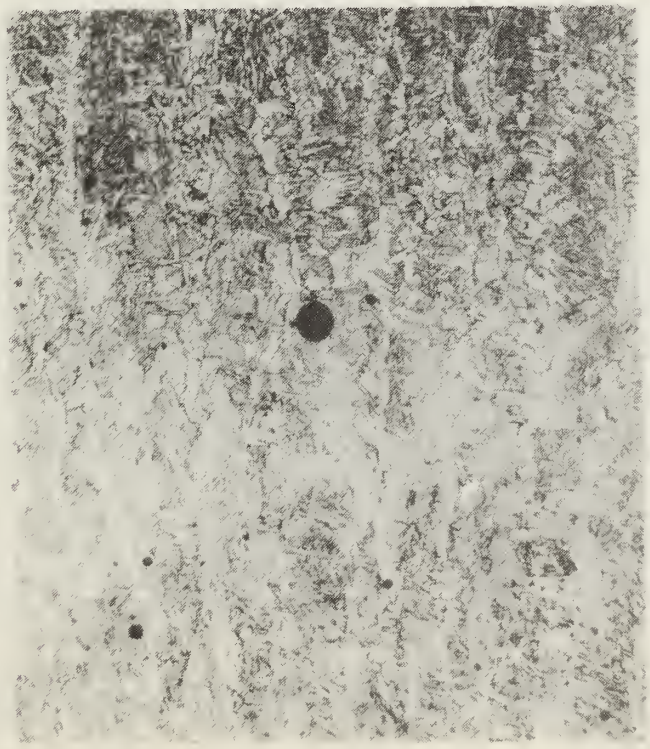

Figure A7.4.1-26 Representative microstructure of the weld metal in transverse section 2BM2 through box beam 8L (NBS 2). The microstructure appears to consist primarily of bainite. Some inclusions are evident. Etchant: two percent nital. X200

Figure A7.4.1-27 Transition zone from weld metal (right) to heat affected zone (left) in section 2BM1. Etchant: two percent nital. X200

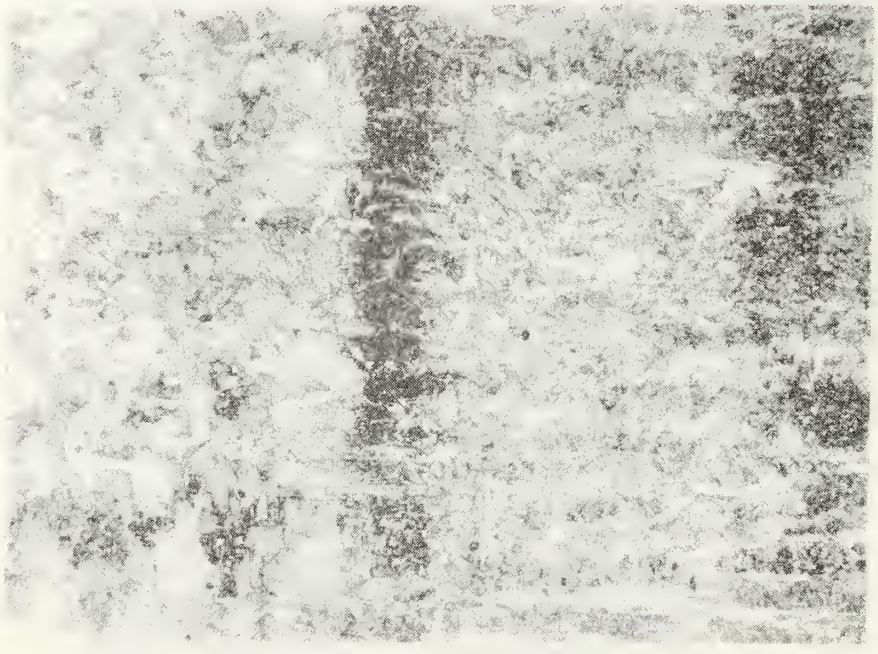

Figure A7.4.1-28 Transition zone from weld metal (right) to heat affected zone (left) in section 2BM2. Etchant: two percent nital. X200

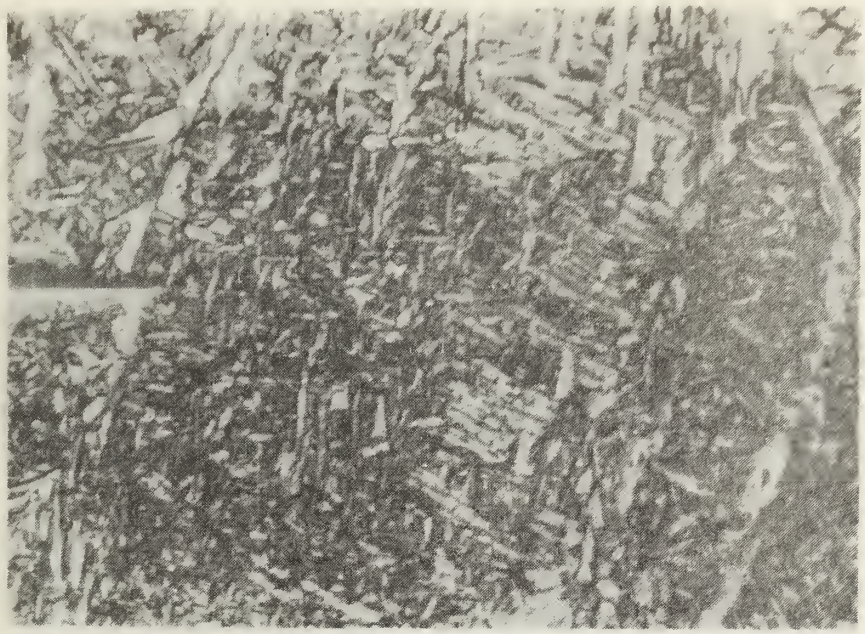

Figure A7.4.1-29 Region of the transition zone from weld metal to the heat affected zone in section 2BM2. This region is one of the hard areas. The microstructure appears to consist of tempered martensite. Part of a hardness test impression can be seen at the left center. Etchant: two percent nital. X1200

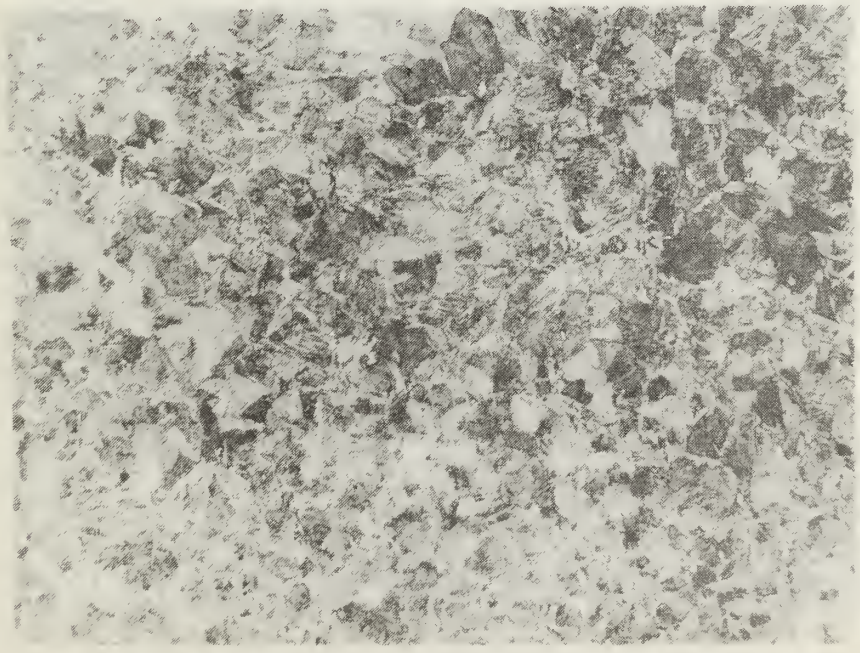

Figure A7.4.1-30 Representative microstructure of the heat affected zone in section 2BM1. The microstructure appears to consist of ferrite, both as a network in prior austenite grain boundaries and as needles, bainite, partially spheroidized carbides, and tempered martensite. Etchant: two percent nital. X200

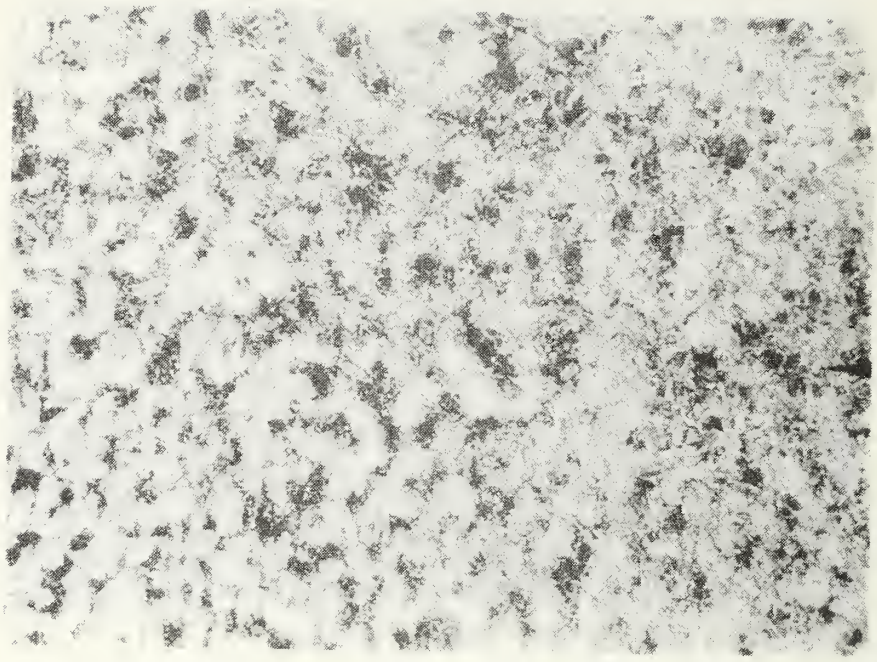

Figure A7.4.1-31 Transition region from heat affected zone (right) to base channel material (left) in section 2BM1. Etchant: two percent nital. X200

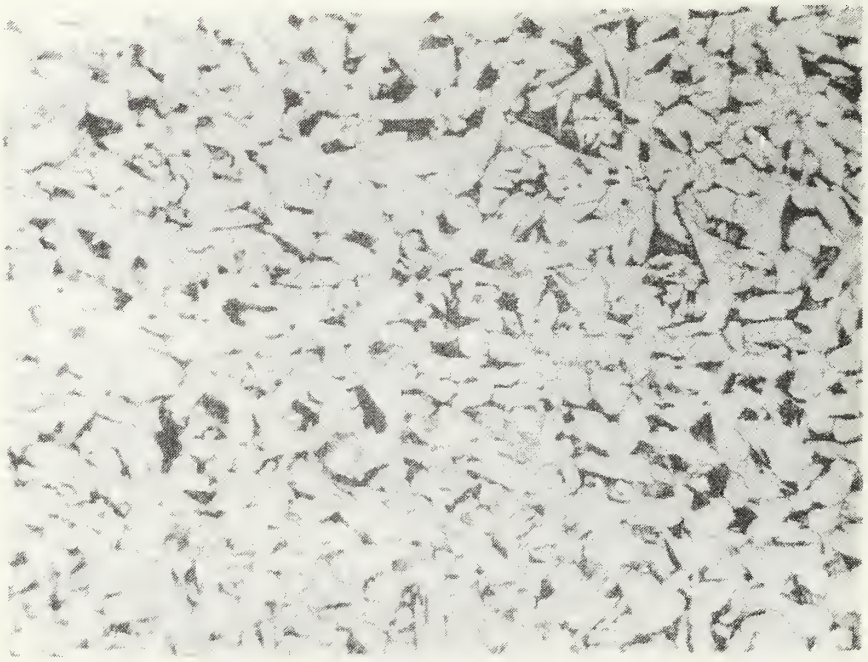

Figure A7.4.1-32 Region of section 2BM1 representative of the base channel material in both sections through box beam 8L. The microstructure consists primarily of ferrite (light) and pearlite (dark) in the normalized condition. Etchant: two percent nital. X200

Figure A7.4.1-33 Transverse section 3BM1 through the bottom of walkway box beam 9M (NBS 3). The south channel of the box beam is to the left and the north channel is to the right. The weld connecting the flanges of the two channels used to fabricate the box beam is in the center. Parts of the web regions of each channel had been removed before this photograph was taken. The indentations appearing on the surface of the section are the result of hardness measurements. Etchant: two percent nital. ~X1

Figure A7.4.1-34 Part of the transverse section shown in figure A7.4.1-33, but at higher magnification. The region at the bottom center is weld metal. The gray regions on either side of the weld metal are the heat affected zones associated with the weld. The lighter regions at either side of the figure beyond the heat affected zone are base channel material. Etchant: two percent nital. X8.5

Figure A7.4.1-35 Transverse section 3BM2 through the bottom of walkway box beam 9M (NBS 3). The south channel of the box beam is to the left and the north channel is to the right. The weld connecting the flanges of the two channels used to fabricate the box beam is in the center. Parts of the web regions of each channel had been removed before this photograph was taken. The indentations appearing on the surface of the section are the result of hardness measurements. Etchant: two percent nital. ~X1

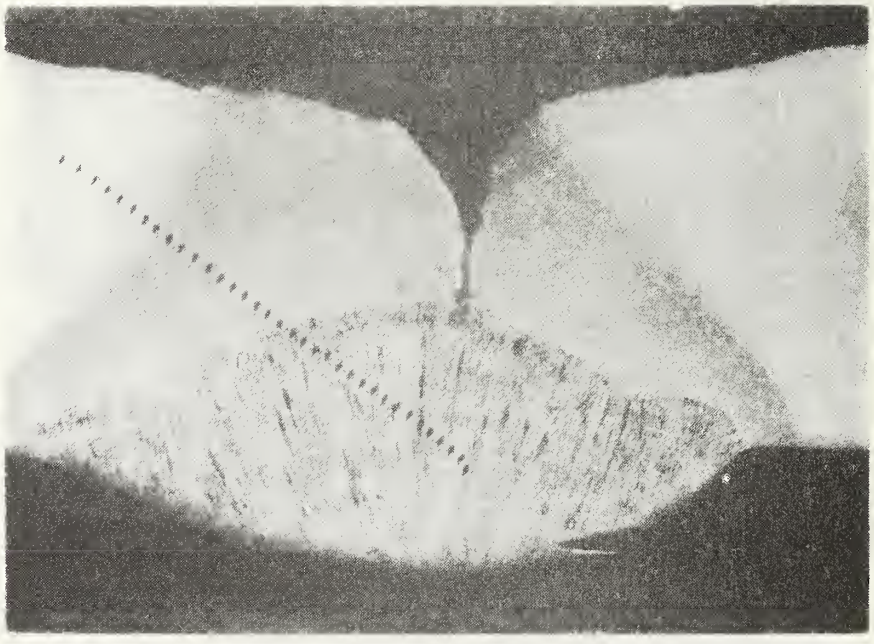

Figure A7.4.1-36 Part of the transverse section shown in figure A7.4.1-35, but at higher magnification. The region at the bottom center is weld metal. The gray regions on either side of the weld metal are the heat affected zones associated with the weld. The lighter regions at either side of the figure beyond the heat affected zones are base channel material. Etchant: two percent nital. X8.5

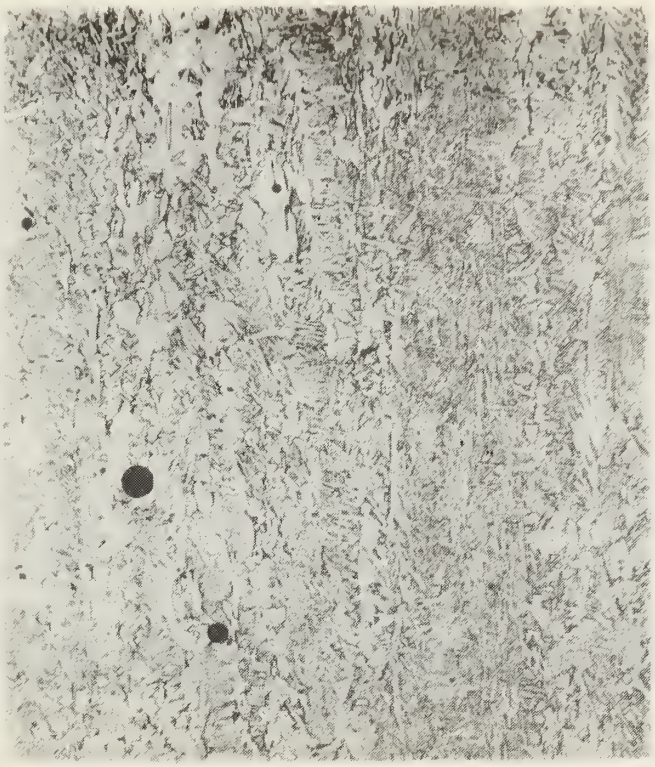

Figure A7.4.1-37 Representative microstructure of the weld metal in transverse section 3BM1 through box beam 9M (NBS 3). The microstructure consists primarily of bainite. Several inclusions are evident. Etchant: two percent nital. X200

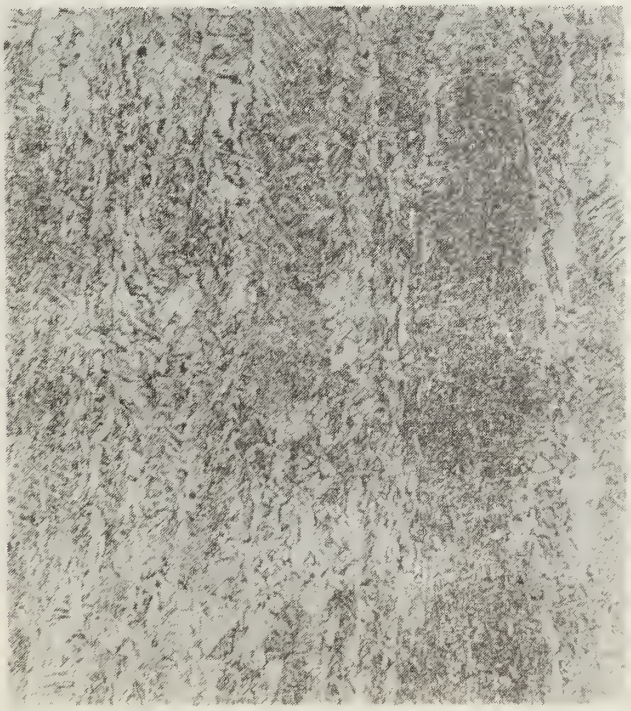

Figure A7.4.1-38 Representative microstructure of the weld metal in transverse section 3BM2 through box beam 9M (NBS 3). The microstructure consists primarily of bainite. Etchant: two percent nital. X200

Figure A7.4.1-39 Transition zone from weld metal (right) to heat affected zone (left) in section 3BM2. Some inclusions can be seen primarily in the weld metal. Etchant: two percent nital. X200

Figure A7.4.1-40 Region representative of the heat affected zone in section 3BM1. The microstructure appears to consist of ferrite both as a network in prior austenite grain boundaries and as needles, bainite, partially spheroidized carbides, and tempered martensite. Etchant: two percent nital. X200

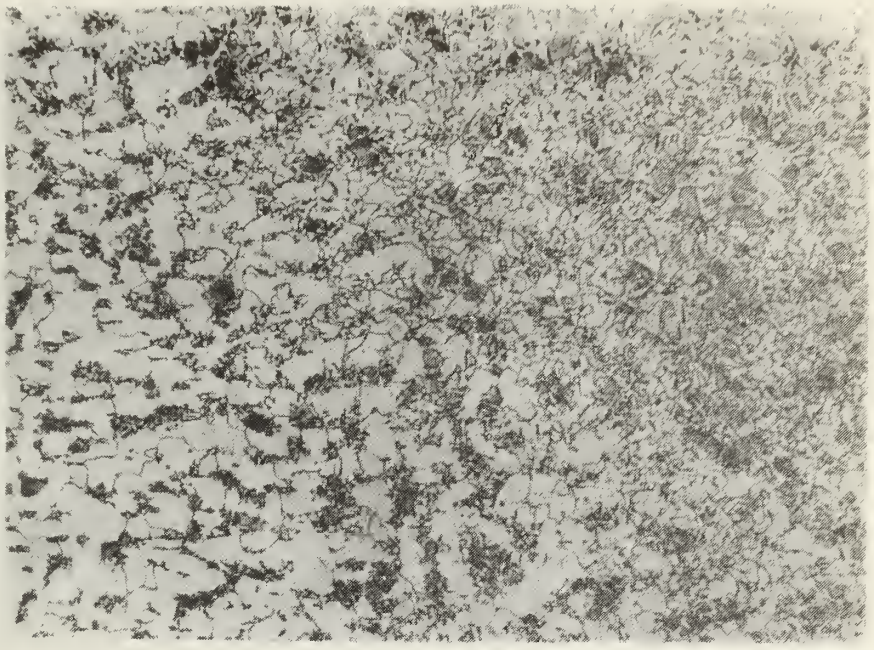

Figure A7.4.1-41 Transition zone from heat affected zone (right) to base channel material (left) in section 3BM2. Etchant: two percent nital. X200

Figure A7.4.1-42 Representative region of base channel material in section 3BM1. The microstructure consists of ferrite (light) and pearlite (dark) in the normalized condition. Etchant: two percent nital. X200

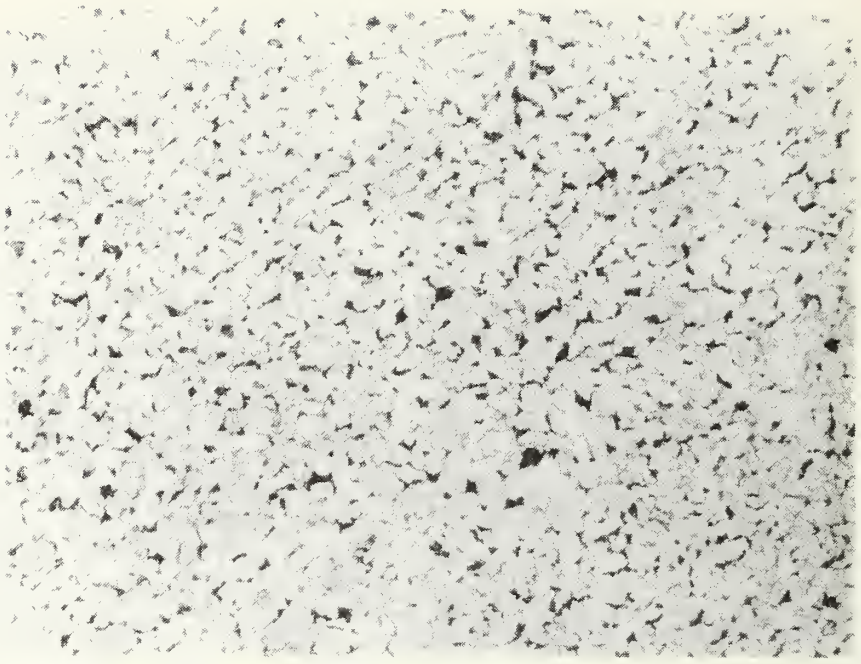

Figure A7.4.2-1 Transverse section through hanger rod NBS 5A showing the representative microstructure. The microstructure consists of relatively fine grained ferrite (light) and pearlite (dark) in a normalized condition.
Etchant: two percent nital. X100

Figure A7.4.2-2 Transverse section through hanger rod NBS 5B showing the representative microstructure. The microstructure consists of ferrite (light) and pearlite (dark) in a normalized condition. Etchant: two percent nital. X100

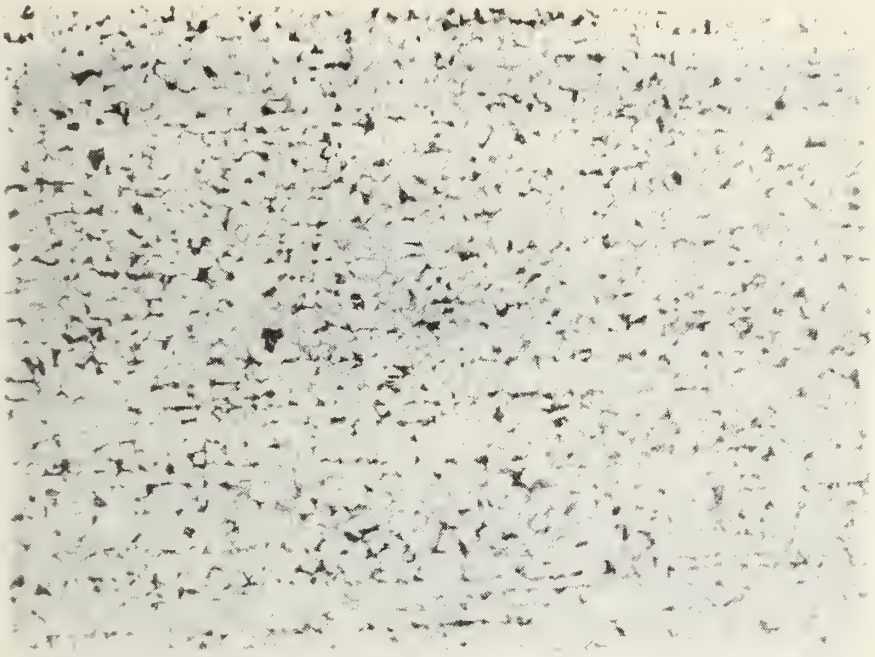

Figure A7.4.2-3 Longitudinal section through hanger rod NBS 5A showing the normalized microstructure consisting of ferrite and pearlite. Etchant: two percent nital. X100

Figure A7.4.2-4 Longitudinal section through hanger rod NBS 5B showing the normalized microstructure consisting of ferrite and pearlite. Etchant: two percent nital. X100

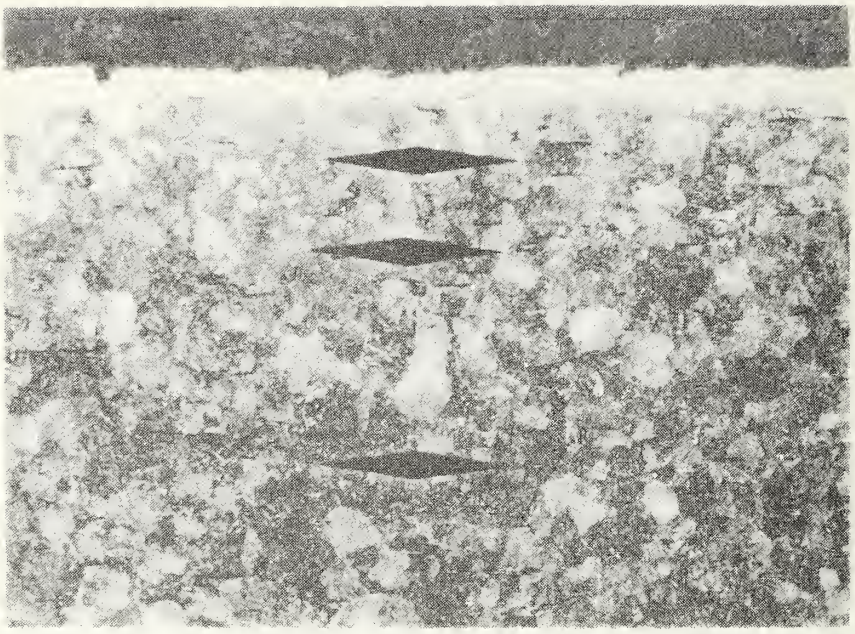

Figure A7.4.3-1 Microstructure of washer from location 9MW in the walkway debris. The thin, light layer at the surface (horizontal near the top in the figure) is the decarburized layer at the washer surface. The microstructure consists primarily of tempered martensite. Etchant: Picral. X200

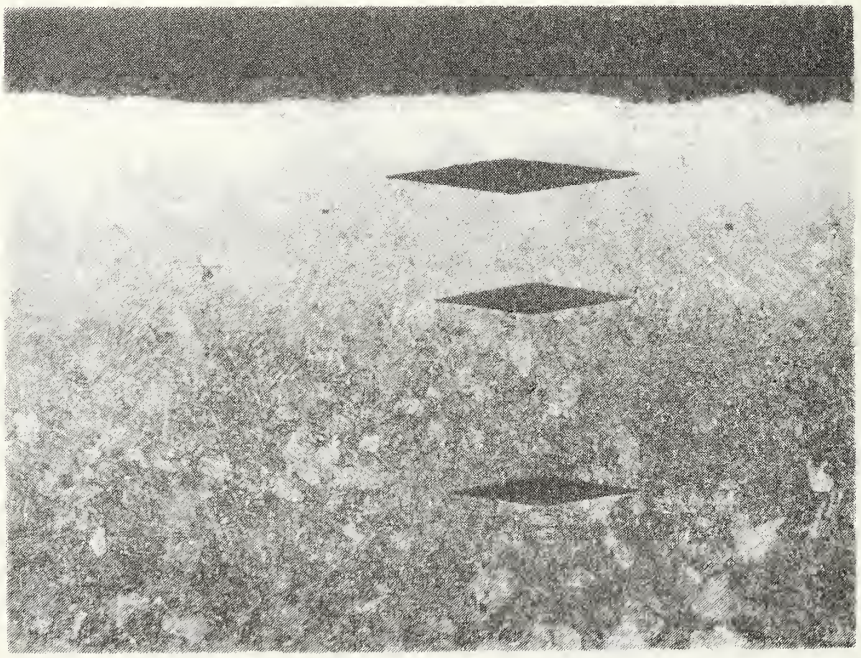

Figure A7.4.3-2 Microstructure of NBS hard washer. The light layer at the surface (horizontal near the top in the figure) is decarburized. The microstructure consists primarily of tempered martensite. Etchant: Picral. X200

Section A7.6

Table A7.6-1 Bulk Specific Gravity of Drilled Concrete Cores

Core Number	Weight (grams)						$\frac{A}{C-D}$ (a)	$\frac{B}{C-D}$ (b)
	A	B	C	D	E	C-D		
4-02	215.4	206.2	222.8	105.1	222.7	117.7	1.83	1.75
03	238.3	227.4	245.5	114.3	245.5	131.2	1.82	1.73
04	282.3	269.4	291.3	137.5	291.3	153.8	1.84	1.75
06	299.2	286.4	310.1	147.0	310.0	163.1	1.83	1.76
08	307.8	292.7	318.1	155.9	318.1	162.2	1.90	1.80
09	287.7	273.7	297.1	140.6	297.1	156.5	1.84	1.75
11	277.5	264.9	290.9	134.7	290.7	156.2	1.78	1.70
14	268.7	256.4	280.8	127.6	281.4	153.3	1.75	1.67
15	265.5	253.6	276.5	130.3	276.4	146.2	1.82	1.73
17	323.9	308.9	336.2	157.0	336.2	179.2	1.81	1.72

Notes: A = original weight
B = 24 hr oven dry weight
C = saturated surface-dry weight
D = weight immersed in water
E = saturated surface-dry weight after immersion

(a) Bulk specific gravity, air-dry

(b) Bulk specific gravity, oven-dry

1 lb = 0.4536 kg

Table A7.6-2 Bulk Specific Gravity of Topping Material

Core Number	Weight (grams)						$\frac{A}{C-D}$ (a)	$\frac{B}{C-D}$ (b)
	A	B	C	D	E	C-D		
4-02	58.7	57.6	62.7	34.2	62.7	28.5	2.06	2.02
03	51.7	51.0	55.7	30.5	55.5	25.2	2.05	2.02
04	41.5	41.1	49.9	24.5	49.9	25.4	1.63	1.62
06	49.9	47.7	52.8	28.6	52.8	24.2	2.06	1.97
11	38.6	38.2	41.2	23.4	41.2	17.8	2.17	2.15
14	46.3	44.5	51.7	23.9	51.7	27.8	1.67	1.60
15	58.3	55.8	64.3	29.1	64.3	35.2	1.66	1.59
17	58.7	56.3	65.6	31.0	65.6	34.6	1.70	1.63

Notes: A = original weight
B = 24 hr oven dry weight
C = saturated surface-dry weight
D = weight immersed in water
E = saturated surface-dry weight after immersion

(a) Bulk specific gravity, air-dry

(b) Bulk specific gravity, oven-dry

1 lb = 0.4536 kg

Table A7.6-3 Compressive Strength of Drilled Concrete Cores

Core Number	Avg. Capped Height L (inches)	Average Diameter D (inches)	L/D	Cross-Sectional Area $(in)^2$	Load at Failure (lbs)	Calculated Compressive Strength (psi)	CF[a]	Corrected Compressive Strength (psi)
4-01	3.829	1.984	1.930	3.09	16,950	5,485	0.993	5,447
05	3.584	1.986	1.805	3.10	15,575	5.024	0.983	4,938
07	3.635	1.980	1.836	3.08	15,975	5,187	0.985	5,109
10	3.425	1.980	1.730	3.08	16,175	5,252	0.978	5,136
12	3.608	1.986	1.817	3.10	15,075	4,863	0.984	4,785
13	3.696	1.981	1.866	3.08	13,850	4,497	0.988	4,443
16	3.150	1.982	1.590	3.08	14,500	4,708	0.967	4,553
18	3.695	1.986	1.861	3.10	17,325	5,589	0.988	5,522
19	3.722	1.985	1.875	3.09	16,525	5,348	0.989	5,289

Note: [a] Strength correction factor. See ANSI/ASTM C42-77, Standard Method of Obtaining and Testing Drilled Cores and Sawed Beams of Concrete.

1 in = 25.4 mm

1 lb = 4.448 N

1000 psi = 6.9 MPa

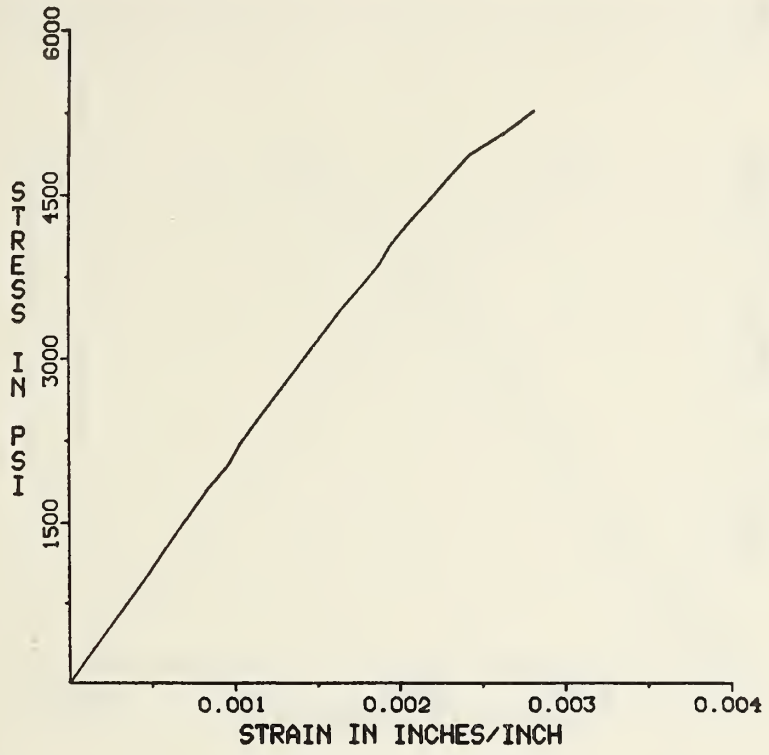

Figure A7.6-1. Stress-strain plot for concrete core 4-01.

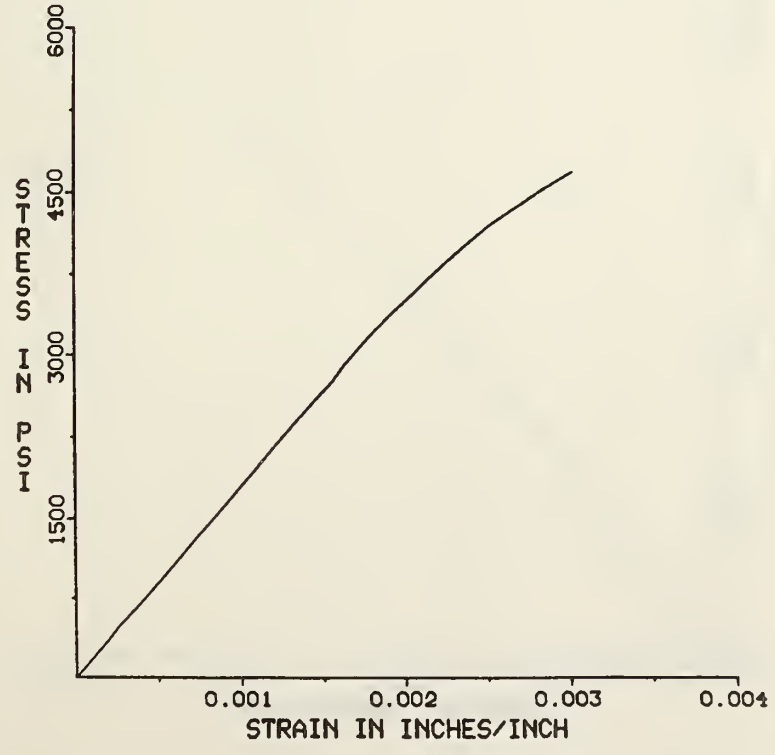

Figure A7.6-2. Stress-strain plot for concrete core 4-05.

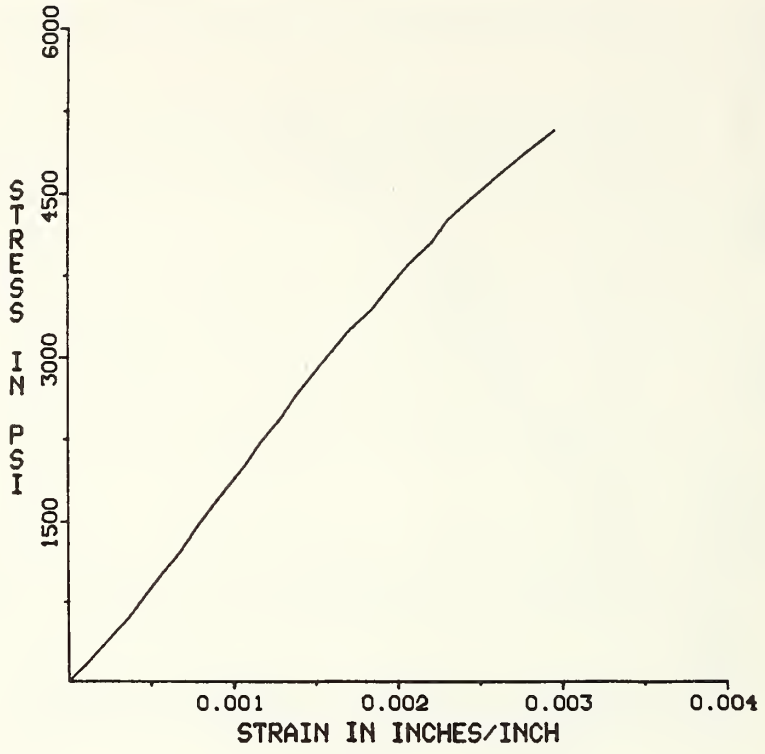

Figure A7.6-3. Stress-strain plot for concrete core 4-07.

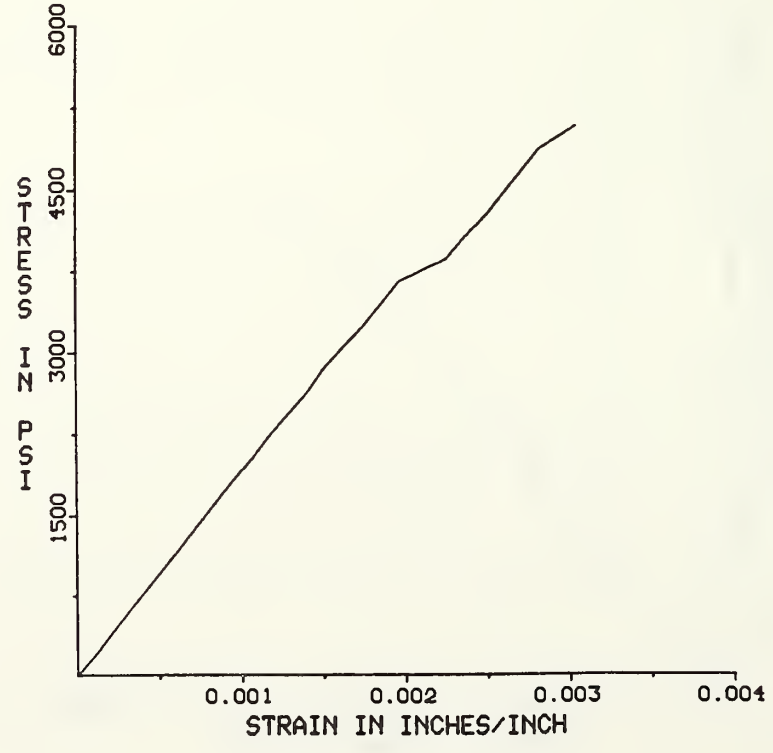

Figure A7.6-4. Stress-strain plot for concrete core 4-10.

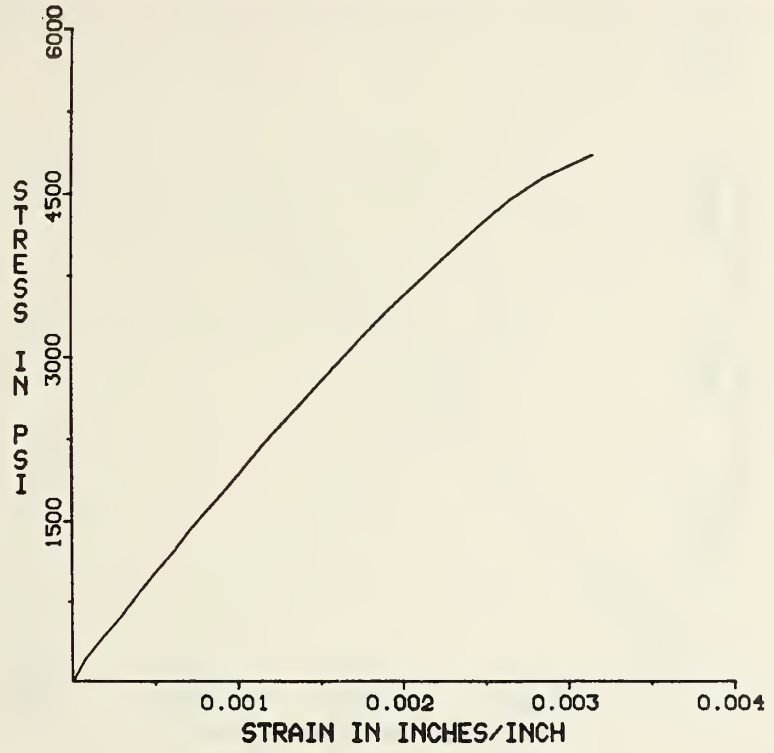

Figure A7.6-5. Stress-strain plot for concrete core 4-12.

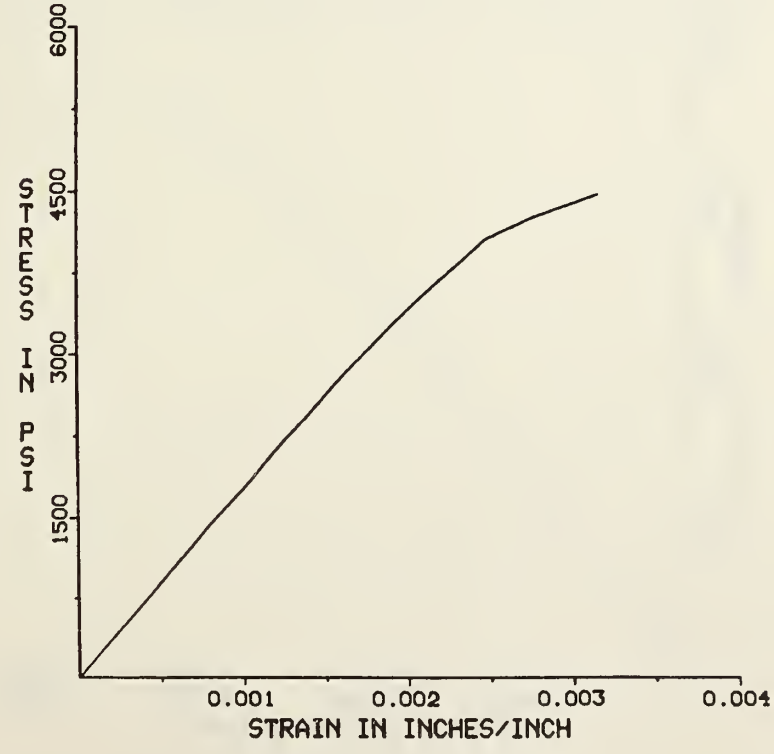

Figure A7.6-6. Stress-strain plot for concrete core 4-13.

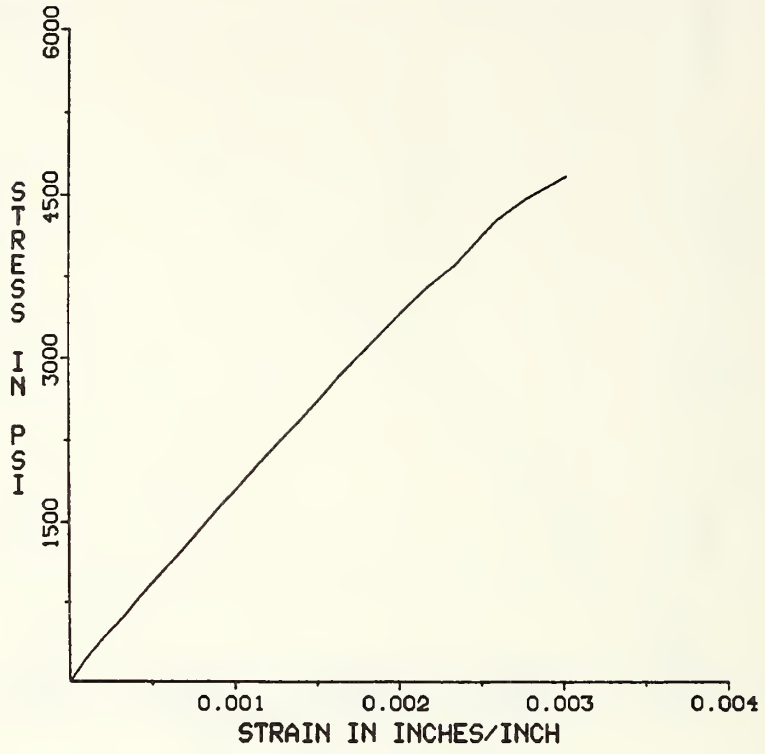

Figure A7.6-7. Stress-strain plot for concrete core 4-16.

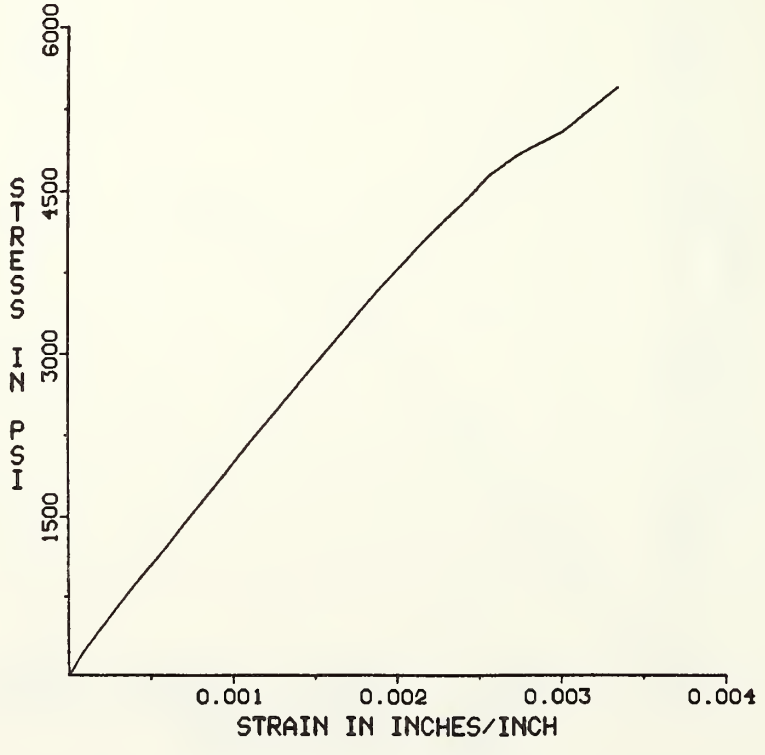

Figure A7.6-8. Stress-strain plot for concrete core 4-18.

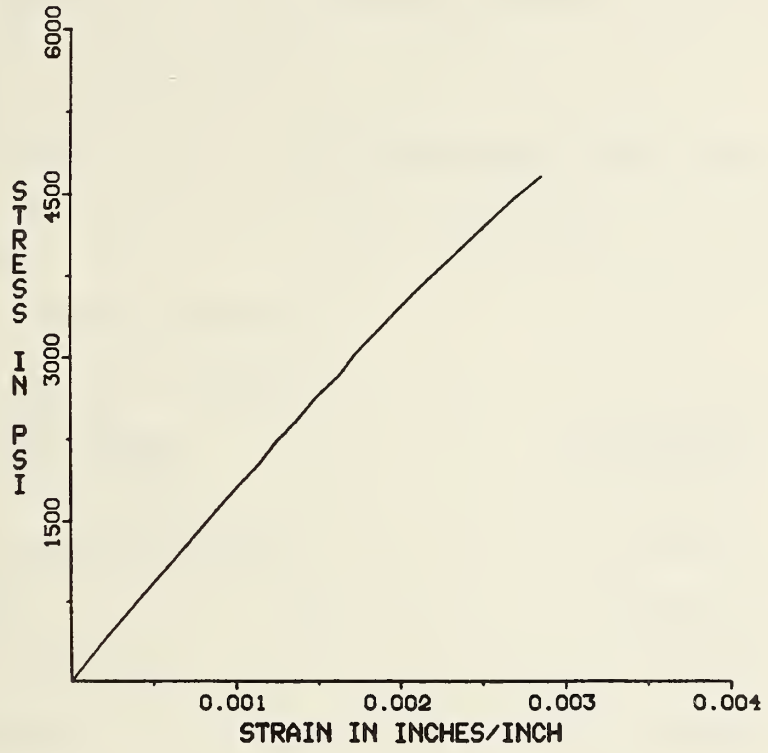

Figure A7.6-9. Stress-strain plot for concrete core 4-19.

Section A9.2

Table A9.2.1-1 Unit Weights of Walkway Materials

Item	Unit Weight
Structural Steel	Per AISC Manual of Steel Construction
1 1/2" x 20 Ga. Formed Steel Deck	2.20 lbs/ft^2
5/8" Type "X" Gyp. Bd. & Framing	
(a) 5/8" Gyp. Bd.	2.56 lbs/ft^2
(b) 24 Ga. Steel Studs	0.39 lbs/ft
(c) 24 Ga. Steel Runners	0.31 lbs/ft
Wood Handrail & Brass Extrusion	5.30 lbs/ft
Top Glass Grip	1.78 lbs/ft
1/2" Tempered Plate Glass	6.54 lbs/ft^2
Bottom Glass Grip	5.19 lbs/ft
Steel Support Angle (4 x 3 x 3/8)	8.50 lbs/ft
Footlights	2.26 lbs each
Footlight Base Plate & Cap	1.33 lbs/ft
Carpet	0.60 lbs/ft^2
Padding	0.25 lbs/ft^2
Sprinkler Pipes and Fittings	Per AISC Manual of Steel Construction
Aluminum Slats	70.4 lbs/span

Table A9.2.1-2 Weight Analysis of Damaged Walkway Spans

Item	Weight/Span (lbs)							
	U7-8	U8-9	U9-10	U10-11	L7-8	L8-9	L9-10	L10-11
Cross Beams & Stringers	2191.7	2057.1	2057.1	2174.5	2191.7		2057.1	2174.5
Box Beams	--	343.8	184.6	--	--		184.6	--
Clip Angles	12.7	--	--	12.7	12.7		--	12.7
1 1/4" ϕ Hanger Rods	--	110.0	--	--	--		--	--
1 1/2" x 20 Ga. Formed Steel Deck	498.9	493.4	493.4	498.9	498.9		493.4	498.9
Gyp. Bd. Attached to Span	1369.2	976.5	968.6	836.8	985.9		932.7	850.1
24 Ga. Steel Framing for Gyp. Bd.	67.6	67.6	67.6	67.6	67.6		67.6	67.6
Gyp. Bd. Scattered on Deck	--	52.0	39.0	41.6	26.0		7.8	--
Handrail Assembly	79.5	297.4	106.2	--	63.6		155.0	--
Top Glass Grip	102.5	--	--	--	52.1		--	--
1/2" Tempered Plate Glass Panels	416.5	520.6	--	--	208.2		--	--
Broken Plate Glass Panels	52.1	156.2	--	13.1	52.1		--	--
Bottom Glass Grip & Support Angle	795.8	790.0	790.0	800.4	795.8		790.0	800.4
Footlights & Baseplate	95.9	89.3	45.8	24.4	69.0		26.7	33.0
Carpet & Padding	187.3	187.3	--	--	187.3		--	--
Sprinkler Pipes	--	--	97.1	64.4	43.7		86.9	58.0
Miscellaneous Metal Work	--	100.0	--	--	100.0		--	--
Miscellaneous Debris	100.0	--	--	--	--		--	20.0
Timber Cribbing	156.2	--	--	--	--		--	59.4
Embedded Steel Plate	--	--	--	--	10.2		--	--
Broken Granite Panels	--	--	--	--	262.5		--	--
Total	6125.9	6241.2	4849.4	4534.4	5627.3		4801.8	4574.6

Span L8-9 not weighed

Table A9.2.1-3 Weights of Undamaged Walkway Span
Excluding Concrete Deck and Topping

Component Description	Weight/Span (lbs)			
	U7-8 L7-8	U8-9 L8-9	U9-10 L9-10	U10-11 L10-11
W16 x 26 Stringers & 1/4 x 6 Bent Plate	1847.0	1798.6	1798.6	1829.8
W8 x 10 Cross Beams & Clip Angles	344.7	258.5	258.5	344.7
MC8 x 8.5 Box Beams & Clp Angles	92.3	184.6	184.6	92.3
1 1/4" ϕ Hanger Rods (Fourth Floor) (Second Floor)	130.5 --	261.0 --	261.0 --	130.5 --
1 1/2" x 20 Ga. Formed Steel Deck	498.9	493.4	493.4	498.9
5/8" Type "X" Gyp. Bd. & Framing	2309.4	2309.4	2309.4	2309.4
Handrail Assy & Top Glass Grip	408.3	408.3	408.3	408.3
1/2" Tempered Plate Glass	1249.4	1249.4	1249.4	1249.4
Bottom Glass Grip & Support Angle	795.8	790.0	790.0	800.4
Footlights & Baseplate	104.8	104.8	104.8	104.8
Carpet & Padding	187.3	187.3	187.3	187.3
Sprinkler Pipes	51.1	88.2	97.1	91.8
Aluminum Slats	70.4	70.4	70.4	70.4
Total for Fourth Floor Spans	8089.9	8203.9	8212.8	8118.0
Total for Second Floor Spans	7959.4	7942.9	7951.8	7987.5

NBS-114A (REV. 2-8C)

U.S. DEPT. OF COMM. BIBLIOGRAPHIC DATA SHEET (See instructions)	1. PUBLICATION OR REPORT NO. NBSIR 82-2465	2. Performing Organ. Report No.	3. Publication Date February 1982

4. TITLE AND SUBTITLE

Investigation of the Kansas City Hyatt Regency Walkways Collapse

5. AUTHOR(S) R D. Marshall, E.O. Pfrang, E.V. Leyendecker, K.A. Woodward, R.P. Reed, M.B. Kasen, and T. R. Shives

6. PERFORMING ORGANIZATION (If joint or other than NBS, see instructions)

NATIONAL BUREAU OF STANDARDS
DEPARTMENT OF COMMERCE
WASHINGTON, D.C. 20234

7. Contract/Grant No.

8. Type of Report & Period Covered

9. SPONSORING ORGANIZATION NAME AND COMPLETE ADDRESS (Street, City, State, ZIP)

10. SUPPLEMENTARY NOTES

☐ Document describes a computer program; SF-185, FIPS Software Summary, is attached.

11. ABSTRACT (A 200-word or less factual summary of most significant information. If document includes a significant bibliography or literature survey, mention it here)

An investigation into the collapse of two suspended walkways within the atrium area of the Hyatt Regency Hotel in Kansas City, Mo., is presented in this report. The investigation included on-site inspections, laboratory tests and analytical studies.

Three suspended walkways spanned the atrium at the second, third, and fourth floor levels. The second floor walkway was suspended from the fourth floor walkway which was directly above it. In turn, this fourth floor walkway was suspended from the atrium roof framing by a set of six hanger rods. The third floor walkway was offset from the other two and was independently suspended from the roof framing by another set of hanger rods. In the collapse, the second and fourth floor walkways fell to the atrium floor with the fourth floor walkway coming to rest on top of the lower walkway.

Based on the results of this investigation, it is concluded that the most probable cause of failure was insufficient load capacity of the box beam-hanger rod connections. Observed distortions of structural components strongly suggest that the failure of the walkway system initiated in the box beam-hanger rod connection on the east end of the fourth floor walkway's middle box beam.

(continued on attached)

12. KEY WORDS (Six to twelve entries; alphabetical order; capitalize only proper names; and separate key words by semicolons)

building; collapse; connection; construction; failure, steel; walkway.

13. AVAILABILITY

☐ Unlimited

☐ For Official Distribution. Do Not Release to NTIS

☐ Order From Superintendent of Documents, U.S. Government Printing Office, Washington, D.C. 20402.

☐ Order From National Technical Information Service (NTIS), Springfield, VA. 22161

14. NO. OF PRINTED PAGES

15. Price

"Investigation of the Kansas City Hyatt Regency Walkways Collapse"

ABSTRACT - (continued)

Two factors contributed to the collapse: inadequacy of the original design for the box beam-hanger rod connection which was identical for all three walkways, and a change in hanger rod arrangement during construction that essentially doubled the load on the box beam-hanger rod connections at the fourth floor walkway. As originally approved for construction, the contract drawings called for a set of continuous hanger rods which would attach to the roof framing and pass through the fourth floor box beams and on through the second floor box beams. As actually constructed, two sets of hanger rods were used, one set extending from the fourth floor box beams to the roof framing and another set from the second floor box beams to the fourth floor box beams.

Based on measured weights of damaged walkway spans and on a videotape showing occupancy of the second floor walkway just before the collapse, it is concluded that the maximum load on a fourth floor box beam-hanger rod connection at the time of collapse was only 31 percent of the ultimate capacity expected of a connection designed under the Kansas City Building Code. It is also concluded that had the original hanger rod arrangement not been changed, the connection capacity would have been approximately 60 percent of that expected under the Kansas City Building Code. With this change in hanger rod arrangement, the ultimate capacity of the walkways was so significantly reduced that, from the day of construction, they had only minimal capacity to resist their own weight and had virturally no capacity to resist additional loads imposed by people.

Supplementary material is contained in an appendix to this report and published as NBSIR 82-2465A.

UNITED STATES DEPARTMENT OF
COMMERCE
NEWS
WASHINGTON, D.C. 20234

NATIONAL BUREAU
OF
STANDARDS

HOLD FOR RELEASE
9:30 a.m., February 25, 1982

Mat Heyman
301/921-3181

TN-5345

CONNECTIONS IN COLLAPSED WALKWAYS AT KANSAS CITY HOTEL FAR FROM ADEQUATE, NBS REPORTS

Critical connections in two Kansas City Hyatt Regency Hotel walkways which collapsed July 17, 1981, were capable of supporting less than one-third of the load expected to be carried by a connection designed under the Kansas City, Mo., building code. That was one of the major conclusions in a report issued today by the Commerce Department's National Bureau of Standards (NBS).

Dr. Edward O. Pfrang, who headed up an NBS investigation of the nation's worst building collapse, today identified the two factors related to those box beam-hanger rod connections which were critical in causing the walkways' failure.

First, Pfrang said, the "connections as initially detailed and approved for construction provided a capacity far below the capacity that would have been required to satisfy the Kansas City Building Code." Second, a change in the supporting hanger rod arrangement "essentially doubled the load to be transferred" by the connections, "thus further aggravating an already critical situation."

- more -

Shortly after the accident which killed 113 people and injured 186 others, Kansas City Mayor Richard L. Berkley asked NBS to investigate the failure. The mayor's request was endorsed by members of the Missouri congressional delegation. NBS, a federal science and engineering research laboratory which traditionally has served in a third party role to resolve technical controversies, agreed to determine the most probable cause of the collapse.

The NBS investigation included a review of various construction-related documents, on-site and laboratory structural and materials investigations--including testing of selected parts of the walkways' debris and NBS replicas of important walkway components--and extensive engineering analyses.

The bureau's findings are given in a 349-page report submitted today to Mayor Berkley in Kansas City and reviewed by Pfrang, Chief of the NBS Structures Division, at a news conference in Gaithersburg, Md.

Walkway's Structure

Three suspended walkways spanned the Hyatt Regency atrium, which connected a high-rise section and a lower "function block." The second floor walkway was suspended from the fourth floor walkway directly above it by six steel hanger rods. In turn, this fourth floor walkway was suspended from the atrium roof framing by another six hanger rods.

The third floor walkway, which was not involved in the collapse, was offset from the other two walkways and was independently suspended from the roof framing by another set of hanger rods.

The hanger rods from the roof and from the second floor walkway passed through the ends of the fourth floor walkway box beams. These box beams were made up of pairs of 8-inch steel channels which were welded together. The hanger rods were secured by washers and nuts after passing through the box beams. Under this arrangement, the fourth floor box beam-hanger rod connections transmitted the loads of both the second and fourth floor walkways.

In the collapse, the second and fourth floor walkways fell to the atrium floor after the fourth floor to ceiling hanger rods pulled through at the walkway box beam connections.

The NBS Investigation

To meet requirements of the Kansas City Building Code, Pfrang said, the fourth floor connections between the walkways' box beams and supporting hanger rods <u>each</u> should have been designed to handle 40,700 pounds--including the weight of the walkways and a specified design live load of people. However, the Kansas City code also incorporates a margin of safety for steel components. Walkway connections designed according to the code to have a capacity of 40,700 pounds would actually be expected to have an ultimate capacity of at least 68,000 pounds.

After weighing the damaged walkway spans and estimating the number of people on the walkways at the time of the collapse, NBS researchers concluded that the maximum load on any of the six connections at the time of the collapse was 21,400 pounds. Thus, the load on the walkways was far below that required to be handled under the Kansas City Building Code.

After conducting extensive structural and materials tests on selected parts of the walkways and NBS-fabricated replicas, bureau researchers determined that the average ultimate capacity of each fourth floor hanger rod-box beam connection was just 18,600 pounds compared to the expected ultimate capacity of 68,000 for code-complying connections. Thus, the connections were capable of supporting only 27 percent of the load expected to be supported by connections designed under the Kansas City Building Code.

Since the loads on the connections from the weight of the walkways and people on the walkways at the time of the collapse were so near to or in excess of the estimated ultimate capacity of the actual connections, failure could have begun at any of the fourth floor box beam-hanger rod connections, NBS researchers determined. Progressive failure of the other connections and the walkways' collapse was assured after any one of the connections failed and the load from that connection was distributed to the other connections. Based on studies of the walkways debris, NBS researchers were able to pinpoint a connection at the middle fourth floor box-beam as the most likely to have failed first.

A key factor contributing to the collapse, the NBS report noted, was that the walkways were not constructed in accordance with the contract drawings. As originally approved for construction by the Kansas City Codes Administration Office, the plan for the walkways called for a single set of hanger rods (attached to the roof framing) which would pass through the fourth floor beams and on through the second floor beams. Under this arrangement, each box beam would transfer its own load directly into the hanger rods.

However, during construction the hanger rod arrangement was changed to an "interrupted" hanger rod scheme so that the fourth floor box beam connections were required to transfer the load of both the fourth and the second floor walkways.

This change essentially doubled the load on those fourth floor connections. While NBS researchers concluded that this original hanger rod-box beam connection detail still would not have satisfied the Kansas City Building Code, they also determined that the original connections as shown on the contract drawings would have had the capacity to resist the loads estimated to have been acting on them at the time of the collapse.

Based on a variety of materials tests of walkway components--including the welds, nuts and washers, steel channels, and hanger rods--NBS researchers determined that "Neither the quality of workmanship nor the materials used in the walkway system played a significant role in initiating the collapse."

The bureau's report also notes that in addition to the box beam-hanger rod connections, the fourth floor to ceiling hanger rods and the third floor walkway hanger rods violated the design provisions of the Kansas City Building Code. According to NBS investigators, though, the hanger rod code violations were not a factor in the collapse.